JSCSEN 74(6)607–706(2009)

Journal of the Serbian Chemical Society

Electronic version

VOLUME 74

No 6

BELGRADE 2009

Available on line at

www.shd.org.rs/JSCS

The full search of JSCS is available through

DOAJ DIRECTORY OF OPEN ACCESS JOURNALS

www.doaj.org

Journal of the Serbian Chemical Society
JSCS@tmf.bg.ac.rs • www.shd.org.rs/JSCS

J. Serb. Chem. Soc. Vol. 74, No. 6 (2009)

CONTENTS

Published by the Serbian Chemical Society
Karnegijeva 4/III, 11000 Belgrade, Serbia
Printed by the Faculty of Technology and Metallurgy
Karnegijeva 4, P.O. Box 35-03, 11120 Belgrade, Serbia

Journal of the Serbian Chemical Society
JSCS@tmf.bg.ac.rs • www.shd.org.rs/JSCS

J. Serb. Chem. Soc. 74 (6) 607–618 (2009)
JSCS–3859

UDC 633.12:577.112.386:547.964.2
Original scientific paper

Successful production of recombinant buckwheat cysteine-rich aspartic protease in *Escherichia coli*

MIRA D. MILISAVLJEVIĆ[1]*, DRAŽEN R. PAPIĆ[1,2], GORDANA S. TIMOTIJEVIĆ[1] and VESNA R. MAKSIMOVIĆ[1]

[1]*Institute of Molecular Genetics and Genetic Engineering, University of Belgrade, Vojvode Stepe 444a, P.O. Box 23, 11010 Belgrade, Serbia and* [2]*Interfaculty Institute for Biochemistry, University of Tübingen, 72076 Tübingen, Germany*

(Received 23 January, revised 10 March 2009)

Abstract: Herein, the expression of recombinant cysteine-rich atypical buckwheat (*Fagopyrum esculentum*) aspartic protease (FeAPL1) in five *Escherichia coli* strains differing in their expression capabilities is presented. It was shown that the expression success depended highly on the choice of FeAPL1 fusion partner. His_6-FeAPL1 was produced in large quantities as an insoluble protein localized in inclusion bodies. On the other hand, MBP-FeAPL1 was localized in both the cytoplasm and inclusion bodies in BL21 and Rosetta-gami strains. Only purified soluble MBP-FeAPL1 from Rosetta-gami cells showed proteolytic activity at pH 3.0 with BSA as the substrate. The results also indicated that FeAPL1 contained a PRO segment that had to be removed for the enzyme activity to appear. The activity of FeAPL1 produced in the Rosetta-gami strain, which enables disulfide bond formation, indicated the importance of the twelve cysteine residues for correct folding and functionality.

Keywords: aspartic protease; His tag; inclusion bodies; MBP; recombinant protein.

INTRODUCTION

Aspartic proteases (APs) are one of the major classes of proteolytic enzymes and are widely distributed in the whole living world. They are most active at an acidic pH, are specifically inhibited by pepstatin A and contain two aspartic acid residues, which are indispensable for catalytic activity.

The majority of plant APs are distinguished from their non-plant homologues by the presence of the so-called plant-specific insert (PSI), which is removed from most mature plant APs together with the signal peptide and autoinhibitory PRO segment.[1] Recently a new class of plant APs, often called atypical or AP-like without PSI, has been identified and is represented by six members.[2–7] One of these is FeAPL1, the cDNA of which was isolated from the buck-

* Corresponding author. E-mail: heljda@sezampro.rs
doi: 10.2298/JSC0906607M

wheat seed cDNA library. Analysis of the polypeptide deduced from the FeAPL1 coding region, predicted an M_w of 48.6 kDa, four *N*-glycosylation sites and a hydrophobic signal peptide in the *N*-terminal region. Active-site sequence motifs DTG/DSG characteristic for APs as well as twelve Cys residues were also registered.[7]

Interestingly, bioinformatics analysis of the Arabidopsis genome sequence revealed 59 AP-like proteins, providing a new perspective concerning the diversity of AP family members in plants.[8] The biological significance of the existence of two types of APs only in plants is not clear.

Little is known about the biological functions and biochemical properties of the AP-like members. Various functions have been proposed. It was reported that they could be involved in pathogen resistance,[4] in the degradation of rubisco during leaf senescence,[6] in prey digestion[5] or in nucellar cell death.[2,3]

One reason for the lack of data related to the AP-like group is that it is very difficult to obtain sufficiently purified enzyme from plant tissues for detailed characterization. One suitable way is to overexpress the gene in heterologous systems, such as microorganisms or cell cultures of higher organisms (yeast, insects, mammals, *etc*.). The most common host for the production of recombinant APs is *Escherichia coli*. However, of the many attempts, those that gave successful expression often yielded a completely insoluble product that had to be refolded to gain activity. This occurred with OsAsp1 from rice,[3] deleted forms of CND41 from tobacco,[9] cardosin A from *Cynara cardunculus*[10] and some non-plant APs––candidapepsin from *Candida tropicalis*,[11] bovine prochymosin,[12] porcine pepsin[13] and human procathepsin D.[14] The successful production of plant APs in higher organisms was reported for cyprosin and phytepsin in *Pichia pastoris*[15] and insect cells,[16] respectively.

The attractiveness of *E. coli* as an expression system lies in its ability to grow rapidly and at high density on inexpensive substrates, its well characterized genetics and the availability of an increasingly large number of cloning vectors and mutant host strains.[17] The most important factors that largely affect efficient recombinant protein expression are: a) a strong and tightly regulated promoter (isopropyl-β-D-thiogalactopyranoside (IPTG)-inducible promoters are mostly used); b) *E. coli* strains deficient in the most harmful proteases and/or thioredoxin and glutathione reductases; c) codon usage difference between the *E. coli* strain and the overexpressed gene; d) solubility of the recombinant protein, which depends on the protein expression rate, presence of disulfide bonds, hydrophobicity and choice of fusion partner (tags).[18] The most commonly used tags are polyhistidine (His tag) and glutathione *S*-transferase (GST tag), but tags such as thioredoxin, MBP (Maltose Binding Protein), NusA (transcription termination anti-terminator factor)[19] or SUMO (small ubiquitin-like modifier)[20] have been shown to be more effective as solubility enhancers of fusion partners. For inso-

luble proteins, it is possible to solubilize aggregates and refold proteins either by dilution, dialysis or on-column refolding methods.[21,22] However, optimization of the refolding procedure for a given protein requires time-consuming efforts and is not always conducive to high product yields.

Herein, the production of recombinant buckwheat aspartic protease-like (rFeAPL1) in several *E. coli* strains with two different tags, His_6 and MBP, and an analysis of their efficiency and "stumbling blocks" are reported.

EXPERIMENTAL

E. coli *strains and expression vectors*

Expression strains: M15(pREP4) (Qiagen), BL21(DE3)pLysS (Promega) BL21-CodonPlus (DE3)-RIL (Stratagene), BL21- CodonPlus (DE3)-RP (Stratagene), Rosetta-gami (Novagen).

Expression vectors: pQE32 (Qiagen), pMAL-c2X (New England Biolabs).

LB medium: 1 % (w/v) trypton; 1 % (w/v) NaCl; 0.5 % (w/v) yeast extract, pH 7.5,[23] with or without 0.2 % glucose.

LA plates – LB medium containing 1.5 % (w/v) of agar.

Competent *E. coli* cells M15, BL21 and Rosetta-gami were prepared and heat shock transformed according to the manufacturer's instructions.

Preparation of expression constructs

Expression vectors pQE32 and pMAL-c2X were linearized by double digestion using *Sma*I/*Hind*III and *Xmn*I/*Hind*III restriction enzymes (Fermentas), respectively.

The coding sequence of the FeAPL1 gene was amplified using P6:

(5'-atgcccggggccacatttcccttg-3') and

P5 (5'-gtcaagcttaatttttggatcgatcgatcacattgttg-3') primers,

which contain *Sma*I and *Hind*III restriction sites on the 5' ends, respectively. The template was *FeAPL1* clone (AY536047).[7]

The polymerase chain reaction (PCR) was cycled 5 times for 30 s at 94 °C, 30 s at 60 °C and 90 s at 68 °C and then 20 times for 30 s at 94 °C and 2 min at 70 °C. Amplification products were cloned in pGEM-T Easy vector (Promega), excised by *Sma*I and *Hind*III restriction enzymes, gel extracted and subcloned into opened pQE32 and pMAL-c2X expression vectors.

Recombinant protein production

Recombinant clones containing FeAPL1 cDNA sequence, cloned in expression vectors pQE32 and pMAL-c2X, were used for the transformation of competent M15, BL21(DE3)-pLysS, BL21-CodonPlus (DE3)-RIL, BL21-CodonPlus (DE3)-RP and Rosetta-gami strains.

Rapid screening of small expression cultures

Bacterial cultures (2 ml) were grown overnight at 37 °C in LB medium containing ampicillin 100 μg/ml, kanamycin 25 μg/ml in the case of M15 cells, ampicillin 100 μg/ml; chloramphenicol 34.5 μg/ml for all BL21 strains and ampicillin 100 μg/ml, kanamycin 15 μg/ml, tetracycline 12.5 μg/ml and chloramphenicol 34.5 μg/ml in the case of the Rosetta-gami strain.

A 1.5 ml aliquot of prewarmed LB medium (including antibiotics) or LB medium (including antibiotics) containing 0.2 % glucose for expression of FeAPL1 from the pMALc2X vector, was inoculated with 500 μl of the overnight cultures and grown at 37 °C for 30 min with vigorous shaking (180 rpm, Lab-Therm shaker). Expression of recombinant protein was induced by adding IPTG at a final concentration of 1mM and the cultures were grown at 37 °C for 3 h.

The induced cultures (1 ml) were centrifuged at 14000 rpm (Eppendorf centrifuge, 5417R) for 1 min. The pellets were resuspended in 100 µl of Buffer B (100 mM NaH_2PO_4, 10 mM Tris-HCl, 8 M urea, pH 8.0). The lysates (10 µl) were analyzed by SDS-PAGE.

Clones that expressed recombinant protein were subjected to determination of protein solubility. One ml of the induced cultures was centrifuged and the pellets were resuspended in the appropriate buffer. Lysis buffer (50 mM NaH_2PO_4, 300 mM NaCl, 10 mM imidazole, pH 8.0) was used when the expression was from the pQE32 vector and Column buffer (20 mM Tris-HCl, pH 7.4, 200 mM NaCl, 1 mM EDTA) for expression from the pMAL-c2X vector. The lysates were sonicated three times for 10 s on ice (Sonipenio 150, MSE (UK) Ltd.) and centrifuged at 14000 rpm (Eppendorf centrifuge, 5417R) for 15 min at 4 °C. The pellets were resuspended in 100 µl of buffer B. The supernatant (20 µl) and pellet (10 µl) were analyzed by SDS-PAGE.

Large scale production: determination of optimal conditions for recombinant protein production

The clones with the highest expression of recombinant protein were selected for large scale production. A suitable LB medium (500 to 1000 ml) containing antibiotics was inoculated 1:50 with the overnight culture and grown at 37 °C with vigorous shaking until an OD_{600} of 0.5 was attained. Expression was induced by adding IPTG to a final concentration of 0.10, 0.30, 0.50 or 1.0 mM.

The cultures were incubated at different temperatures (16, 25, 30 or 37 °C) for 15 min, 30 min, 1, 2 or 3 h. The cells were harvested by centrifugation at 4000 rpm at room temperature for 20 min and resuspended in Lysis buffer or its modifications (300 or 1 mM NaCl, with or without 0.2 % Triton X-100 or Tween 20, 10 % or 50 % of glycerol and 10 mM 2-mercaptoethanol) or Column buffer at 2–5 ml of buffer per gram wet weight of cells. Lysozyme (1 mg/ml) was added and the lysate incubated on ice for 30 min. After sonication three times for 10 s on ice, the lysate was centrifuged at 10000 rpm for 20 min at 4 °C. Both the supernatant and pellet were analyzed by SDS-PAGE.

The supernatants were used for further recombinant protein purification under native conditions and pellets for purification under denaturing conditions and further refolding of FeAPL1.

Purification under native conditions

The cleared lysate (supernatant) was mixed with 200–1000 µl of prewashed 50 % Ni-NTA slurry (expression from pQE32) or amylose resin (expression from pMALc2X) and gently shaken at 4 °C for 1 h or overnight. The resin was collected by centrifugation for 30 s at 1000 rpm. The resins were washed 2 to 4 times with 5–10 volumes of Wash buffer (50 mM NaH_2PO_4, 300 mM NaCl, 20 mM imidazole, pH 8.0) for 30 min at 4 °C. The protein was eluted in 200–1000 µl of Elution buffer (50 mM NaH_2PO_4, 300 mM NaCl, 250 mM imidazole, pH 8.0) (expression from pQE32) or Column buffer containing 10 mM maltose (expression from pMAL-c2X) and analyzed by SDS-PAGE and immunoblot.

Purification under denaturing conditions

The pellet resuspended in Buffer B was mixed with 200–1000 µl of prewashed 50 % Ni-NTA slurry by gently shaking at room temperature for 1 h. After collection, the resin was washed once in 5 ml of Buffer B and 2 to 3 times in 5–10 ml Buffer C for 30 min each time. The recombinant FeAPL1 was eluted in 1 to 2 ml of Elution buffer and analyzed by SDS--PAGE and immunoblot.

Immunoblot analysis

The antibodies used for immunodetection were mouse Anti-His HRP monoclonal antibodies (Qiagen) and Anti-MBP rabbit antiserum (New England Biolabs).

For immunodetection, rFeAPL1 was electrophoresed and transferred to a PVDF membrane (Millipore) in a Fastblot B43 transfer system (Biometra) according to the manufacturer's instructions. After transfer, all immunodetection steps were performed at room temperature. For detection with Anti-His HRP antibodies, the membranes were washed twice for 10 min with TBS buffer (10 mM Tris-HCl, pH 7.5, 150 mM NaCl) and incubated in blocking buffer (0.5 % Blocking reagent in 1X Blocking reagent Buffer, Qiagen) for 1 h. After two washings in TBS-Tween/Triton (20 mM Tris-HCl, pH 7.5, 500 mM NaCl, 0.05 % Tween-20, 0.2 % Triton X-100) and one in TBS buffer, the membranes were incubated with Anti-His HRP Conjugate solution (1:2000 dilution) in blocking buffer for 1 h. The membranes were washed twice in TBS-Tween/Triton buffer and once in TBS for 10 min each time.

For detection with Anti-MBP rabbit antiserum, the membranes were washed in TBST buffer (20 mM Tris-HCl, pH 7.5, 150 mM NaCl, and 0.1 % Tween-20) and incubated in Blocking buffer (5 % non-fat dry milk in TBST buffer) overnight. The membranes were incubated with Anti-MBP antiserum in 1:10000 dilution in TBST buffer for 1 h. After washing with TBST buffer three times for 5 min each, the membranes were incubated with anti-rabbit IgG peroxidase conjugate (Sigma) (1:10000 dilution) in TBST buffer.

In both cases, chemiluminescence was detected by an ECL-Plus Western Blotting Detection System (GE Healthcare) according to the manufacturer's recommendations. The membranes were covered with mixed reagent A and B (40:1) for 5 min at RT and exposed to X-ray film for 3 to 10 s.

Protease digestion

Recombinant His_6-FeAPL1 expressed in M15 cells, or MBP-FeAPL1 produced in BL21 (DE3)pLysS or Rosetta-gami (3 to 20 μg) was mixed with 20 μg of BSA, casein or hemoglobin in 100 μl of suitable buffer and incubated at 37 °C overnight. Samples were analyzed by SDS-PAGE.

Buffers used for digestion: 0.10 M sodium citrate, pH 3.0 and 4.0; 0.10 M sodium acetate, pH 5.0; 0.10 M phosphate, pH 6.0 and 7.0; 0.10 M Tris-HCl, pH 8.0.

RESULTS

To produce recombinant FeAPL1, its cDNA without the putative signal peptide (1–20 amino acids) was cloned in two expression vectors (pQE32 and pMAL--c2X) and the resulting constructs were introduced into several *Escherichia coli* strains. Cloning into the pQE32 vector resulted in the fusion of six histidines (His tag) in front of FeAPL1 (construct rHis6-FeAPL1). Cloning into the pMAL-c2X vector resulted in the fusion of the MBP tag in front of FeAPL1 (construct rMBP-FeAPL1) (Scheme 1a and 1b).

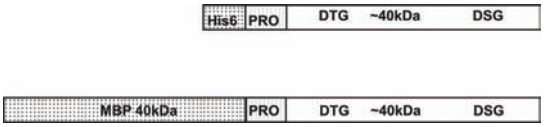

Scheme 1. Scheme of recombinant constructs: rHis6-FeAPL1 (a) and rMBP-FeAPL1 (b). His6 – polyhistidine tag; PRO – auto-inhibitory PRO segment; DTG and DSG – two catalytic sequence motifs; MBP – maltose binding protein tag.

Expression of rHis$_6$-FeAPL1

Several bacterial strains (M15(pREP4), BL21(DE3)pLysS, BL21-CodonPlus (DE3)-RIL, BL21-CodonPlus (DE3)-RP and Rosetta-gami) with different properties for expression of recombinant His$_6$-FeAPL1 (experimental) were chosen. Eight clones of each strain were screened for recombinant protein production. In every strain, except Rosetta-gami (which did not produce recombinant protein) at least three clones out of eight produced His$_6$-FeAPL1 of approximately 46 kDa and no significant difference in quantity was observed. The produced clones were analyzed for protein localization. After induction of expression, cell pellets were resuspended in native Lysis buffer and centrifuged. Both fractions (pellet and supernatant) were analyzed by 12 % SDS-PAGE (Fig. 1a). The recombinant protein was dominantly localized in the pellet-insoluble inclusion bodies in all clones and it was easily visualized by Coomassie staining. On the other hand, recombinant protein in the soluble fraction could only be detected by anti-His antibodies, due to the small amount (Fig. 1b). Approximately 100 μg of soluble protein from 3 l of culture was purified on Ni-NTA resin but the purified protein did not show any activity.

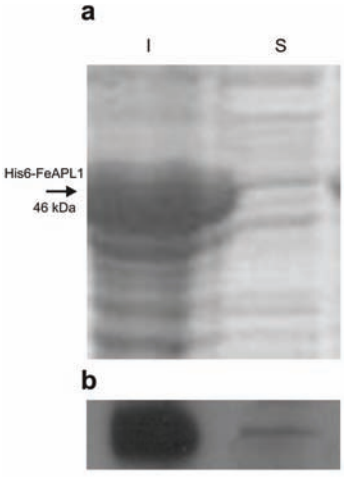

Fig. 1. Expression of rHis6-FeAPL1. a) Coomassie brilliant blue G250 staining of 12 % SDS-PAGE of insoluble (I) and soluble (S) fractions of the protein extract of transformed M15 strain. b) Western blot hybridization of the same fractions with Anti-His HRP antibodies.

All efforts to enlarge the soluble fraction, such as altering the induction conditions (temperature, culture OD_{600}, time of induction, IPTG concentration), changing the Lysis buffer content, or conditions for binding and elution of protein from NI-NTA resin did not give positive results.

Expression of rMBP-FeAPL1

In order to increase the solubility of FeAPL1, an MBP-FeAPL1 construct in the pMAL-c2X vector was made. BL21(DE3)pLysS and Rosetta-gami strains were selected for the expression of this construct. A fusion protein of approxima-

tely 90 kDa was localized in both the insoluble (inclusion bodies) and soluble fractions, with more protein in the inclusion bodies. The recombinant protein from both fractions could be visualized either by Coomassie brilliant blue G250 staining (Fig. 2) or anti-MBP antibody (data not shown). Approximately 1 mg of soluble protein could be purified on amylose resin from one liter of induced bacterial culture.

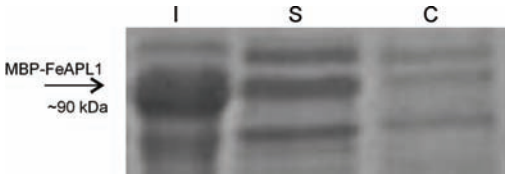

Fig. 2. Expression of rMBP-FeAPL1. Coomassie staining of 12 % SDS-PAGE of insoluble (I) and soluble (S) fractions of protein extract of transformed Rosetta-gami strain and crude protein extract of the untransformed cells (C).

Enzyme activity of rMBP-FeAPL1

In order to test if the rMBP-FeAPL1 produced from BL21(DE3)pLysS and Rosetta-gami cells showed proteolytic activity, an increasing amount of recombinant enzyme (3, 10 or 20 μg) was mixed with 20 μg of BSA, casein or hemoglobin in buffers of different pH (experimental). The products of proteolysis were analyzed by SDS-PAGE. Proteolytical cleavage was observed only with BSA in citrate buffer (pH 3.0) with rMBP-FeAPL1 purified from Rosetta-gami cells. The main product was a band of approximately 50 kDa with several lower bands (Fig. 3a). In the presence of 10 μM pepstatin A, an inhibitor of aspartic proteases, proteolysis of MBP-FeAPL1 was not observed (Fig. 3b). Purified supernatants from untransformed BL21/Rosetta-gami cells and BSA alone in suitable buffers were used as control reactions (data not shown).

The same reactions were analyzed for autoproteolytic processing of rMBP--FeAPL1 by immunodetection with anti-MBP antibodies. At lower pH values (3.0 and 4.0), there was a clear decrease of the full-length rMBP-FeAPL1 band (≈ 90 kDa) and the appearance of an approximately 44 kDa band, which could correspond to the fusion protein MBP-PRO segment of FeAPL1. This could be evidence that FeAPL1 possesses a PRO segment that has to be removed from the active enzyme. At higher pH values, this band could not be detected and the amount of full-length protein increased with increasing pH (Fig. 4).

DISCUSSION

In order to gain insight into the function of FeAPL1 after analysis of its cDNA,[7] it was necessary to obtain the protein itself. It is usually very difficult to isolate sufficiently purified enzyme from plant tissues for detailed characterization, mainly due to the low amounts and poor stability. Therefore, the production of a recombinant protein was chosen. In general, aspartic proteases are “hard pro-

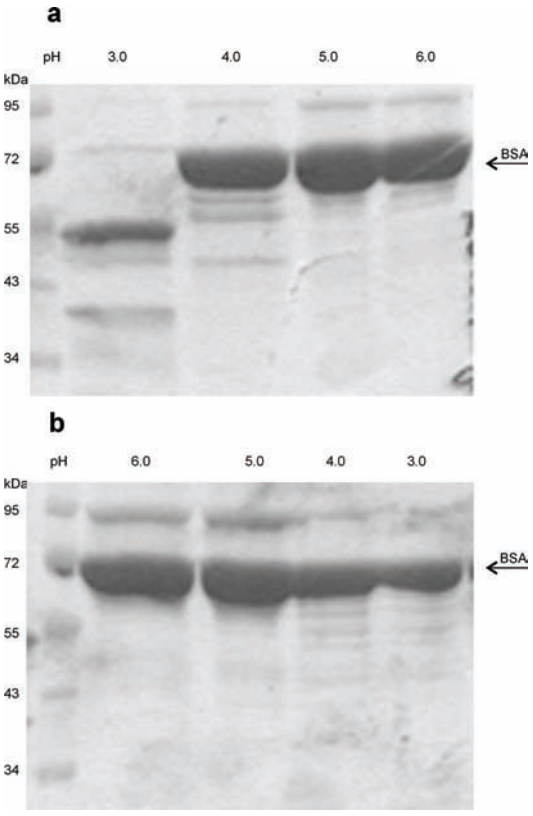

Fig. 3. Enzyme activity of rMBP-FeAPL1. a) Proteolysis of BSA by purified soluble rMBP-FeAPL1 from Rosetta-gami cells in buffers of pH 3.0, 4.0, 5.0 and 6.0 respectively; b) the same reactions in the presence of 10 μm pepstatin A. On the left (a) and (b) – PageRuler marker (Fermentas)-bands from top to bottom: 95, 72, 55, 43 and 34 kDa.

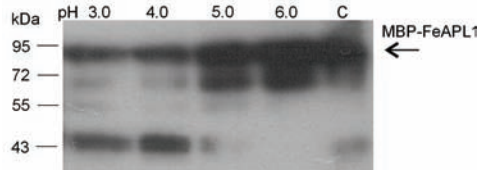

Fig. 4. Autoproteolytic processing of rMBP-FeAPL1. Western blot analysis with Anti-MBP antibodies of the reactions shown in Fig. 3a and purified rMBP-FeAPL1 in Column buffer with 10 mM maltose (C).

teins" for overexpression in heterologous systems. Thus, in *Escherichia coli*, the most frequently used expression system, recombinant APs usually ended up in inclusion bodies. Refolding by different techniques had to be performed in order to make them soluble and active. This justified initial attempts at overexpression in more complex and expensive systems, such as yeast and insect cells. Unfortunately, *Pichia pastoris* did not produce FeAPL1 protein at all, probably due to differences in codon usage, while the protein expressed in insect cells was completely insoluble and inactive. Therefore, it was decided to analyze the *E. coli* system in more detail, being aware that, despite the above-mentioned short-

comings, this system offers many opportunities for variation of all constituents. Production of FeAPL1 was examined in several *E. coli* strains with two different tags – His_6 and MBP.

The difference in codon usage between FeAPL1 and *E. coli* is 27.89 % (Graphical Codon Usage Analyzer, http://gcua.schoedl.de). Thus, BL21 RIL and RP strains were chosen in order to overcome possible problems with synthesis of the protein. These strains possess plasmid carrying genes for tRNA for Arg, Ile, Leu and Pro, respectively. Since all strains produced equal amounts of protein, the codon usage difference was shown to have no significance in the efficiency of FeAPL1 expression.

The polyhistidine tag was added to the N terminus of FeAPL1 cDNA without the signal peptide. This tag is poorly immunogenic, small at pH 8.0 and uncharged, and hence does not generally affect compartmentalization or folding of the fusion protein and thus its structure and function.

This system proved very efficient since a large amount of rHis_6-FeAPL1 (50 mg/l culture) was produced and purified on Ni-NTA resin. However, the crucial problem was the almost complete insolubility of the fusion protein. Factors that might be involved in the formation of inclusion bodies are: a high local concentration of recombinant protein; the reducing environment of the *E. coli* cytoplasm, which prevents disulfide bond formation; the lack of post-translational modification; improper interactions with chaperones and other enzymes involved in folding *in vivo*; intermolecular cross-linking *via* disulfide bonds and other covalent bonds; and increased aggregation of folding intermediates due to their limited solubility. The primary structure of FeAPL1 largely contributes to its insolubility. It contains twelve cysteine residues able to form disulfide bonds. Since all these residues are conserved within the AP-like group, they are certainly important for proper folding into the correct structure and, therefore, functionality of the enzyme. There is no evidence whether all cysteines are included in disulfide bond formation or not. Probably due to the inability of disulfide bond formation, the protein starts to fold improperly, exposing insoluble hydrophobic regions and, together with the factors mentioned above, is prone to aggregation.

For this kind of cysteine-rich protein, it is very challenging to find conditions throughout isolation that will enable the formation of correct intramolecular disulfide bonds instead of intermolecular disulfide bonds leading to protein aggregation. Decreasing the amount of produced protein (decrease of IPTG concentration and/or time of induction), lowering the temperature-increase of protein solubility, and induction of different *E. coli* growth phases did not give any positive results. Therefore, purified His_6-FeAPL1 from inclusion bodies was subjected to several refolding methods in different buffers. Buffers of different ionic strength, containing detergents such as Triton X-100 or Tween 20, 2-mercaptoethanol as reductant or glutathione oxidized/reduced did not lead to refolding of the FeAPL1.

In order to improve the solubility of FeAPL1, cDNA was inserted downstream from the *malE* gene coding for MBP. MBP has a solubilizing effect on structurally, functionally, chemically and evolutionary diverse proteins, but the exact mechanism is not clear.[24–26]

MBP-FeAPL1 was overexpressed in BL21 and Rosetta-gami cells. Both strains produced a satisfactory amount of soluble fusion protein. The Rosetta-gami strain was chosen because it has a less reducing environment in the cytoplasm (due to disruption of thioredoxin and glutathione reductases), thereby facilitating disulfide bond formation. In addition, it supplies tRNAs for AGG, AGA (arg), AUA (ile), CUA (leu), CCC (pro), GGA (gly). The combination of an MBP-tag and this *E. coli* strain might be crucial for proper folding and correct cysteine positioning for disulfide bond formation. The native structure enables functional proteolytic activity as detected by hydrolysis of BSA at an acidic pH. At an acidic pH, the full-length rMBP-FeAPL1 band (≈ 90 kDa) decreased and a 44 kDa band appeared, that might correspond to the fusion protein MBP-PRO segment of FeAPL1, as indicated with anti-MBP antibodies. This could be evidence that FeAPL1 possesses a PRO segment that has to be removed from the active enzyme, as occurs with many plant APs.[1] This removal was detected at pH 3.0, 4.0, 5.0 but hydrolysis of BSA occurred only at pH 3.0. Broader pH values at which APs are active could be expected.[1,3,5,27] In this study, FeAPL1 activity was detected at pH 3.0, but not at pH 4.0, 5.0 or 6.0. This observation is unusual but one explanation may be that at pH 3.0, when MBP is autocatalytically removed, the protein remains in its native structure and exhibits protease activity. At higher, but still acidic pH values, the protein may possess autocatalytic activity, successfully removing PRO+MBP but after losing MBP, the protein unfolds and loses its activity. Also, the possibility that FeAPL1 is only active in a narrow pH range around pH 3.0 cannot be excluded. Sets of control reactions were set up to confirm that BSA hydrolysis was due to FeAPL1 activity and not to the acidic environment, co-purified bacterial proteases or any other proteases than aspartic. Proteolysis was not detected in reactions with the purified soluble fraction of *Rosetta gami* cells without overexpression of MBP-FeAPL1, or in reactions with BSA in digestion buffers without rMBP-FeAPL1. Finally, when a pepstatin A-specific inhibitor of APs was added, hydrolysis of BSA was absent. The fact that only BSA was hydrolyzed (no casein or hemoglobin) may be interpreted as high substrate specificity of the enzyme, although for such an interpretation, more analyses with different natural and synthetic substrates are required.

One more strategy that could be implemented for FeAPL1 overexpression in *E. coli* is to target it to the periplasm. The beneficial effects achieved through secretion of the gene product include enhanced disulfide bond formation and a considerable reduction in the amount of contaminating proteins in the starting material for purification.

CONCLUSIONS

Expression of recombinant proteins is a challenging process that demands empirical investigations of all expression system actors, as it is usually impossible to predict the behavior and features of the recombinant protein. Therefore, there are no “hard proteins” if all actors in the expression system are analyzed. These investigations should lead toward obtaining a satisfactory amount of soluble and biologically active protein.

In the case of FeAPL1, the less reducing cytoplasm of the *Rosetta gami* strain in combination with the MBP tag with solubilizing properties on its fusion partner, enabled the production of a satisfactory amount of soluble and, more importantly, proteolytically active enzyme.

Acknowledgment. This work was supported by the Ministry of Science and Technological Development of the Republic of Serbia, Grant 143017. We would also like to thank Dr Anna Nikolić for editing the manuscript and Dr Miroslav Konstantinović for the artwork.

ИЗВОД

УСПЕШНА ПРОИЗВОДЊА РЕКОМБИНАНТНЕ АСПАРТАТНЕ ПРОТЕИНАЗЕ ХЕЉДЕ БОГАТЕ ЦИСТЕИНОМ У *E.coli*

МИРА Д. МИЛИСАВЉЕВИЋ, ДРАЖЕН Р. ПАПИЋ, ГОРДАНА С. ТИМОТИЈЕВИЋ и ВЕСНА Р. МАКСИМОВИЋ

Институт за молекуларну генетику и генетичко инжењерство, Универзитет у Београду, Војводе Степе 444а, п.пр. 23, 11010 Београд

У овом раду представљена је експресија рекомбинантне атипичне аспартатне протеиназе хељде (*Fagopyrum esculentum*) богате цистеином, где су тестирана различита експресиона својства пет сојева *E. coli*. Такође је анализиран и утицај фузионих партнера (His_6 и MBP) на ефикасност експресије. У случају His_6-FeAPL1, добијена је велика количина нерастворног протеина, смештеног у инклузионим телима. С друге стране, MBP-FeAPL1 је био локализован и у цитоплазми и у инклузионим телима у оба употребљена соја *E. coli* (BL21 и Rosetta-gami). Међутим, само за рекомбинантни протеин произведен у сој Rosetta-gami, доказана је протеолитичка активност на супстрату BSA, при pH 3,0. Резултати су такође указали да FeAPL1 садржи PRO сегмент, чије је одстрањивање неопходно за његову протеолитичку активност. Активност FeAPL1, показана само у сој Rosetta-gami, где је могуће формирање дисулфидних веза, указује на значај 12 цистеина у успостављању правилне структуре која омогућава функционалност ензима.

(Примљено 23. јануара, ревидирано 10. марта 2009)

REFERENCES

1. I. Simoes, C. Faro, *Eur. J. Biochem.* **271** (2004) 2067
2. F. Chen, M. Foolad, *Plant Mol. Biol.* **35** (1997) 821
3. X. Bi, G. Khush, J. Bennett, *Plant Cell Physiol.* **46** (2005) 87
4. Y. Xia, H. Suzuki, J. Borevitz, J. Blount, Z. Guo, K. Patel, R. A. Dixon, C. Lamb, *EMBO J.* **23** (2004) 980
5. S. Athauda, K. Matsumoto, S. Rajapakshe, M. Kuribayashi, M. Kojima, N. Kubomura, A. Iwamatsu, C. Shibata, H. Inoue, K. Takahashi, *Biochem. J.* **381** (2004) 295

6. Y. Kato, S. Murakami, Y. Yamamoto, H. Chatani, Y. Kondo, T. Nakano, A. Yokota, F. Sato, *Planta* **220** (2004) 97
7. M. D. Milisavljević, G. S. Timotijević, S. R. Radović, M. M. Konstantinović, V. P. Maksimović, *J. Plant Physiol.* **165** (2008) 983
8. E. Beers, A. Jones, A. Dickerman, *Phytochemistry* **65** (2004) 43
9. T. Nakano, S. Murakami, T. Shoji, S. Yoshida, Y. Yamada, F. Sato, *Plant Cell* **9** (1997) 1673
10. I. Simões, E. C. Mueller, A. Otto, D. Bur, A. Y. Cheung, C. Faro, E. Pires, *FEBS J.* **272** (2005) 5786
11. X. Lin, J. Tang, G. Koelsch, M. Monod, S. Foundling, *J. Biol. Chem.* **268** (1993) 20143
12. H. G. Menzella, H. C. Gramajo, E. A. Ceccarelli, *Protein Expr. Purif.* **25** (2002) 248
13. X. L. Lin, R. N. Wong, J. Tang, *J. Biol. Chem.* **264** (1989) 4482
14. G. E. Conner, G. Richo, *Biochemistry* **31** (1992) 1142
15. P. C. White, M. C. Cordeiro, D. Arnold, P. E. Brodelius, J. Kay, *J. Biol. Chem.* **274** (1999) 16685
16. S. Glathe, J. Kervinen, M. Nimtz, G. H. Li, G. J. Tobin, T. D. Copeland, D. A. Ashfort, A. Wlodawer, J. Costa, *J. Biol. Chem.* **273** (1998) 31230
17. G. Georgiou, *Protein Engineering: Principles and Practice*, Wiley-Liss, New York, 1996, p. 101
18. J. R. Swartz, *Curr. Opin. Biotechnol.* **12** (2001) 195
19. K. Terpe, *Appl. Microbiol. Biotechnol.* **60** (2003) 523
20. T. R. Butt, S. C. Edavettal, J. P. Hall, M. R. Mattern, *Protein Expr. Purif.* **43** (2005) 1
21. A. Middelberg, *Trends Biotechnol.* **20** (2002) 437
22. H. P. Sørensen, H. U. Sperling-Petersen, K. K. Mortensen, *Protein Expr. Purif.* **32** (2003) 252
23. J. Sambrook, E. F. Fritsch, T. Maniatis, *Molecular Cloning. A Laboratory Manual*, Cold Spring Harbor Laboratory Press, New York, 1989
24. R. B. Kapust, D. S. Waugh, *Protein Sci.* **8** (1999) 1668
25. J. C. Spurlino, G. Y. Lu, F. A. Quiocho, *J Biol Chem.* **266** (1991) 5202
26. . D. Fox, R. B. Kapust, D. S. Waugh, *Protein Sci.* **10** (2001) 622
27. I. Simões, R. Faro, D. Bur, C. Faro, *J. Biol. Chem.* **282** (2007) 31358.

Journal of the Serbian Chemical Society
JSCS@tmf.bg.ac.rs • www.shd.org.rs/JSCS

J. Serb. Chem. Soc. 74 (6) 619–628 (2009)
JSCS–3860

UDC 582.272+551.468(262.4):615.28–188:
:665.52/54
Original scientific paper

Antimicrobial and antioxidant activity of brown algae from the Aegean Sea

ZELIHA DEMIREL[1], FERDA F. YILMAZ-KOZ[2], ULKU N. KARABAY-YAVASOGLU[1], GUVEN OZDEMIR[1]* and ATAKAN SUKATAR[1]

[1]*Ege University, Faculty of Science, Department of Biology, Izmir and* [2]*Ege University, Faculty of Pharmacy, Department of Pharmaceutical Microbiology, Izmir, Turkey*

(Received 9 December 2008, revised 26 January 2009)

Abstract: The present study was conducted to evaluate the antioxidant and antimicrobial activity of methanol, dichloromethane and hexane extracts, as well as the essential oils of brown algae (Phaeophyta) *Colpomenia sinuosa*, *Dictyota dichotoma*, *Dictyota dichotoma* var. *implexa*, *Petalonia fascia* and *Scytosiphon lomentaria*. The essential oil of the macroalgae was obtained by steam distillation and analyzed by GC and GC/MS. The antioxidant activity of the algal extracts was determined using the procedures of inhibition of β-carotene bleaching and $ABTS^+$ methods. The antioxidant effects of the extracts were compared with those of commercial antioxidants, such as butylated hydroxytoluene (BHT), butylated hydroxyanisol (BHA) and α-tocopherol. The hexane extracts of *D. dichofoma* var. *implexa* had a higher phenolic content than the other extracts. The dichloromethane extract of *S. lomentaria* was found to be more active in the decolorization of $ABTS^+$ than the other extracts and generally the dichloromethane extracts were more active than the methanol and hexane extracts. Antimicrobial activities of the extracts were assessed against Gram (+) and Gram (–) bacteria and one yeast strain by the disk diffusion method. According to the results, the dichloromethane extracts generally showed more potent antimicrobial activity than the methanol and hexane extracts at concentrations 1.5 and 1.0 mg/disk.

Keywords: brown algae; antioxidant activity; antimicrobial activity; essential oil.

INTRODUCTION

Marine organisms are rich sources of structurally new and biologically active metabolites.[1] In recent years, there have been many reports of macroalgae derived compounds that have a broad range of biological activities, such as antibiotic, antiviral, antioxidant, antifouling, anti-inflammatory, cytotoxic and antimitotic activities.[2] Seaweeds are known to contain reactive antioxidant mole-

* Corresponding author. E-mail: guven.ozdemir@ege.edu.tr
doi: 10.2298/JSC0906619D

cules, such as ascorbate and glutathione (GSH) when fresh, as well as secondary metabolites, including carotenoids (α- and β-carotene, fucoxanthin, astaxanthin), mycosporine-like amino acids (mycosporine-glycine) and catechins (*e.g.*, catechin, epigallocatechin, epigallocatechin), gallate, phlorotannins (*e.g.*, phloroglucinol), eckol and tocopherols (α-, χ-, δ-tocopherols).[3] Brown-algal polyphenols phlorotannins worked as antioxidants, antibacterial and anti-algal compounds.[4,5]

Antibacterial halogenated compounds, such as bromophenols, have been isolated from many types of seaweed.[6] *Colpomenia sinuosa* synthesize fatty acids and sterols, and the main sterol of this alga is found as fucosterol.[7,8] The *Dictyota dichotoma*-isolated dolabellane (dolabellane, and perhydroazulene diterpenes, diterpenoids) derivatives possess antimicrobial activity against bacteria.[9] *C. sinuosa* exhibited significant antitumoral, antileukemic, antiprotozoan[10] and hypolipidemic activity.[11]

Thus, the objectives of this study were: 1) to analyze the chemical composition of the essential oil of *C. sinuosa*, *D. dichotoma*, *D. dichotoma* var. *implexa*, *Petalonia fascia* and *Scytosiphon lomentaria*, which were collected from the Aegean Sea in the Izmir Bay, by GC/MS in order to determine the essential oil chemotype; 2) to investigate the antimicrobial and antioxidant activities of the methanol, dichloromethane and hexane extracts, and the essential oil from these algae.

EXPERIMENTAL

Algal material

Field collections of seaweeds, *Colpomenia sinuosa* (No. EGE 40777), *Dictyota dichotoma* (no EGE 40775), *Dictyota dichotoma* var. *implexa* (No. EGE 40774), *Petalonia fascia* (No. EGE 40773) and *Scytosiphon lomentaria* (No. EGE 40776) were deposited in the EGE herbarium (Ege University, Department Herbarium, Izmir, Turkey). Macroalgae were obtained from several reefs (depths of 1–2 m) along the Izmir coast (Turkey) and identified by Dr. Atakan Sukatar. The harvested fresh macroalgae samples were cleaned from their epiphytes, frozen immediately after harvesting and stored at –20 °C until they were freeze-dried.

Preparation of algal extracts

Freeze-dried samples were pulverized and 15 g of each were sequentially extracted as reported by Vlachos *et al.*[12] in 150 mL methanol, dichloromethane and hexane for 24 h using a Soxhlet extraction apparatus. The solvents were evaporated and the resulting extracts were kept at +4 °C. All employed solvents were of analytical reagent grade and obtained from Sigma Chemical Co. (St. Louis, CA).

Isolation of the essential oil

To obtain the essential oil, dried samples of each alga (10 g) were exposed to steam distillation for 4 h using a Clevenger-type apparatus according to the European Pharmacopoeia (1975)[13] and the obtained distillate was diluted with hexane.

GC/MS analysis

The steam-distilled components were analyzed by GC and GC/MS. An HP 6890 gas chromatograph equipped with an FID and a 5 m×0.2 mm HP-1 capillary column (0.33 μm coating) was employed for the GC analysis. GC/MS analysis was performed using a HP 5973

mass selective detector coupled with an HP 6890 gas chromatograph, equipped with a HP-1 capillary column. Identification of the individual components was performed by comparison of mass spectra with literature data and by comparison of their retention indices (*RI*) relative to a C8–C32 *n*-alkene mixture.[14] A computerized search was performed using the Wiley 275 L GC/MS library and the ARGEFAR GC/MS library created with authentic samples.

Antimicrobial activity

Eight bacteria strains (*Bacillus subtilis* ATCC 6633, *Staphylococcus aureus* ATCC 6538P, *Enterobacter aerogenes* ATCC 13048, *Escherichia coli* ATCC 29998, *Proteus vulgaris* ATCC 6897, *Salmonella typhimurium* CCM 583), two specific pathogenic strains (methicillin-oxacillin-resistant *Staphylococcus aureus* ATCC 43300, hemorrhagic *Escherichia coli* (O157: H7) RSSK 232 and one yeast strain *Candida albicans* ATCC 10239 were obtained from the Microbiology Department Culture Collection of Ege University, Faculty of Science, Turkey.

Disk diffusion method

20 and 30 μL each algal solvent extracts (1.0 and 1.5 mg disk^{-1}) were applied per sterile 6 mm diameter filter paper disks (Schleicher and Schüll, No. 2668, Dassel, Germany).[15]

The suspensions of organisms were initially adjusted with sterile distilled water to a density equivalent to the 0.5 McFarland standards. 0.20 ml of a 24 h-broth culture (10^6 cfu/ml) of the bacteria species were spread on the surface of gelled sterile Mueller-Hinton Agar plates. The algal extracts were prepared with methanol, dichloromethane and hexane and then adsorbed onto the sterile disks (20 and 30 μL) and the same volume of solvent was used as the negative control. The paper disks containing the extracts were air-dried and placed on the surface of each plate. The antimicrobial activity of the extracts against the test bacteria was indicated by the growth-free "zone of inhibition" near the respective disk. Methanol, dichloromethane and hexane did not show any antimicrobial activity. All tests were performed under sterile conditions in duplicate and repeated three times. Tobramycin disks (Bioanalyse, 10 μg/disk) and nystatin disks (Oxoid, 30 μg/disk) were used as the positive controls.

Antioxidant activity

ABTS radical cation decolorization assay. The experiments were performed using an improved ABTS (2,2'-azinobis(3-ethylbenzothiazoline-6-sulfonic acid)) decolorization assay.[16] BHA (butylated hydroxyanisol), BHT (butylated hydroxytoluene) and α-tocopherol (Vitamin E) were used as the positive controls. All determinations were performed in triplicate. The inhibition percentage, *I*, of the absorbance was calculated as follows (1):

$$I = 100\left(\frac{A_0 - A_1}{A_0}\right) \quad (1)$$

where A_0 is the $ABTS^+$ absorbance value at the initial time and A_1 is the $ABTS^+$ absorbance value after 6 min incubation.

β-*Carotene bleaching assay*. This experiment was performed by measuring the coupled auto-oxidation of β-carotene and linoleic acid.[17] The antioxidant activity, *AA*, is expressed as percent inhibition relative to the control after 120 min incubation using the following equation:

$$AA = 100\left[1 - \left(\frac{A_0 - A_t}{A_0^o - A_t^o}\right)\right] \quad (2)$$

where A_0 and A_0^o are the absorbance values measured at the initial incubation time for the sample and control, respectively, while A_t and A_t^o are the absorbance values measured in the samples or standards and control at t = 120 min, respectively.

Total phenolic content. The total phenolic compound concentrations were determined as described previously.[18] The phenolic content is expressed as gallic acid equivalent (GAE) in milligram per 1 g algal extract.

Statistics

The antioxidant activities of the data are expressed as means ±*SE*. Statistical analysis was performed by ANOVA with LSD test and Student's *t*-test. A *P* value of 0.05 or less was taken to indicate statistical significance.

RESULTS AND DISCUSSION

Antimicrobial activity

The methanol, dichloromethane and hexane extracts of five lyophilized brown algae were investigated for *in vitro* antimicrobial activity (Table I). The concentrations of 1.0, 1.5 mg/disk of the algae extracts inhibited the growth of all microorganisms. Some studies concerning the effectiveness of extraction methods highlight that methanol extraction yields higher antimicrobial activity than hexane and ethyl acetate, whereas others report that chloroform extraction is better than methanol and benzene.[19] According to the present experimental results, the dichloromethane extracts caused better halo-zones than methanol for all strains. The seaweed extracts are responsible for its activity against Gram (+) bacteria, especially *Bacillus subtilis* and *Staphylococcus aureus*. The dichloromethane extracts exhibited a higher degree of activity as compared to the methanol and hexane extracts. There are some reports regarding the antimicrobial activity of seaweeds from the Aegean Sea, Turkey.[19–21] The previous reports showed that the algal extracts were generally more effective against Gram (+) than Gram (–) bacteria, probably due to the more complex structure of the cell wall of Gram (–) bacteria.[22] Salvador *et al.*[2] described the antimicrobial activities of 82 seaweeds extracts (18 Chlorophyceae, 25 Phaeophyceae and 39 Rhodophyceae) as fresh and freeze-dried forms in each season. The effect of freeze-drying on the bioactivity of algal sample was generally such that it enabled greater extraction rates of the compounds. Taskin *et al.*[21] showed that the methanolic extracts of *Dictyota dichotoma* inhibited *S. aureus*. The dichloromethane extract of *Dictyota dichotoma* var. *implex*, *D. dichotoma*, exhibited antibacterial activity against *Salmonella typhimurium*. Only one species, *Scytosiphon lomentaria*, showed antimicrobial activity against nine test microorganisms.

Composition of the essential oil

The composition of the volatile compounds of the five brown macroalgae was determined by GC/MS. Different groups of compounds were identified, such as hydrocarbons, terpenes, acids, phenols, sulfur-containing compound, aldehy-

des, naphthalene skeleton and alcohols (Table II). Eight for *D. dichotoma* var. *implexa*, twelve for *D. dichotoma*, four for *Petalonia fascia*, six for *S. lomentaria* and fourteen compounds for *Colpomenia sinuosa* were identified from the distillate, accounting for 58.41, 83.53, 91.71, 87.89 and 74.17 % of the total composition of the essential oil, respectively. In recent years, many studies on volatile compounds from marine algae have been published.[22] The most common volatile compounds determined from marine algae were terpenoids, thymol, carvacrol, β-cubebene, β-eudesmol, β-ionone, dactylol and pachydictol A. It is known that β-ionone has a deterring action against some arthropods, and that it possesses antibacterial and antifungal activity.[23] Alcoholic and phenolic compounds have not been found in *D. dichotoma*, *P. fascia* and *S. lomentaria*. Heptadecane and hexadecane have been reported as common major volatile components in seaweeds.[20] The highest concentration of crown ether (18-crown-6-ether) was found in *S. lomentaria.* One sulfur-containing compound, dihexylsulfide, which are rarely found in algae,[23] was also identified in *C. sinuosa*.

TABLE I. Antimicrobial activity (diameter of zone of inhibition, including the diameter of the filter paper disk (6 mm), in mm, mean value of three independent experiments) of brown macroalgae extracts; I – *D. dichotoma* var. *implexa*, II – *D. dichotoma*, III – *P. fascia*, IV – *S. lomentaria* V – *C. sinuosa*, VI – Standards; 1. *B. subtilis* (ATCC 6633), 2. *S. aureus* (ATCC 6538-p), 3. *S. aureus*, methicillin-oxacillin resistant (ATCC 43300), 4. *E. aerogenes* (ATCC 13048), 5. *E. coli* (ATCC 29908), 6. *E. coli* hemorrhagic, O157:H7 (RSSK 232), 7. *P. vulgaris* (ATCC 6897), 8. *S. typhimurium* (CCM 5445), 9. *C. albicans* (ATCC 10239)

Algae	Extractant	Extract concentration mg/disk	Microorganisms								
			1	2	3	4	5	6	7	8	9
			Gram								
			+	+	+	–	–	–	–	–	
I	Methanol	1	na[a]	na	na	na	na	na	na	na	na
		1.5	6.5	6.5	na	na	na	na	6.5	na	na
	Dichloromethane	1	6.5	7	7	9	8	8	10	10	na
		1.5	7	8	8	11	12	11	12	13	na
	Hexane	1	8	7	na	na	na	na	na	na	na
		1.5	9	10	10	na	na	na	na	na	6.5
II	Methanol	1	na	7	7	na	na	na	na	na	na
		1.5	6.5	7.5	7.5	na	na	na	na	na	na
	Dichloromethane	1	6.5	na	6.5	na	na	na	9	na	na
		1.5	7	na	7	6.5	6.5	6.5	11	7	na
	Hexane	1	8	7	na	na	na	na	na	na	na
		1.5	9	7.5	na	na	na	na	na	na	na
III	Methanol	1	na	na	na	na	na	na	na	na	na
		1.5	na	na	na	na	na	na	na	na	na
	Dichloromethane	1	6.5	6.5	na	na	na	na	na	na	na
		1.5	7	7	6.5	6.5	na	na	na	na	na
	Hexane	1	na	na	na	na	na	na	na	na	na
		1.5	na	6.5	na	na	na	na	na	na	na

TABLE I. Continued

Algae	Extractant	Extract concentration mg/disk	Microorganisms								
			1	2	3	4	5	6	7	8	9
			Gram								
			+	+	+	–	–	–	–	–	
IV	Methanol	1	7	7	6.5	na	na	na	na	na	na
		1.5	7.5	7.5	7	na	na	na	na	na	na
	Dichloromethane	1	7.5	7.5	7	na	na	7	7	na	na
		1.5	8.5	8.5	7.5	6.5	9	9.5	7.5	6.5	6.5
	Hexane	1	6.5	7	9	6.5	6.5	6.5	7	7	6.5
		1.5	7.5	8	11	7	7	7	8	8	7.5
V	Methanol	1	na	8	6.5	na	na	na	na	na	na
		1.5	na	9	8	na	na	na	6.5	na	na
	Dichloromethane	1	7	7	7.5	na	na	na	na	na	na
		1.5	7.5	7.5	8.5	na	na	na	6.5	na	na
	Hexane	1	na	6.5	na	na	na	na	na	na	na
		1.5	na	7	na	na	na	na	6.5	na	na
VI	Tobramycin	10	24	16	7	19	10	25	13	10	NT[b]
	Nystatin	30	NT	NT	NT	NT	NT	NT	NT	NT	18

[a]No activity; [b]not tested

TABLE II. Content (GC/MS analysis) of essential oil components (%) as parts of the total volatile compounds; I – *D. dichotoma* var. *implexa*, II – *D. dichotoma*, III – *P. fascia*, IV – *S. lomentaria*, V – *C. sinuosa*, VI – t_R / min

Component	Algae					
	I	II	III	IV	V	VI
Hydrocarbons						
n-Tridecane	–	–	4.11	–	–	10.87
n-Eicosane	–	–	12.65	–	–	18.91
Methylcyclohexane	–	–	–	–	8.37	6.36
n-Heptane	–	–	–	–	3.92	6.51
3-Methylheptane	–	–	–	–	0.85	6.70
2,3,4-Trimethylhexane	–	–	–	–	1.62	7.33
2,4-Dimethyl-1-heptene	–	–	–	–	2.69	7.55
2,4,6-Trimethyldecane	–	–	–	–	1.16	11.46
5-Methylundecane,	–	–	–	–	0.80	12.37
n-Nonadecane	–	–	–	–	2.54	26.31
n-Pentadecane	9.13	1.24	–	5.69	–	12.18
Crown ether						
18-crown-6-ether	9.45	0.44	–	41.27	–	23.75
Terpenes						
Thymol	–	–	12.48	–	–	25.12
Carvacrol	–	–	62.47	–	–	25.39
β-Cubebene	4.23	2.95	–	–	–	16.24
β-Eudesmol	–	2.42	–	–	–	19.62
β-Ionone	5.80	1.95	–	15.11	–	20.02

TABLE II. Continued

Component	Algae					
	I	II	III	IV	V	VI
Terpenes						
Dactylol	–	7.90	–	–	–	20.84
Pachydictol A	–	39.54	–	–	–	28.29
Acids						
Palmitic acid	–	–	–	–	1.60	16.07
Phenols						
2,4-Bis(1,1-Dimethylethyl)phenol	–	–	–	–	2.96	20.41
S-Containing compounds						
Dihexylsulfide	–	–	–	–	6.72	19.65
Aldehydes						
Stearaldehyde	–	–	–	–	6.33	24.70
Olealdehyde	–	–	–	–	9.18	29.64
Myristaldehyde	12.28	9.81	–	10.29	–	17.89
Hexadecanal		6.64	–	6.69	–	21.32
(*Z*)-13-Octadecenal	14.56	7.68	–	–	–	22.02
Alcohols						
1-Octen-3-ol	1.99	–	–	–	–	11.19
Others						
2,2,4-Trimethyl-1,3-dioxolane	–	–	–	–	25.43	6.18
Hexaethylene glycol	0.97	0.92	–	8.57	–	20.13
Naphthalene skeleton						
Mixture of 1-isopropyl-4,6-dimethyl-1,2,3,4--tetrahydronaphthalene and 4-isopropyl-1,6--dimethyl-1,2,3,4-tetrahydronaphthalene	–	2.04	–	–	–	25.85
Total	58.41	83.53	91.71	87.89	74.17	–

Antioxidant activity

Antioxidant activities of different extracts from the five brown macroalgae were analyzed by means of different *in vitro* tests, such as the presented antioxidant activity in terms of scavenging of hydrosoluble radicals ($ABTS^+$ decolorization), inhibition of β-carotene bleaching (β-carotene-linoleate model system) and the total phenolic compounds (Table III). The phenolic content of the brown algae extracts varied form 0.4±0.2 mg GAE/g to 189.6 ± 8.6 mg GAE/g. Hexane extracts of *D. dichotoma* var. *implexa* were found to have the highest phenolic contents. In this way, within the brown seaweeds, *Dictyota* sp. has been described as a significant source of terpenoids.[24] Several studies have shown a highly significant correlation between the phenolic content and the antioxidant activity in seaweed extracts. In addition, some studies described the antioxidant activity of some phenolic compounds purified from *Eisenia bicyclis* and *Sargassum kjellmanianum*.[25] Kulevanova *et al.*[26] reported that phenolic compounds have more effective antioxidant properties than α-tocopherol and an activity com-

TABLE III. Antioxidant activity of brown macroalgae extracts; I – *D. dichotoma* var. *implexa*, II – *D. dichotoma*, III – *P. fascia*, IV – *S. lomentaria*, V – *C. sinuosa*, VI – BHT, VII- α-tocopherol, VIII – BHA; 1 – ABTS inhibition, %; 2 – β-carotene inhibition, %; 3 – mg GAE/g

Algae	Concentration mg/ml	Extractant								
		Methanol			Dichloromethane			Hexane		
		1	2	3	1	2	3	1	2	3
I	0.5	19.3±0.7	32.8±1.2	24.5±1.3	21.2±1.3	15.5±4.4	66.3±3.2	8.2±1.7	4.4±1.7	79.3±0.5
	1	33.4±0.3	37.4±1.5	47.9±0.9	37.8±0.5	48.5±2.9	81.7±1.7	16.9±1.3	16.8±7.3	123.9±1.1
	2	49.8±1.9	57.9±1.5	78.5±1.2	59.6±0.5	70.2±1.5	119.8±1.8	38.7±0.1	28.6±1.6	189.6±8.6
II	0.5	19.4±1.7	–	0.4±0.2	25.3±0.9	21.8±4.5	35.4±2.8	25.3±0.6	10.1±1.7	23.9±0.8
	1	29.9±0.2	7.6±1.5	21.3±3.4	42.2±1.5	29.0±1.8	62.1±1.4	39.5±0.7	25.0±0.9	43.4±1.3
	2	44.8±0.8	41.2±6.4	41.6±0.5	67.6±0.7	84.8±2.9	78.4±5.2	63.8±0.3	46.2±1.8	65.1±2.0
III	0.5	26.3±1.2	6.0±2.0	3.5±1.2	38.1±2.0	26.4±3.2	31.1±2.6	10.2±3.3	9.1±5.4	10.8±1.5
	1	45.5±0.4	8.7±2.7	10.5±0.8	58.5±1.0	56.6±2.6	51.8±0.5	19.4±0.6	25.4±3.1	24.0±0.4
	2	66.5±3.2	23.5±1.2	26.6±0.8	71.9±0.9	56.7±7.5	83.4±0.5	31.3±0.9	43.5±4.2	40.0±1.5
IV	0.5	5.6±1.4	–	–	51.9±3.1	22.9±2.1	47.7±2.0	32.2±2.5	20.0±7.5	29.8±5.1
	1	7.5±0.5	–	–	73.4±1.8	34.3±2.1	69.8±0.9	53.6±1.7	38.3±6.2	33.4±5.2
	2	11.4±0.7	–	3.4±0.5	79.4±0.8	38.5±7.1	107.5±3.9	69.8±3.1	59.8±6.9	61.0±1.0
V	0.5	6.2±0.9	–	–	36.8±2.3	8.8±1.5	28.1±1.4	19.5±4.3	–	13.6±1.8
	1	9.2±0.1	–	–	55.4±1.5	20.6±6.0	42.4±0.9	35.7±1.5	0.6±4.2	23.4±2.2
	2	14.0±0.3	2.6±4.3	1.1±0.4	62.1±1.1	40.3±6.5	76.4±0.8	49.9±4.2	7.3±3.8	39.0±1.0
VI	0.1	94.3±3.1	97.1±1.6	–	94.4±3.0	97.1±1.6	–	94.4±3.0	97.1±1.6	–
VII	0.1	84.7±4.1	94.4±3.6	–	85.2±3.9	94.4±3.6	–	85.0±4.0	94.4±3.6	–
VIII	0.1	97.9±0.4	93.9±1.3	–	98.0±0.4	93.9±1.3	–	98.0±0.4	93.9±1.3	–

parable to that of synthetic antioxidants, BHA and BHT. There is a decrease in the absorbance of β-carotene and linoleic acid undergoes oxidation in the absence of an antioxidant.[27] Another colorimetric antioxidant activity screening method, the ABTS radical cation decolorization assay, showed quite similar results compared to those obtained in the β-carotene bleaching assay (Table III).

CONCLUSIONS

Marine organisms have several active chemicals such as antioxidant and antimicrobial compounds. In this research, the antioxidant and antimicrobial activity of brown algae from the Aegean Sea were investigated. Marine organisms are currently undergoing detailed investigations with the objective of isolating biologically active molecules along with the search for new compounds. Moreover, it was indicated that the Aegean Sea is a potential source of a variety of biologically active marine organisms and it is hope that the present results will provide a starting point for investigations aimed at exploiting new natural antioxidant substances present in the extracts of algae collected from the Izmir Bay.

Acknowledgements. The authors would like to thank Bulent Olmez for his help in performing the GC/MS analysis.

И З В О Д

АНТИМИКРОБНА И АНТИОКСИДАТИВНА АКТИВНОСТ МРКИХ АЛГИ ИЗ ЕГЕЈСКОГ МОРА

ZELIHA DEMIREL[1], FERDA F. YILMAZ-KOZ[2], ULKU N. KARABAY-YAVASOGLU[1], GUVEN OZDEMIR[1] и ATAKAN SUKATAR[1]

[1]*Ege University, Faculty of Science, Department of Biology, Izmir, и* [2]*Ege University, Faculty of Pharmacy, Department of Pharmaceutical Microbiology, Izmir, Turkey*

Циљ описане студије је био да процени антиоксидативну и антимикробну активност метанолног, дихлорметанског и хексанског екстракта, као и есенцијалног уља мрких алги (Phaeophyta) *Colpomenia sinuosa*, *Dictyota dichotoma*, *Dictyota dichotoma* var. *implexa*, *Petalonia fascia* и *Scytosiphon lomentaria*. Етарско уље макроалги је добијено дестилацијом воденом паром и анализирано је методама GC и GC/MS. Антиоксидативна активност екстраката алги је одређена применом методе инхибиције губитка боје β-каротена и $ABTS^+$ методом. Антиоксидативни ефекти екстраката су упоређивани са ефектима комерцијалних антиоксиданаса, као што су бутил-хидрокситолуен, бутил-хидроксианизол и α-токоферол. Хексански екстракт *D. dichotoma* var. *implexa* је садржао више фенола него други екстракти. Дихлорметански екстракт *S. lomentaria* је био потентнији у обезбојавању $ABTS^+$ од осталих екстраката. Уопштено, дихлорметански екстракти су имали већу активност од метанолних и хексанских. Антимикробна активност екстраката је одређивана спрам Грам (+) и Грам (-) бактерија, укључујући два специфична соја: метицилин-оксацилин резистентни *Staphylococcus aureus* ATCC 43300 и *Escherichia coli* O157:H7 RSSK 232, као и спрам квасца, методом дифузије на диску. Према нашим резултатима, дихлорметански екстракти су испољили већу антимикробну активност од метанолних и хексанских екстраката, при концентрацији од 1,5 и 1,0 mg по диску.

(Примљено 9. децембра 2008, ревидирано 26. јануара 2009)

REFERENCES

1. R. Ely, T. Supriya, C. G. Naik, *J. Exp. Mar. Biol. Ecol.* **309** (2004) 121
2. N. Salvador, A. G. Garreta, L. Lavelli, M. Ribera, *Sci. Mar.* **71** (2007) 101
3. Y. V. Yuan, D. E. Bone, M. F. Carrington, *Food Chem.* **91** (2005) 485
4. T. Kuda, T. Kunii, H. Goto, T. Suzuki, T. Yano, *Food Chem.* **103** (2007) 900
5. T. Shibata, Y. Hama, T. Miyasaki, M. Ito, T. Nakamura, *J Appl. Phycol.* **18** (2006) 787
6. H. Yamada, N. Itoh, S. Murakami, Y. Izumi, *Agric. Biol. Chem.* **49** (1985) 2961
7. G. D. Kanias, H. Scaltsa, E. Tsitsa, A. Loukis, J. Bitis, *Fresenius J. Anal. Chem.* **344** (1992) 334
8. H. I. Heiba, H. S. Al-Easa, A.-F. M. Rizk, *Plant Foods Hum. Nutr.* **51** (1997) 27
9. V. Amico, G. Oriente, M. Piattelli, C. Tringali, E. Fattorusso, S. Mango, L. Mayol, *Tetrahedron* **36** (1980) 1409
10. K. R. Sridhar, N. Vidyavathi, *Acta Hydrochim. Hydrobiol.* **19** (2006) 455
11. J. Ara, V. Sultana, R. Qasim, V. U. Ahmad, *Phytother. Res.* **16** (2002) 479
12. V. Vlachos, A. T. Critchley, A. von Holy, *Microbios* **88** (1996) 115
13. *European Pharmacopoeia*, Maisonneuve S.A., Sainte-Ruffine, France, 3 (1975) 68
14. R. P. Adams, *Identification of Essential Oil Components by Gas Chromatography/Mass Spectroscopy*, Allured Publishing Corporation, Carol Streem, IL, 1995, p. 469
15. L. J. Bradshaw, *Laboratory Microbiology*, Saunders College Publishing, New York, 1992, p. 435
16. Y. Sun, S. Hayakawa, M. Ogawa, K. Izumori, *Food Control* **18** (2007) 220
17. A. Ismail, Z. M. Marjan, C. W. Foong, *Food Chem.* **87** (2004) 581
18. T. Kuda, M. Tsunekawa, T. Hishi, Y. Araki, *Food Chem.* **89** (2005) 617
19. I. Tuney, B. H. Cadirci, D. Unal, A. Sukatar, *Fresenius Environ. Bull.* **16** (2007) 428
20. G. Ozdemir, Z. Horzum, A. Sukatar, N. U. Karabay-Yavasoglu, *Pharm. Biol.* **44** (2006) 183
21. E. Taskin, M. Ozturk, E. Taskin, O. Kurt, *Afr. J. Biotechnol.* **6** (2007) 2746
22. W. A. Stirk, D. L. Reinecke, J. V. Staden, *J. Appl. Phycol.* **19** (2007) 271
23. Z. Kamenarska, S. Dimitrova-Konaklieva, K. Stefanova, H. Najdenskic, I. Tzvetkovac, S. Popova, *Bot. Mar.* **45** (2002) 502
24. Y. Freile-Pelegrin, J. L. Morales, *Bot. Mar.* **47** (2004) 140
25. M. Zubia, D. Robledo, Y. Freile-Pelegrin, *J. Appl. Phycol.* **19** (2007) 449
26. S. Kulevanova, T. K. Panovska, *Bull. Chem. Technol. Macedonia* **20** (2001) 61
27. H. Huang, B. Wang, *J. Agric. Food Chem.* **52** (2004) 4993.

Journal of the Serbian Chemical Society
JSCS@tmf.bg.ac.rs • www.shd.org.rs/JSCS

J. Serb. Chem. Soc. 74 (6) 629–640 (2009)
JSCS–3861

UDC 546.732+547–304.4+547.466
Original scientific paper

A study of novel cobalt(II) octaazamacrocyclic complexes with aminocarboxylates or their derivatives

GORDANA VUČKOVIĆ[1*#], SLAĐANA B. TANASKOVIĆ[2#], MIRJANA ANTONIJEVIĆ-NIKOLIĆ[3], VUKOSAVA ŽIVKOVIĆ-RADOVANOVIĆ[1] and GORDANA GOJGIĆ-CVIJOVIĆ[4]

[1]Faculty of Chemistry, University of Belgrade, P.O. Box 158, 11001 Belgrade, [2]Faculty of Pharmacy, Vojvode Stepe 450, 11000 Belgrade, [3]Higher Technological School of Professional Studies, 15000 Šabac and [4]Institute of Chemistry, Technology and Metallurgy, Department of Chemistry, Njegoševa 12, P. O. Box 473, Belgrade, Serbia

(Received 26 December 2008, revised 27 February 2009)

Abstract: Four new air-stable mixed-ligand Co(II) complexes having the general formula $[Co_2(Y)tpmc]Z_3 \cdot q(H_2O/CH_3CN)$ (HY = *N*-methylglycine/*N*,*N*-dimethylglycine, Z = BF_4^-, qH_2O = 4 or 3; HY = *S*-norvaline/*S*-valine Z = ClO_4^-, qCH_3CN = 0.5; qH_2O = 0.5; tpmc = *N*,*N*',*N*'',*N*'''-tetrakis(2-pyridylmethyl)--1,4,8,11-tetraazacyclotetradecane) were prepared. The composition, some physical and chemical properties and their tentative geometries were evaluated based on elemental analysis (C, H, N), conductometric and magnetic measurements, spectroscopic data (UV/Vis, IR) and cyclic voltammetry. The data were compared with earlier described analogous complexes containing the macrocyclic ligand and aliphatic aminocarboxylates. It is assumed that all complexes are binuclear with an *exo* coordination mode of the octaazamacrocyclic pendant ligand in the boat conformation. In addition, two $–N–(CH_2)_2–N–$ portions of the cyclam ring within the tpmc ligand and Co(II) ions in the high-spin state are most probably bridged *via* oxygen atoms from the anion of the aminocarboxylate/derivatives, whereas nitrogen atoms rest uncoordinated. In all cases, a combined chelate-bridged coordination is proposed as the most probable. The complexes were electrochemically stable in the potential range –1.0 to 1.0 V. They were also preliminary assayed toward some microorganisms together with the ligands, starting simple salts and solvents as test substances. In some cases, certain antimicrobial activity of the complexes was detected.

Keywords: cobalt(II) complexes; pendant octaazamacrocycle; aminocarboxylates and derivatives.

* Corresponding author. E-mail: gordanav@chem.bg.ac.rs
# Serbian Chemical Society member.
doi: 10.2298/JSC0906629V

INTRODUCTION

The field of investigation concerning azamacrocyclic and/or aminocarboxylic transition metal complexes is widely explored[1–5] with regard to their properties: some of them are models for the active centres of metalloenzymes, are potentially bioactive and could be used as drugs, catalysts or represent new materials with specific electrical and magnetic properties.[6,7] In most hitherto described complexes, aminocarboxylato ligands are bonded in one of many modes *via N*: as *N*-monodentate; *N,O*-bonded as chelate in mononuclear complexes or as a bridging ligand between two metallic centres (Scheme 1a); *N,O,O'*-mode (Scheme 1b). In some binuclear complexes, one or both oxygens are included in the coordination, with the $-NH_2$ group resting uncoordinated: unsymmetrically (Scheme 1c), symmetrically (Scheme 1d) or in a combined chelate-bridged manner (Schemes 1e and 1f).[1,4] Depending on the reaction conditions, the nature of the central metal ion, pH, the presence of other ligands, steric hindrance *etc.*, one of the mentioned coordination modes is favoured. In addition, for such complexes some biological activity is expected or found. In previous papers, the synthesis and study of a series of cationic binuclear high-spin Co(II) complexes containing besides a pendant octaazamacrocycle *N,N',N'',N'''*-tetrakis(2-pyridylmethyl)-1,4,8,11-tetraazacyclotetradecane (tpmc), a coordinated aminocarboxylate with an aliphatic side chain, were described.[8,9] The proposed general formula was $[Co_2(A)tpmc](ClO_4)_3$, where HA = glycine/*S*-alanine/*S*-α-aminobutyric/α-aminoisobutyric acid or β-aminobutyric/isobutyric acid. Different amounts of crystal solvents (H_2O/CH_3CN) were present in some of them. μ-*O,O'*-Bonding of the aminocarboxylato ligands was proposed, while tpmc adopted a boat conformation and the *exo* coordination mode (Schemes 1d and 2, where A is the corresponding anion of the mentioned aminocarboxylates).

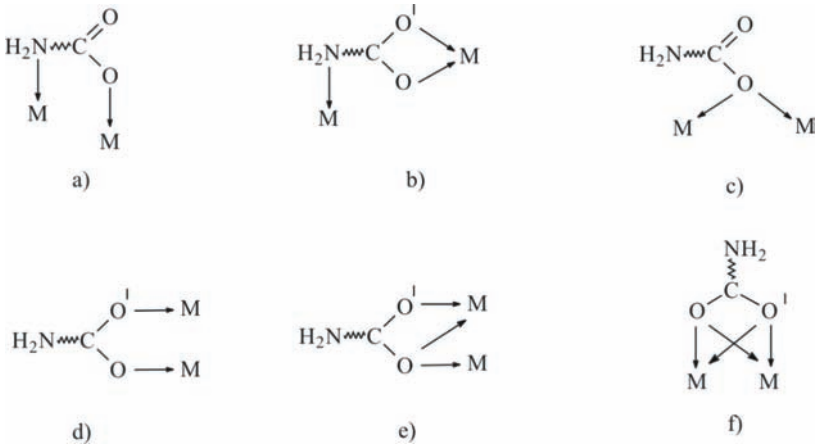

Scheme 1. Selected possible coordination modes of aminocarboxylates in binuclear complexes.

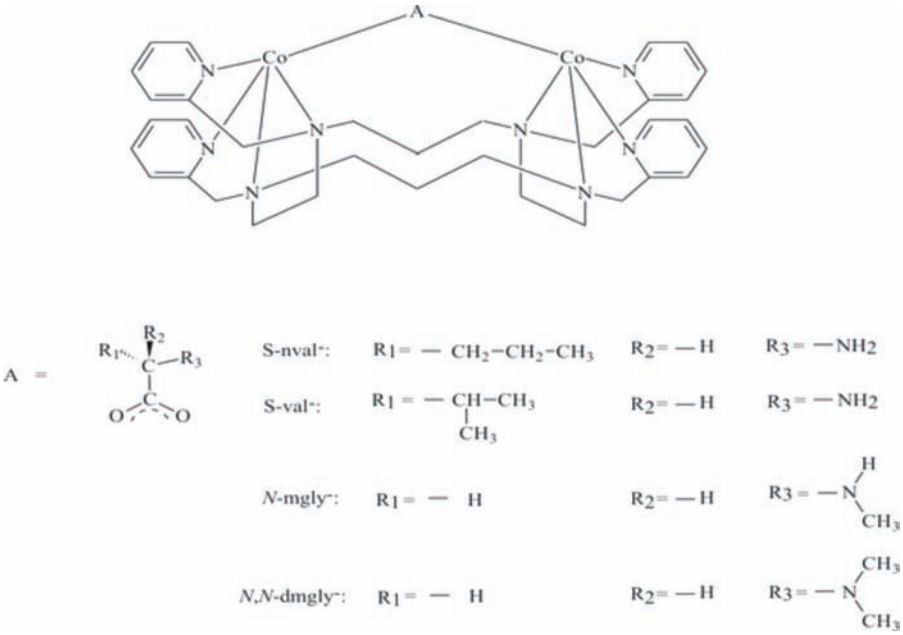

Scheme 2. Boat conformation in the complex cation of $[Co_2(A)tpmc](ClO_4)_3$; A = bridged monoanion of aminocarboxylates/derivatives (*S*-norvaline/*S*-valine/ /*N*-methylglycine/*N*,*N*-dimethylglycine).

The objective of this study was the preparation and study of Co(II)-tpmc complexes with *N*-derivatives of glycine (*N*-methyl/*N*,*N*-dimethylglycine), and amino acids of longer aliphatic side chain (*S*-norvaline/*S*-valine). In addition, an attempt was made to reduce $[Co_2(OH)tpmc](ClO_4)_3$ complex formation,[10] which is always present as an impurity which drastically decreases the yield of the target mixed-ligand complexes. Some of their physical and chemical properties were investigated. Finally, the results were compared mutually and with already published data with the aim of proposing the most probable mode of ligand(s) coordination.

EXPERIMENTAL

Preparation and optimization of the reaction conditions

CAUTION! Perchlorate metal salts with organic ligands are potentially explosive and should be handled with extreme caution although in this work such properties were not observed! Always prepare a small amount of the complex and do not heat more than a few crystals in the solid state! Cobalt tetrafluoroborate hexahydrate is a corrosive substance not yet fully tested!

The ligand tpmc[11] and $Co(ClO_4)_2 \cdot 6H_2O$[12] were prepared and purified as described in the literature. The other chemicals as *p.a.* commercial products were provided by Merck, Germany; *S*-valine, cyclam and 2-picolyl chloride hydrochloride by Aldrich, USA, *S*-norvaline by Fluka, Switzerland; $Co(BF_4)_2 \cdot H_2O$ by Acros Organics, USA.

[Co_2(Y)tpmc](BF_4)$_3$·qH_2O (HY = N-*methylglycine*, N,N-*dimethylglycine, abbreviated below as* N-*mgly*/N,N-*dmgly;* q = *4* (***A***) *or 3* (***B***))

General procedure. $Co(BF_4)_2·6H_2O$ (0.170 g, 0.500 mmol) and *N*-methyglycine/*N,N*-dimethylglycine (0.0334g/0.0387g, 0.375 mmol) (previously neutralized to pH 6.0 with NaOH, c = 0.10 mol/dm^3, checked with indicator strips) were dissolved in a minimum amount of CH_3OH and refluxed on a water bath (80 °C) for 30 min with stirring. After that, a suspension of tpmc (0.141 g, 0.250 mmol) in CH_3OH was added. The reaction mixture was continuously stirred and heated for the following 2 h, concentrated to 1/4 of its initial volume and left in a refrigerator overnight. The purple microcrystalline product was separated by suction, dried at room temperature, powdered, washed properly with small portions of cold water, and the procedure was repeated until a pure product was obtained (checked using a microscope).

[Co_2(N-*mgly)tpmc](BF_4)$_3$·4H_2O (**A**)*. Yield: 78 % (0.215 g). Anal. Calcd. for $C_{37}H_{59}O_6N_9B_3Co_2F_{12}$ (FW = 1103): C, 40.28; H, 5.30; N, 11.42. Found: C, 39.94; H, 5.33; N, 11.41.

[Co_2(N,N-*dmgly)tpmc](BF_4)$_3$·3H_2O (**B**)*. Yield: 75 % (0.206 g). Anal. Calcd. for $C_{38}H_{59}O_5N_9B_3Co_2F_{12}$ (FW = 1099): C, 41.52; H, 5.31; N, 11.46. Found: C, 41.30; H, 5.25; N, 11.50.

[Co_2(S-*nval)tpmc](ClO_4)$_3$·0.5CH_3CN (*S-*nvalH* = S-*norvaline) (**C**)*. To a suspension of tpmc (0.141 g; 0.250 mmol) in 5 cm^3 of CH_3CN, a solution of $Co(ClO_4)_2·6H_2O$ (0.176 g; 0.500 mmol) in 4.0 cm^3 of deionised H_2O was added. The mixture was stirred for 10 min, when a saturated aqueous solution of *S*-norvaline (0.0440 g; 0.375 mmol) (previously neutralized with 0.10 mol/dm^3 aqueous NaOH to pH 6.2, checked with indicator strips) was slowly added dropwise. The reaction mixture of intensive purple colour was refluxed on a water bath (80 °C) for 2 h with continuous stirring. The purple precipitate separated by suction was slightly contaminated with violet $[Co_2(OH)tpmc](ClO_4)_3$.[10] The product was recrystallized several times from a mixture of CH_3CN:H_2O (5:1, v/v), washed with cold CH_3CN and deionised water to give pure purple microcrystals, which were dried and kept in a desiccator over anhydrous $CaCl_2$. Yield: 42 % (0.117 g); Anal. Calcd. for $C_{40}H_{55.5}O_{14}N_{9.5}Cl_3Co_2$ (FW = 1117.70): C, 42.98; H, 5.00; N, 11.90. Found: C, 43.14; H, 5.29; N, 11.54.

[Co_2(S-*val)tpmc](ClO_4)$_3$·0.5H_2O (*S-valH* = S-*valine) (**D**)*. The procedure and colour of complex **D** was like for complex **C** with *S*-norvaline, except for using *S*-valine (0.0440 g, 0.375 mmol) and neutralization to pH 6.0. Yield: 46% (0.129 g); Anal. Calcd. for $C_{39}H_{57}O_{15.5}N_9Cl_3Co_2$ (FW = 1124.20): C, 41.67; H, 5.11; N, 11.21. Found: C, 41.68; H, 5.27; N, 11.68.

The complexes **A**–**D** are well soluble in CH_3CN, sparingly in DMSO and DMF, and insoluble in CH_3OH, C_2H_5OH and cold water. The complexes did not melt or decompose up to 250 °C (checked with a hot plate equipped with a microscope).

Analytical methods and applied instruments

Elemental analyses were performed by standard methods in the Centre for Instrumental Analyses, ICTM in Belgrade.

Electronic absorption spectra of complex in CH_3CN solution (c = 1.0×10^{-3} mol/dm^3) were recorded on a GBC UV/Vis spectrophotometer Cintra 20. IR spectra were recorded on a NICOLET 6700 FTIR (ATR technique) in the range 400–4000 cm^{-1}.

Molar conductivities were measured on an HI 8820N conductometer, Hanna Instruments at 20±2 °C in CH_3CN (c = 1.0×10^{-3} mol/dm^3).

Optical rotation measurements for the complexes **C** and **D** in CH_3CN were measured at 589 nm and ambient temperature (20±2 °C) using a tube of 1 dm on a Polarimeter AUTOPOL IV automatic, Rudolf Research Analytical (c = 9.8×10^{-3} mol/dm^3 for complex **C** and 1.2×10^{-3} mol/dm^3 for complex **D**).

Magnetic susceptibilities were measured on MSB-MKI magnetic balance, Sherwood Scientific Ltd., England, at room temperature (23±2 °C). For all complexes, the data were corrected for diamagnetism using Pascal's constants.[13]

Cyclic voltammetry (CV) measurements for complexes **A**–**D** were performed using METHROME 797 VC Compurtrace electronic equipment in a standard three-electrode cell with a Pt disc as the working, standard Ag/AgCl as the reference electrode and Pt as the auxiliary electrode. The measurements were first performed in 10 cm^3 of CH_3CN as the electrolyte, and then in the same volume of complex solution (c = 1.0×10^{-4} mol/dm^3). CV was performed at sweep rates of 50, 100 and 200 mV/s within the potential range from –1.0 to 1.0 V *vs.* Ag/AgCl. To remove O_2 from the system, N_2 was continuously bubbled before each experiment. All measurements were done at room temperature (20±2 °C).

Antimicrobial test

For the determination of antimicrobial activity of the complexes, cultures of the following six microorganisms were used. Gram(+) bacteria: *Micrococcus lysodeikticus* ATCC 4698, *Staphylococcus aureus* ATCC 25923, *Bacillus subtilis* ATCC 6633 and *Bacillus cereus*; Gram(–) bacterium: *Escherichia coli* ATCC 25922; yeast: *Candida albicans* ATCC 24433 and mould: *Aspergillus niger* ATCC 12066. The bacteria were cultivated on Mueller–Hinton agar and the fungi on Sabouraud dextrose agar. Inoculation was performed by mixing 0.10 mL of the microorganism suspension in physiological solution (0.80 g/L NaCl) with 20 mL of cold molten medium.[14] Holes (Ø 0.8 cm) were formed in the inoculated agar plates and 100 μL of the tested complexes (1.0 mg/mL in DMSO) were separately introduced into the holes. Apart from the complexes **A**–**D**, tpmc, amino acids/derivatives, $Co(ClO_4)_2\cdot6H_2O$ and $Co(BF_4)_2\cdot6H_2O$ were tested. The incubation temperature was 37 °C for the bacteria and 28 °C for the fungi. The zones of inhibition were measured after 24 h for the bacteria and 48 h for the fungi if microbiological activity was detected.

RESULTS AND DISCUSSION

The reaction conditions for the preparation of the mixed-ligand complexes were carefully adjusted. At ambient temperature, usually used for Co(II) complexes, the yield was very low (less than 1 %) even if the reaction time was several days. Nevertheless, pure products were thus isolated. At elevated temperatures, the yield was much better but side-products in saturated solutions and decomposition in dilute ones are possible. In both cases, the very stable violet side--product $[Co_2(OH)tpmc](ClO_4)_3$ was formed. In this work, its formation was maximally avoided by careful control of the pH to which the aminocarboxylates were previously neutralized, taking into account that tpmc itself is a weak base. In addition, CH_3CN was replaced as the solvent by CH_3OH in the procedure for *N*-methyl derivatives of glycine.

All attempts to prepare Co(II)tpmc complexes of *N*-methyl/*N*,*N*-dimethylglycinate ligands as ClO_4^- salts from various solvents failed, due to the formation of an oily product which was difficult to purify by ordinary methods (fraction crystallization, chromatographically, by adding infusorial earth, by changing solvents, *etc.*). Instead of ClO_4^-, BF_4^- was used as the counter ion and CH_3OH as the solvent. Under these conditions, $Co(BF_4)_2\cdot6H_2O$, tpmc and neutralized *N*--methyl/*N*,*N*-dimethylglycine in a molar ratio 2:1:1.5 gave purple microcrystal-

line products by direct syntheses. It was very important to neutralize the *N*-alkyl derivatives of the aminocarboxylates to pH equal to their pK_a±1, taking into account that tpmc itself is a weak base and the formation of the unavoidable hydroxo complex could be favoured when the solutions were slightly alkaline. The presence of H_2O during synthesis should also be minimized to suppress hydrolysis of BF_4^-. On the other hand, the preparation of analogous complex with glycine as BF_4^- salt also failed, for the above given reasons.

The complexes with *S*-norvaline/*S*-valine were isolated using a similar procedure as for the already published analogous complexes, but pH of the neutralized amino acids was lower (about pK_a±1).

All the complexes were unexpectedly air-stable. However, stable single crystal(s) suitable for X-ray analysis could not be grown. Even if regular size and shiny crystals were isolated, they decompose on prolonged standing in an open atmosphere by losing crystal solvent(s). It can be seen from the Experimental and Table I that elemental analyses and conductivity measurements suggested binuclear and cationic nature for all the newly synthesized complexes, being consistent with the same general formula as for the previously prepared analogous complexes. The values of the molar electrical conductivities in their 1.0×10^{-3} mol/dm^3 CH_3CN solutions at room temperature laid in the range 340–366 S cm^2 mol^{-1} (Table I), corresponding to a 1:3 electrolyte type (the literature range is 340–420 S cm^2 mol^{-1}).[15]

TABLE I. Vis spectral, magnetic and molar conductivity data in a CH_3CN complex solution (c = 1.0×10^{-3} mol dm^{-3}) at room temperature

Complex[a]	λ / nm (ε / dm^3 mol^{-1} cm^{-1})			Λ_M S cm^2 mol^{-1}	μ_{eff}(per Co) μ_B
$[Co_2(OH)tpmc](ClO_4)_3$[b]	489 (60)	–	574 (80)	–	4.46
$[Co_2(gly)tpmc](ClO_4)_3$[c]	458 (80)	511 (96)	548 (79) *sh*[d]	–	4.70
$[Co_2(N\text{-mgly})tpmc](BF_4)_3\cdot4H_2O$	455 (30)	508 (53)	544 (35) *sh*	360	4.75
$[Co_2(N,N\text{-dmgly})tpmc](BF_4)_3\cdot3H_2O$	487 (38)	510 (42)	546 (28) *sh*	366	4.70
$[Co_2(S\text{-nval})tpmc](ClO_4)_3\cdot0.5\ CH_3CN$	458 (42)	514 (57)	555 (44) *sh*	355	4.65
$[Co_2(S\text{-val})tpmc](ClO_4)_3\cdot0.5\ H_2O$	456 (50)	512 (66)	552 (47) *sh*	340	4.63

[a]glyH = glycine, *N*-mglyH = *N*-methylglycine, *N*,*N*-dmglyH = *N*,*N*-dimethylglycine, *S*-nvalH = *S*-norvaline, *S*-valH = *S*-valine; [b]data taken from ref. 10; [c]data taken from ref. 9; [d]shoulder

Cobalt(II) complexes are coloured due to d-d transitions. All the complexes described in this paper had an intensive purple colour. The UV/Vis data and μ_{eff}/Co(II) at room temperature (Table I) for all complexes are in agreement with the high-spin state of Co(II).[16,13b] The complexes containing *N*-methyl substituted derivatives of glycine, **A** and **B** (Table I) have two absorption maxima and one shoulder in the range 487–546 nm and molar extinction coefficients (ε) values of 28–53 dm^3 cm^{-1} mol^{-1}. They were comparable with the corresponding glycinato complexes in spite of the fact that the counter anion was not the same

(BF_4^- instead of ClO_4^-). The intensities of the bands were lower than those found for the corresponding analogous glycinato complexes. It is known that pentacoordinated Co(II) complexes, owing to their lower symmetry, have higher ε values than hexacoordinated ones in the case of the same chromophore.[16] The more pronounced bathochromic shift of the first absorption maxima by about 30 nm in the spectrum of the *N*,*N*-dimethylglycinato analogue could be ascribed to a possible exchange of this ligand with OH^- (Table I). However, the absence of an absorption maximum at 574 nm and the appearance of a maximum at 510 nm, as well as the lower intensities, might suggest a higher degree of symmetry. Thus, it is supposed that in complexes **A** and **B** containing *N*-methylglycinato/*N*,*N*-dimethylglycinato anions, the Co(II) is hexacoordinated (Scheme 1e or 1f).

The Vis spectra of the complexes **C** and **D** with *S*-norvalinato/*S*-valinato ligands are of similar shape and corresponding band positions. They are also similar to those containing amino acids of the preceding members of the homologous series (glycine/*S*-alanine/*S*-α-aminobutyric/α-aminoisobutyric acid), although of lower intensities, but this trend on enlarging the side hydrocarbon chain had already been observed. In addition, for complex **D**, with a branched aminocarboxylato side chain, the values of ε were higher than those for complex **C**, having the isomeric normal side chain ligand. The same was observed earlier for complexes with isomeric *S*-α-aminobutyrato/α-aminoisobutyrato ligands.[8,9]

In UV part of the electronic spectra, very intense multiple bands ascribed to CT appeared in the 230–300 nm range (ε was in the range 5000–5500 $dm^3\ mol^{-1}\ cm^{-1}$ for the *N*-methylglycinato/*N*,*N*-dimethylglycinato complexes and 3750––3900 $dm^3\ mol^{-1}\ cm^{-1}$ for the *S*-norvalinato/*S*-valinato complexes).

The origin of the optical activity of the complexes $[Co_2(A)tpmc](ClO_4)_3$ where HA = *S*-alanine/*S*-α-aminobutyric acid was earlier ascribed to the "vicinal effect", *i.e.*, to the optical activity of A^- alone.[9] Namely, the values of $[M]_{589}^{20}$ for the *S*-alaninato/*S*-α-aminobutyrato complex were +167.7 and +125.5°. The calculated $[M]_{589}^{20}$ values for complexes **C** and **D** (containing *S*-norvalinato/*S*-valinato ligand) were +279.4 and +459.7°, respectively. This strongly suggests an enhanced conformational and configurational contribution to the overall asymmetry of these complexes. Complex **D**, containing a branched side chain and thus larger steric hindrance, has a substantially higher molecular rotation value than its analogue with the isomeric normal side chain ligand (complex **C**).

In the IR spectra of the complexes, there are some characteristic bands:[17] a broad multiple band around 3600 (for complex **A**) or 3580 cm^{-1}(for complexes **B** and **D**), arising from ν(O–H) of crystal water; at 3244 cm^{-1} of ν(NH) for the secondary amino group excluded from coordination (complex **A**), a doublet at 3310 and 3277 cm^{-1} belonging to the primary non-coordinated amino group in the spectra of **C** and **D**; a sharp strong band at 1603–1609 cm^{-1} from the skeletal stretching valence vibration of the tpmc pyridine included in coordination (in the

spectra of all complexes); a very strong broad band at about 1070 cm^{-1} from $\nu(ClO_4^-)$ and a medium sharp band around 631 cm^{-1} from $\delta(ClO_4^-)$ for complexes **C** and **D**, and around 1020–1030 cm^{-1} of $\nu(BF_4^-)$ for complexes **A** and **B**. Sharp weak bands in the spectra of all complexes assigned to ν(Co–N) appeared in the range 475–485 cm^{-1} and ν(Co–O) in the range 412–420 cm^{-1}. Additionally, in the region of 1560–1392 cm^{-1}, asymmetrical (ν_a) and symmetrical (ν_s) valence vibrations of the OCO group of weak to strong intensities were observed (Table II). The observed changes of the $\Delta\nu = \nu_a - \nu_s$ values for the complexes compared with those found for their corresponding sodium salts[18] showed that the aminocaroxylato/derivatives ligand are coordinated using both oxygen atoms. Moreover, the $\Delta\nu$ values in all cases were significantly lower than in the spectra of the respective free ligand. It is obvious that the $\Delta\nu$ values decrease in the following order: *S*-ala^{-9} > gly^{-9} > *α*-aibu^{-8} > *S*-abu^{-9} > *S*-val$^-$/*S*-nval$^-$. Such an order suggests the formation of weaker Co–O bonds in the complexes **C** and **D** containing the longest chains than those predicted for the other aminocarboxylates from the same homologous series[8,9] As for the *N*-methyl derivatives of glycine, the strength of the Co–O bond parallels the decrease in $\Delta\nu$ in the order: gly^{-9} > *N*-mgly > *N*,*N*-dmgly, which could be explained by the steric hindrance produced by the introduction of voluminous $-CH_3$ group(s) on the nitrogen atom instead of the smaller H atom(s). In addition, the formation of stronger H-bonds within complexes **A** and **B** containing BF_4^- than in the glycinato complexes hav-

TABLE II. Selected IR spectral data of OCO^- (asymmetrical, ν_a, symmetrical valence vibrations, ν_s, and $\Delta\nu$ values in cm^{-1}) for uncoordinated alkaline salts and the corresponding aminocarboxylates/derivatives in the complexes

Compound[a]	ν_a	ν_s	$\Delta\nu$
Na-gly	1595 *s*[c]	1399 *s*	196
$[Co_2(gly)tpmc](ClO_4)_3$[b]	1580 *m*	1365 *m*	215
Na-*N*-mgly	1580 *m*	1391 *m*	190
$[Co_2(N\text{-mgly})tpmc](BF_4)_3\cdot H_2O$	1585 *sh*, *m*	1481 *w*, 1446 *m*, 1392 *m*, 1439[e]	146
Na-*N*,*N*-dmgly	1593 *vs*	1375 *vs*	218
$[Co_2(N,N\text{-dmgly})tpmc](BF_4)_3\cdot 3H_2O$	1573 *sh*, *m*	1481 *w*, 1443 *m*, 1405 *m*, 1443[e]	130
Na-*S*-ala	1595 *s*	1406 *s*	189
$[Co_2(S\text{-ala})tpmc](ClO_4)_3\cdot H_2O$[d]	1575 *m*	1350 *w*	225
K-*S*-abu	1587 *s*	1408 *s*	179
$[Co_2(S\text{-abu})tpmc](ClO_4)_3\cdot H_2O$[d]	1575 *m*	1390 *m*	185
K-*α*-aibu	1577 *s*	1416 *vs*	161
$[Co_2(\alpha\text{-aibu})tpmc](ClO_4)_3$[d]	1555 *s*	1361 *w*	194
Na-*S*-nval	1569 *vs*	1410 *s*	159
$[Co_2(S\text{-nval})tpmc](ClO_4)_3\cdot 0.5CH_3CN$	1560 *m*	1483 *w*, 1442 *m*, 1462[e]	99
Na-*S*-val	1549 *vs*	1395*s*	154
$[Co_2(S\text{-val})tpmc](ClO_4)_3\cdot 0.5H_2O$	1560 *m*	1482 *w*, 1467 *w*, 1441 *m*, 1463[e]	97

[a]abbreviations as in Table I; [b]data taken from ref. 9 and [c]from ref. 8; [d]*m* = medium; *s* = strong; *vs* = very strong; *w* = weak; [e]calculated as the average value of two or three bands

ing ClO_4^- are to be expected. Similar shifts of ν(OCO) were already observed for some bulky dicarboxylato ligands in the Co(II)tpmc moiety,[19,20] for which hexacoordination was proposed or confirmed by X-ray analysis. Hence, it is proposed that in the complexes **A**–**D**, the anions of *N*-methyl derivatives/aminocarboxylates are coordinated through OCO in a combined chelate-bridged manner (Scheme 1e or 1f). The participation of the amino nitrogen is excluded in all cases, although it can form H-bonds with the counter ions or crystal solvents molecules. The strength of the Co–O bonds in the above-described complexes is the consequence of various factors, such as: steric repulsions between the alkyl groups from the aminocarboxylates/derivatives and the pyridyl groups from tpmc; changes of the inductive effects of the introduced $–CH_2–$/$–CH_3$ groups and their positions; the size of the alkyl group in relation to the size of the macrocyclic cavity; non-covalent interactions; *etc*. It is difficult to determine the contribution of each of them, as they are all responsible for the overall structure.

The electrochemical behaviour of the complexes **A**–**D** was studied by cyclic voltammetry. The absence of any peaks on all voltammograms under the investigated conditions suggests electrochemical stability of the complexes. This fact gives the possibility of their use as catalysts. A previous electrochemical study of some congeneric complexes with *α*-amino acids showed that complexes with a gly$^-$/*S*-ala$^-$ ligand undergo a two-step reversible electrochemical oxidation and are destroyed at a potential of 0.60 V, which was ascribed to ligand oxidation. The complex containing *α*-aibu$^-$ exhibited another type of electrochemical behaviour. It adsorbed on the electrode surface without charge transfer. A similar stability was observed for Co(II)-tpmc complexes containing some of the dicarboxylates.[20,21]

The results of the antimicrobial tests are presented in Table III. It is obvious that the complexes showed moderate antibacterial and antifungal activity. Furthermore, the complexes **A** and **D** are active against all tested microorganisms, while the solvent and ligands were inactive under the same conditions.

TABLE III. Antimicrobial activity of the prepared complexes

Microorganism	Zone diameter, mm			
	Compound[a]			
	A	**B**	**C**	**D**
Bacillus cereus (Gram(+) bacterium)	22	26	16	18
Micrococcus lysodeikticus ATCC 4698 (Gram(+) bacterium)	25	20	–[b]	20
Bacillus subtilis ATCC 6633 (Gram(+) bacterium)	16	–	–	18
Staphylococcus aureus ATCC 25923 (Gram(+) bacterium)	20	–	–	15
Escherichia coli ATCC 25922 (Gram(–) bacterium)	16	19	16	17
Aspergillus niger ATCC12066 (mold)	20[c]	15[c]	16[c]	18[c]
Candida albicans ATCC 24433 (fungus)	15	17	16	16

[a]Abbreviations as in Table I; [b]activity was not found; [c]fungistatic activity

CONCLUSIONS

Four novel Co(II) complexes with the pendant octaazamacrocyclic ligand *N*,*N*',*N*'',*N*'''-tetrakis(2-pyridylmethyl)-1,4,8,11-tetraazacyclotetradecane (tpmc) and *N*-methylglycine/*N*,*N*-dimethylglycine/*S*-norvaline/*S*-valine anions were prepared in good yields. They were characterized by some physical properties and by valuable methods and techniques (elemental analyses, molar electrical conductivity, spectroscopic data, magnetic measurements, cyclic voltammetry) and compared with already described analogous Co(II) complexes.

All complexes are binuclear with an *exo* coordination mode of tpmc in the boat conformation. The Co(II) ions are coordinated to the four nitrogen atoms of tpmc and bridged *via* oxygen atoms from the aminocarboxylate/derivatives, while the nitrogen atoms are uncoordinated. In all complexes, a combined chelate--bridged mode with hexacoordinated cobalt atom is suggested as the most probable. The complexes are electrochemically stable and showed some antimicrobial activity.

Acknowledgements. We gratefully acknowledge the financial support of the Ministry of Science and Technological Development of the Republic of Serbia (Project No. 142028) and Dr Dragan Manojlović of the Faculty of Chemistry, Belgrade, Serbia, for the CV measurements.

ИЗВОД

ПРОУЧАВАЊЕ НОВИХ КОМПЛЕКСА КОБАЛТА(II) СА ОКТААЗАМАКРОЦИКЛОМ И АМИНОКАРБОКСИЛАТИМА ИЛИ ЊИХОВИМ ДЕРИВАТИМА

ГОРДАНА ВУЧКОВИЋ[1], СЛАЂАНА Б. ТАНАСКОВИЋ[2], МИРЈАНА АНТОНИЈЕВИЋ-НИКОЛИЋ[3], ВУКОСАВА ЖИВКОВИЋ-РАДОВАНОВИЋ[1] и ГОРДАНА ГОЈГИЋ-ЦВИЈОВИЋ[4]

[1]Хемијски факултет, Универзитет у Београду, п.пр. 158, 11001 Београд, [2]Фармацеутски факултет, Универзитет у Београду, Војводе Степе 450, 11000 Београд, [3]Виша техничка школа струковних студија, 15000 Шабац и [4]Институт за хемију, технологију и металургију, Центар за хемију, Његошева 12, 11000 Београд

Добијена су четири нова мешовито-лигандна комплекса Co(II), стабилна на ваздуху, опште формуле $[Co_2(Y)tpmc]Z_3 \cdot q(H_2O/CH_3CN)$ (HY = *N*-метилглицин/*N*,*N*-диметилглицин, $Z = BF_4^-$, qH_2O = 4 или 3); HY = *S*-норвалин/*S*-валин, $Z = ClO_4^-$, qCH_3CN = 0,5; qH_2O = 0,5; tpmc = *N*,*N*',*N*'',*N*'''-тетракис(2-пиридилметил)-1,4,8,11-тетраазациклотетрадекан). Састав, нека физичка и хемијска својства и њихове приближне геометрије су изведене на основу елементалне анализе (C, H, N), кондуктометријских и магнетних мерења, спектроскопских података (UV/Vis, IR) односно цикличне волтаметрије. Подаци су упоређени са раније описаним аналогим комплексима који садрже макроциклични лиганд и алифатичне аминокарбоксилате. Претпостављено је да су сви комплекси динуклеарни са егзо координацијом пендантног октаазамакроцикла у конформацији лађе. Поред два $–N–(CH_2)_2–N–$ дела цикламовог прстена унутар tpmc-а, јони високо-спинског Co(II) су највероватније премошћени ангажовањем кисеоникових атома са анјона аминокарбоксилата/деривата, док атоми азота остају некоординовани. За све комплексе предложен је комбиновани хелатно-мостовни начин везивања. Комплекси су били електрохемијски стабилни у опсегу потенцијала –1,0 до 1,0 V. Они су прелиминарно тести-

рани на микроорганизме заједно са лигандима, полазним простим солима и растварачима као тест супстанцама. У неким случајевима је нађена извесна антимикробна активност комплекса.

(Примљено 26. децембра 2008, ревидирано 27. фебруара 2009)

REFERENCES

1. F. A. Cotton, G. Wilkinson, C. A. Murillo, M. Bochmann, *Advanced Inorganic Chemistry*, 6th ed., Wiley, New York, 1999
2. L. F. Lindoy, *The Chemistry of Macrocyclic Ligand Complexes*, Cambridge University Press, Cambridge, 1989
3. a) V. M. Rao, M. P. Latha, T. S. Rao, G. N. Rao, *J. Serb. Chem. Soc.* **73** (2008) 1169; b) H. Hongwei, C. Shuhui, W. Liya, M. Lufang, *J. Coord. Chem.* **61** (2008) 2690
4. M. N. Hughes, *Comprehensive Coordination Chemistry*, Pergamon Press, Oxford, 1987, p. 642
5. C. P. Pradeep, P. S. Zacharias, S. K. Das, *Inorg. Chem. Commun.* **9** (2006) 1071
6. a) Z. H. Chohan, M. Arif, M. A. Akhtar, C. T. Supuran, *Bioinorg. Chem. Appl*. (2006), Article ID 83131; b) G. Vučković, S. B. Tanasković, U. Rychlewska, D. D. Radanović, J. Mroziński, M. Korabik *J. Mol. Struct.* **827** (2007) 80; c) G. Vučković, M. Antonijević-Nikolić, T. Lis, J. Mroziński, M. Korabik, D. D. Radanović, *J. Mol. Struct.* **872** (2008) 135
7. a) W. Sibert, A. H. Cory, J. G. Cory, *J. Chem. Soc. Chem. Commun.* (2002) 154; b) S. J. Paisey, P. J. Sadler, *J. Chem. Soc. Chem. Commun.* (2004) 306; c) X. Liang, J. A. Parkinson, M. Weishaulp, R. O. Gould, S. J. Paisey, H. Park, T. M. Hunter, C. A. Blindauer, S. Parsons, P. J. Sadler, *J. .Am. Chem. Soc*. **124** (2002) 9105
8. G. Vučković, D. Opsenica, S. P. Sovilj, D. Poleti, M. Avramov-Ivić, *J. Coord. Chem.* **42** (1997) 241
9. G. Vučković, D. Opsenica, S. P. Sovilj, D. Poleti, *J. Coord. Chem*. **47** (1999) 331
10. H. Harada, M. Kodera, G. Vučković, N. Matsumoto, S. Kida, *Inorg. Chem*. **30** (1991) 1190
11. a) S. Chandrasekhar, W. L. Waltz, L. Prasad, J. W. Quail, *Can. J. Chem*. **75** (1997) 1363; b) J. Narayanan, M. E. Sosa-Torres, R. A. Toscana, *J. Chem. Crystallogr*. **3** (2001) 129
12. A. Kiss, Z. M. Gerendas, *Phys. Chem. A* **180** (1937) 117
13. E. König, *Magnetic Properties of Coordination and Organometallic Transition Metal Compounds*, Springer-Verlag, Berlin, 1966
14. a) J. F. Acar, F. W. Goldstein, in *Antibiotics in Laboratory Medicine*, 4th ed., V. Lorian, Ed., Williams and Wilkins, Baltimore, MD, 1996, p. 1; b) C. R. Mahon, G. Manuselis, *Textbook of Diagnostic Microbiology*, W. B. Saunders Company, Philadelphia, PA, 1995, p. 67
15. W. J. Geary, *Coord. Chem. Rev*. **7** (1971) 81
16. B. P. Lever, *Inorganic Electronic Spectroscopy*, 2nd ed., Elsevier, Amsterdam, 1984, pp. 481–505, 554–573
17. K. Nakamoto, *Infrared and Raman Spectra of Inorganic and Coordination Compounds*, Part B, 5th ed., Wiley, New York, 1997, pp. 23–26, 59–62, 83, 271–272; b) N. B. Colthup, L. H. Daly, S. E. Wiberley, *Introduction to Infrared and Raman Spectroscopy*, 2nd ed., Academic Press, London, 1975, pp. 284, 408
18. G. B. Deacon, R. J. Philips, *Coord. Chem. Rev*. **33** (1980) 227

19. G. Vučković, S. B. Tanasković, Z. M. Miodragović, V. Stanić, *J. Serb. Chem. Soc.***72** (2007) 1295
20. S. P. Sovilj, G. Vučković, K. B. Babić-Samardžija, N. Matsumoto, V. M. Jovanović, J. Mroziński, *Synth. React. Inorg. Met. Org. Chem.* **29** (1999) 785
21. Z. M. Miodragović, G. Vučković, S. P. Sovilj, D. D. Manojlović, *J. Serb. Chem. Soc.* **63** (1998) 781.

Journal of the Serbian Chemical Society
JSCS@tmf.bg.ac.rs • www.shd.org.rs/JSCS

J. Serb. Chem. Soc. 74 (6) 641–650 (2009)
JSCS–3862

UDC 547.759.32–386+546.732'742'472:
535.33.004.12:537.621
Original scientific paper

Estimation of the dipole moments of the excited state of di(2-methyl-6-chlorophenyl)carbazone and its Co(II), Ni(II) and Zn(II) complexes from the effect of solvent on their ultraviolet absorption spectra

ASHOK F. DODAMANI*, MOHAMMEDSHAFI A. PHANIBAND and SHREEDHAR D. DHUMWAD

Department of Chemistry, Karnatak University's Karnatak Science College, Dharwad-580001, Karnataka, India

(Received 15 October, revised 17 December 2008)

Abstract: Di(2-methyl-6-chlorophenyl)carbazone (2M6CPC) and its Co(II), Ni(II) and Zn(II) complexes were synthesized and characterized by magnetic moment, and infrared and ^{1}H-NMR spectral measurements. The solvent effect in a series of polar and non-polar solvents of varying dielectric constants and refractive indices was estimated by recording the electronic spectra (S1 band) of the above compounds. The data was used to determine the magnitude and direction of the electric dipole moments in the first electronically excited state. The results indicate that the observed band systems in these compounds may be attributed to a $\pi \rightarrow \pi^*$ transition.

Keywords: carbazone; electric dipole moments; dielectric constants; $\pi \rightarrow \pi^*$ transition.

INTRODUCTION

Transition metal complexation has played a vital role in the fields of biochemistry and medicine.[1] After work on the chelation of biologically active ligands,[2] it was thought justifiable to study the dipole moments of some adducts. A survey of the literature revealed that in addition to investigating the problems of electronic structure, bonding stereochemistry and stability constants of metal complexes with diphenyl carbazone (DPC)[3] and its derivatives, an increasing number of studies have been devoted to the dynamic and mechanism of the reaction of metal complexes and their heterocyclic nitrogen base adducts.[4,5] Through spectrophotometry, the synthesis and characterization of Co(II), Ni(II) and Zn(II) complexes with di(2-methyl-6-chlorophenyl)carbazone (2M6CPC) and also the electric dipole moments of these compounds in the first electronically excited

* Corresponding author. E-mail: dodamani_ic@rediffmail.com
doi: 10.2298/JSC0906641D

state are reported here. The dipole moment is an important parameter[6,7] which gives an idea of the electronic structure of the molecule and is of prime importance in the understanding of molecular interactions.[8] The present studies were undertaken keeping these views in mind. From the study of the solvent effect on the ultraviolet absorption spectra of each of the above-cited compounds, it is possible to determine its electric dipole moment in its electronically excited state.[9] This so-determined parameter gives some insight into the electron distribution, reactivity, photochemical, reactions, *etc*., of the solute molecule in its electronically excited state.[10] Apart from obtaining the permanent dipole moment, it is also possible from these studies to determine the shape parameters, yet another important parameter that gives knowledge about the shape of the cavity in which a solute molecule is supposed to lie.[11]

EXPERIMENTAL

Carbon tetrachloride, 2-propanol, dimethylformide, 1-butanol, chloroform, 1,4-dioxane and *n*-propanol used were of Fisher AR grade; the cobalt, nickel and zinc chloride used were also of Fisher AR grade.

Ultraviolet absorptions were recorded on Hitachi 150-20 UV–Vis spectrophotometer. Elemental analyses were realized on a Perkin–Elmer 240.C, H and N analyzer. IR and ^{1}H-NMR Spectra were recorded on Nicolet-170 FT-IR spectrometer and a VXR 300 S Varian spectrometer, respectively. The magnetic moments of the Co(II) and Ni(II) complexes were determined by the Gouy method. The metal estimation was performed by the EDTA titration method. The dielectric measurements were recorded with the aid of a Forbes Tinsley (FT) 6421 LCR Data Bridge at 10 kHz frequencies. The refractive indices of various dilute solutions (Sodium D line) were determined using an Abbe's refractometer.

The dielectric constants of the dilute solutions were measured in a suitably fabricated cell of usually small capacitance, where the accurate determination of small changes in the capacitance would be possible. This small change in capacitance can be measured with the help of Forbes Tinsley (FT) 6421 LCR Data B ridge at a frequency of 10 kHz. The dielectric sample holder consisted of two concentric brass cylinders kept in position with small strips (to achieve electric isolation) and their leads were coated with gold. This assembly was kept in a glass beaker so the dilute solution could be filled into the cell and the capacitance of the empty cell (air) would be of the order of a pF.

Synthesis of the ligand di(2-methyl-6-chlorophenyl)carbazone (2M6CPC)

The ligand was synthesized by the method described earlier.[12,13] Briefly, di(2-methyl-6-chlorophenyl)carbazone (2M6CPC) was prepared by heating a mixture of 2-methyl-6-chlorophenylhydrazine and urea (2:1) at 155–160 °C for about 3 h. The so-obtained crude carbazide was crystallized from ethanol. About 1 g of the carbazide was dissolved in a mixture of 60 mL glacial acetic acid, 20 mL of 1.0 N sulfuric acid and 2–3 drops of 10 % ferric alum, and oxidized by the addition of 20 ml of aqueous 0.060 M potassium persulfate ($K_2S_2O_8$) added drop wise under vigorous stirring over about 30 min. The resulting carbazone was extracted with diethyl ether, washed several times with water, dried and purified by column chromatography using silica gel (60–120 mesh) column. A mixture of methanol and chloroform (1:4) was used as the eluent. The structure of the ligand is as given in Fig. 1.

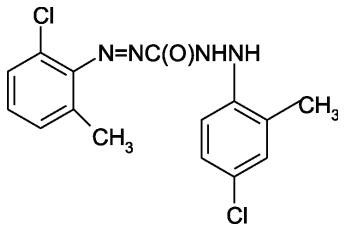

Fig. 1. Structure of the ligand.

Synthesis of the complexes

Cobalt chloride (1.0 g) was dissolved in acetate buffer (pH 6.2) and added drop wise to a 0.010 M EtOH solution (12 ml) of 2M6CPC at room temperature. The mixture was stirred and the resulting precipitate was collected under suction and washed several times with H_2O. The complex was dried over P_2O_5 under vacuum at room temperature and purified by the Soxhlet method,[14] using a 1:1 Et_2O:petroleum ether mixture as the solvent (3 h). The pure complex was obtained as a shining crystalline powder in the Soxhlet tube. The Ni(II) and Zn(II) complexes were similarly prepared using nickel and zinc chloride, respectively. The structures of the complexes are as given in Fig. 2.

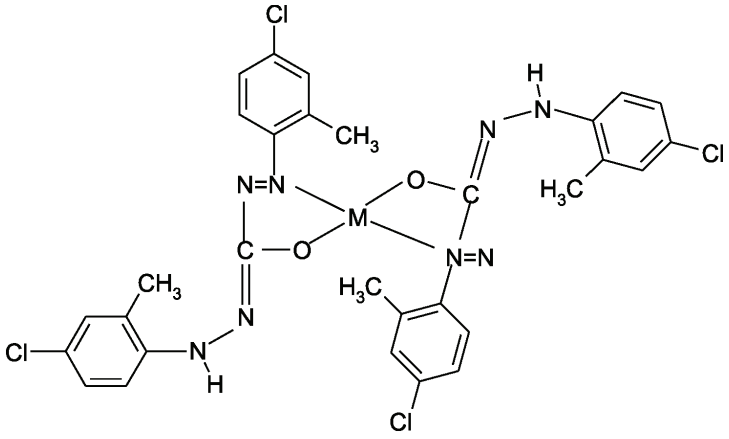

M= Co (II), Ni(II) or Zn(II)

Fig. 2. Proposed structure of the adduct.

RESULTS AND DISCUSSION

Physico-chemical methods

The elemental analyses of the ligand and the complexes together with the magnetic data are reported in Table I. The C, H, N and metal analyses confirm that the stoichiometry of the complexes is 1:2 metal to ligand. The observed magnetic moment for the Co(II) complex was 2.57 μ_B. The low value of the observed magnetic moment is attributed to the orbital contribution, as it is higher in the case of square planar Co(II) complexes.[15] The subnormal magnetic moment for

the Ni(II) complex requires more explanation, since the spin-only value (2.83 μ_B) is expected for tetrahedral and octahedral geometries.

TABLE I. Analytical and magnetic data of the compounds

Compound	Molecular formula	Elemental analysis (found (calcd.), %)				μ_{eff}
		C	H	N	M	μ_B
[D2M 6CPC]	$C_{15}H_{11}N_4OCl_2$	53.34 (53.43)	4.10 (4.18)	16.41 (16.62)	–	–
$[Co(D2M6CPC)_2]$	$Co(C_{30}H_{26}N_8O_2Cl_4)$	49.14 (49.27)	3.43 (3.57)	15.22 (15.32)	8.00 (8.06)	2.57
$[Ni(D2M6CPC)_2]$	$Ni(C_{30}H_{28}N_8O_2Cl_4)$	49.24 (49.28)	3.50 (3.59)	15.40 (15.30)	8.06 (8.03)	2.31
$[Zn(D2M6CPC)_2]$	$Zn(C_{30}H_{25}N_8O_2Cl_4)$	48.80 (48.84)	3.50 (3.55)	15.16 (15.19)	8.80 (8.86)	dia

Infrared spectra

The IR spectra of the ligand and its complexes were recorded in the 4000––400 cm^{-1} range. The ligand showed bands at 3301 and 3150 cm^{-1} attributed to intra and intermolecular bonded ν_{N-H} vibrations. The band at 1684 cm^{-1} is assigned to $\nu_{C=O}$ stretching. The disappearance of this $\nu_{C=O}$ stretching band in the spectra of the complexes indicated that an oxygen atom of the ligand was involved in the coordination with the metal through the enolic form. This was further confirmed by the appearance of a band in the region 1572–1609 cm^{-1} due to $\nu_{C=N}$ stretching in the spectra of the complexes.[16]

^{1}H-NMR spectra

The ^{1}H-NMR spectrum of the ligand was recorded in chloroform using TMS as the internal reference. Singlets were observed at δ 2.35 and 2.76 ppm due to $-CH_3$ protons. The broad peaks observed at δ 6.13 and 8.20 are due to aromatic –NH and amide –NH groups, respectively. The multiplets observed in the region of δ 6.75–7.70 may be attributed to aromatic hydrogen atoms. For the diamagnetic Zn(II) complex, it was observed that the broad peak of the amide –NH had disappeared, indicating that the azomethine atom is involved in the coordination to the central metal atom *via* deprotonation. Based on the analytical and spectral data given in Table II, the structures of the ligand and the complexes are assigned as shown in Figs. 1 and 2, respectively.

Methodology

For the evaluation of the ground state and excited state dipole moment, the UV absorption spectra (for the S1 band) of a single particular weight fraction (concentration) of each of the pure samples, 2M6CPC and its Co(II), Ni(II) and Zn(II) complexes, were recorded on a Hitachi 150-20 UV–Vis spectrophotometer

with a cell path length of 1 cm in various polar and non-polar solvents (concentration 0.010–0.030 g ml^{-1}). The data is presented in Table III. The permanent dipole moments in the excited states (μ_e) and the radius of the cavity in which solute molecules are supposed to lie were obtained using a method reported in the literature and is given below.

TABLE II. IR and ^{1}H-NMR spectral data for the compound (IR frequencies in cm^{-1})

Compound	ν_{N-H}	$\nu_{C=O}$	$\nu_{C=N}$	$\nu_{C=C}$ aromatic	ν_{C-O}	ν_{N-H} bend	^{1}H-NMR
D2M6CPC	3301 3150	1684	–	1486	–	763	2.35, 2.76(S–CH_3); 6.13 (br–NHAr); 8.20 (br–NH, amide); 6.75–7.70 (*m*, Ar–H)
Co(D2M6CPC)$_2$	3380	–	1609	1498	1158	854	2.63 (S–CH_3); 6.42 (br–NH–Ar), 7.24–7.64 (*m*, Ar–H)
Ni(D2M6CPC)$_2$	3005	–	1573	1505	1011	832	2.64 (S–CH_3), 6.38 (br–NH–Ar), 7.10–7.80 (*m*, Ar–H)
Zn(D2M6CPC)$_2$	3320	–	1572	1492	1164	828	2.72 (S–CH_3), 6.60 (br–NH–Ar), 7.20–7.84 (*m*, Ar–H)

Following Suppan and Tsiamis,[14] the change in the permanent dipole moment for a series of solvents of different static dielectric constants (ε) but similar refractive indices (n) are related to the observed energy shift ΔV_{a-b} between solvents "a" and "b" by:

$$-\Delta V_{a-b} = \mu_g \Delta\mu_g - e/hca_g^3(\Delta(f(\varepsilon)) - f(n^2))_{a-b}) + \mu^2 e - \mu_g^2 \Delta(n^2)_{a-b} - e/hca_g^3 \quad (1)$$

where μ_g is the permanent dipole moment in the ground state, h is the Planck's constant, c is the velocity of light, a_g is the radius of the cavity in which the solute molecule is supposed to lie and $f(\varepsilon)$ and $f(n^2)$ are the polarity and polarizability functions, respectively, defined by:

$$f(\varepsilon) = 2(\varepsilon - 1) / (2\varepsilon - 1) \text{ and } f(n^2) = 2(n^2 - 1) / (2n^2 - 1)$$

Recently, a method was proposed by Ayachit *et al.*[17] to determine *M*e by expressing $Ef(i)$ in the form:

$$x/\mathrm{C1} + y/\mathrm{C2} = 1 \quad (2)$$

which is an equation of a straight line with intercepts on either axes.

By plotting a graph:

$$x = (\Delta(f(\varepsilon)) - f(n^2))_{a-b} / -\Delta V_{a-b}) \textit{ vs. } y = \Delta f(n^2)_{a-b} / -\Delta V_{a-b}$$

the intercepts:

$$\mathrm{C1} = hca_g^3 / (\mu_g \Delta\mu_g - e) \text{ and } \mathrm{C2} = hca_g^3 / (\mu e^2 - \mu_g^2)$$

on the x and y axes, respectively, are determined and the magnitude and direction of them are obtained. The required data were obtained by measuring the static per-

TABLE III. Dielectric constants and refractive indices of the compounds in benzene at 25 °C ($\rho_1 = 0.874$ g cm^3; $\varepsilon_1 = 2.278$; $n_1 = 1.5015$)

Compound	Molecular weight $M_{r,2}$	Weight fraction $w_2 \times 10^3$	Dielectric constant ε_{12}	$\varepsilon_{12}-\varepsilon_1/w_2$	Refractive index n_{12}	$n_{12}-n_1/w_2$	Intercepts			Calculated μg / D	
							Δ'	Δ''	Δ	Eq. (3)	Eq. (4)
D2M6CPC	337.09	0.5991	2.4033	209.147	1.5040	12.5417	196.0	12.2	183.80	23.96	24.37
		1.1560	2.4650	161.76	1.5050	9.1027					
		1.7100	2.5205	141.8128	1.5055	7.0339					
		2.3302	2.5630	122.3070	1.5060	5.8084					
		2.8943	2.5900	108.4890	1.5063	4.9812					
Co[D2M6CPC]$_2$	731.350	0.5564	2.3926	205.9264	1.5050	18.9122	152.00	14.40	137.60	30.53	31.60
		1.1364	2.42037	125.2815	1.5055	10.5843					
		1.7146	2.4765	115.7704	1.5060	7.8932					
		2.2991	2.4927	93.3843	1.5065	6.5416					
		2.8966	2.5159	82.1307	1.5070	5.7124					
Ni(D2M6CPC)$_2$	731.11	0.5957	2.3510	122.5440	1.5035	10.0889	139.00	9.00	130.00	29.67	30.21
		1.2715	2.4069	101.3763	1.5040	5.9093					
		1.7561	2.4329	88.2068	1.5045	5.1352					
		2.3302	2.4452	71.7534	1.5050	4.5158					
		2.8966	2.4576	62.0037	1.5055	4.1524					
Zn[D2M6CPC]$_2$	737.75	0.5968	2.4165	232.0710	1.5045	15.1105	188.00	10.80	177.20	34.79	35.30
		1.1791	2.4365	134.1701	1.5050	8.9243					
		1.7446	2.4460	96.2971	1.5060	7.7575					
		2.329	2.4633	79.5620	1.5070	7.1046					
		2.8966	2.4788	69.3226	1.5080	6.7533					

mitivities of the solvents and various dilute solutions (in benzene only for this purpose) at 10 kHz with the help of FT 6421, LCR Data Bridge. The estimated values of μ_g using the modified Guggenheim equation[18] were found to be accurate up to the second decimal place. The equations used are as follows:

$$\mu_g = 0.0128(3/(E_1 + 2)2M_{r,2} / \rho_1 T\Delta]^{0.5} \quad (3)$$

where

$$\Delta = \Delta' - \Delta'' = ((E_{12} - E_1) / w_2)\, w_2^0 - (n_{12}^2 - n_1^2/w_2)w_2$$

$$\mu_g = 0.0128(3/(e_1 + 2)^2 M_{r,2} / \rho_1 T0.97((E_{12} - E_1) / w_2) \quad (4)$$

The quantities n, ρ, M_r, w and T involved in Eqs. (3) and (4) are the refractive index, density, molecular weight, weight fraction and absolute temperature, respectively. The subscripts 1, 2, and 12 refer to the solvent, solute, and solution, respectively. The data of dielectric constants, the refractive indices and hence the ground state dipole moments for the compounds are presented in Table IV. The ultraviolet spectral data of the compounds in different solvents are summarized in Table V. The values of the x and y intercepts are presented in Table VI.

TABLE IV. The electronic spectral data of the compounds in different solvents

Solvent	D2M6CPC		$Co(D2M6CPC)_2$		$Ni(D2M6CPC)_2$		$Zn[D2M6CPC]_2$	
	ν_{max} cm^{-1}	ν cm^{-1}	ν_{max} cm^{-1}	ν cm^{-1}	ν_{max} cm^{-1}	ν cm^{-1}	ν_{max} cm^{-1}	ν cm^{-1}
Cyclohexane	44247	Ref	44404	Ref	44563	Ref	44722	Ref
Carbon tetrachloride	33738	10509	34340	10064	34819	9744	34530	10192
Benzene	34722	9525	36023	8381	34843	9720	34867	9855
2-Propanol	46296	2049	35460	8944	45955	1392	36040	1318
Dimethyl formamide	34698	9549	35511	8893	36927	7636	35511	9211
1-Butanol	43706	541	43029	1375	42589	1974	40916	3806
Chloroform	40916	3331	40716	3688	40983	3580	40849	3873
1,4-dioxane	32051	12196	31766	12638	31806	12757	31928	12799
1-propanol	47348	3101	47258	2854	46992	2429	47080	2358

The magnitude and directions of the dipole moments for the first excited state together with the corresponding ground state dipole moment values are given in Table VI. It may be observed that the excited state dipole moment values are rather higher compared to the values obtained using the Guggenheim Equation for ground state ones C, as entered in the third column of Table VI. Such large values are reported in the literature for some polymers both in polar and non-polar solvents. The method of calculation (vector addition of group moments) has its own limitation of not accounting for the possible inductive/mesmeric/hydrogen bonding effects in these systems. Under these circumstances, if it is assumed that these values would not improve much when bonding effects are also

taken into account; the presently observed dipole moment values remain higher. In the light of these considerations, the observed values of the dipole moments may be considered as inductive and hence the present ligand and complexes may be associated with rather large values of dipole moments, which in turn may be taken as suggestive of their structure.[19]

TABLE V. Values of the x and y intercepts and the molecular radius (a_g) of the compounds

Solvent	D2M6CPC		$Co(D2M6CPC)_2$		$Ni(D2M6CPC)_2$		$Zn[D2M6CPC]_2$	
	$x\times10^5$	$y\times10^5$	$x\times10^5$	$y\times10^5$	$x\times10^5$	$y\times10^5$	$x\times10^5$	$y\times10^5$
Carbon tetrachloride	0.2326	0.0207	0.2429	0.2162	0.2509	0.2230	0.2398	0.2135
Benzene	0.0747	0.0495	0.0849	0.5634	0.0732	0.4850	0.0722	0.4791
1-Propanol	27.14	–0.1655	6.218	–0.3793	39.95	–2.437	42.20	–2.574
Dimethyl formamide	6.180	0.0031	6.636	0.0336	7.729	0.3910	6.4074	0.0324
1-Butanol	98.53	–0.3460	38.77	–1.361	27.01	–0.9480	14.01	–0.4918
Chloroform	8.966	0.0394	8.099	0.3560	0.8343	0.3660	7.712	0.3390
1,4-Dioxane	0.3585	–0.0021	0.3459	–0.0211	0.3430	–0.0209	0.3417	–0.0208
1-Propanol	17.88	–0.0939	19.43	–1.021	22.82	–1.199	23.51	–1.236
$C_1\times10^5$	11.5		7.10		12.0		6.60	
$C_2\times10^5$	0.128		0.570		1.12		0.500	
a_g / Å	3.955		4.978		4.985		5.006	

The dipole moment values of the excited states are expected to be greater than their ground state values. In the present investigation, the excited state dipole moment values are certainly greater than the ground state ones. Based on these observations, it may be presumed that the observed transitions belong to $\pi\rightarrow\pi^*$ transitions.

TABLE VI. Ground state and excited state dipole moments

Compound	Equation	μ_g / D	μ_e / D	θ / °
D2M6CPC	(3)	23.9566	39.1620	60 08' 29"
	(4)	24.3650	39.4137	59 32' 22"
$[Co(D2M6CPC)_2]$	(3)	30.5318	72.3362	74 35' 22"
	(3)	29.6718	55.4710	65 31' 31"
	(4)	30.2179	55.7651	65 09' 07"
$Zn[(D2M6CPC)_2]$	(3)	34.7989	78.7067	72 10' 00"
	(4)	35.3019	78.9304	71 50' 06"

CONCLUSIONS

An interesting dynamic and mechanistic way of viewing the reaction involving the metal complexes was traced in the present study by application of spectrophotometry. The electric dipole moments of the synthesized compounds in

their first electronic excited state were determined. An attempt at predicting the structure and geometry of the complexes was made. All these observations put together lead us to propose the structures shown in Fig. 2.

Acknowledgements. The authors thank the USIC, Karnataka University Dharwad, RSIC, IIT, Powai, Mumbai, for providing spectral facilities and the C, H, N analysis. The authors are also grateful to Dr. H. D. Patil and Y. F. Nadaf, Department of Physics, Basaveshwar Science College, Bagalkot, India, for their illuminating discussions.

ИЗВОД

ПРОРАЧУН ДИПОЛНИХ МОМЕНАТА ЕКСЦИТОВАНОГ СТАЊА ДИ(2-МЕТИЛ-6-ДИХЛОРОФЕНИЛ)КАРБАЗОНА И ЊЕГОВИХ Co(II), Ni(II) И Zn(II) КОМПЛЕКСА НА ОСНОВУ УТИЦАЈА РАСТВАРАЧА НА ЊИХОВЕ УЛТРАЉУБИЧАСТЕ АПСОРПЦИОНЕ СПЕКТРЕ

ASHOK F. DODAMANI, MOHAMMEDSHAFI A. PHANIBAND и SHREEDHAR D. DHUMWAD

Department of Chemistry, Karnatak University's Karnatak Science College, Dharwad-580001, Karnataka, India

Добијен је ди(2-метил-6-хлорофенил)карбазон (2M6CPC) и његови Co(II), Ni (II) и Zn(II) комплекси који су окарактерисани магнетним моментом, инфрацрвеним спектрима и ^{1}H-NMR спектралним мерењима. Утицај растварача у серији поларних и неполарних растварача променљивих диелектричних константи и индекса рефракције су прорачунати снимањем електронских спектара (S1 траке) поменутих једињења. Подаци су искоришћени за одређивање величине и правца електричног диполног момента у првом електронском ексцитованом стању. Резултати указују да се примећена трака у овим једињењима може приписати $\pi \rightarrow \pi^*$ прелазу.

(Примљено 15. октобра, ревидирано 17. децембра 2008)

REFERENCES

1. A. Jaromin, A. Kozubek, K. S. Lukaniuk, M. M. Blaszkiewicz, W. P. Czoch, L. Kaczmarek, *Drug Delivery* **15** (2008) 49
2. M. A. Phaniband, S. D. Dhumwad, *Trans. Met. Chem*. **3** (2007) 1117
3. N. M. Balton, O. M. Peeters, C. J. Ranter, C. J. Willaims, *Acta. Cryst. B* **55** (1970) 629
4. A. H. M. Siddalingarah. R. B. Bhat, *Trans. Met. Chem.* **22** (1997) 105
5. S. A. Hiremath, R. B. Bhat, *Trans. Met. Chem.* **21** (1996) 327
6. J. Cernicharo, A. M. Heras, A. M. Tielens, J. R. Pardo, F. Herpin, M. Guélin, L. M. Waters, *Astrophys. J.* **123** (2001) 546
7. H. L. Bethlem, M. R. Tarbutt, J. Kupper, D. Carty, K. Wohlfart, E. A. Hinds, G. Meijer, *J. Phys. Chem.* **B 39** (2006) R263
8. B. Simard, C. Masoni, P. A. Hackett, *J. Mol. Spectrosc.* **136** (1989) 44
9. R. S. Ram, P. F. Bernath, S. P. Davis, *J. Mol. Spectrosc*. **210** (2001) 110
10. R. S. Ram, P. F. Bernath, S. P. Davis, *J. Mol. Spectrosc*. **215** (2002) 163
11. Z. Kisiel, B. A. Pietrewicz, P. W. Fowler, A. C. Legon, E. Steiner, *J .Phys. Chem*. **104** (2000) 6970
12. S. A. Hiremath, M. Y. Karidurganavar, *Asian J. Chem.* **7** (1995) 621
13. S. A. Hiremath, M. Y. Karidurаganvar, *Asian J. Chem*. **8** (1996) 183
14. P. Suppan, C. Tsiamis, *Spectrochim. Acta* **36A** (1983) 971
15. B. A. Goodman, J. B. Raynor, *Adv. Inorg. Radiochem.* **13** (1970) 135

16. P. G. Avaji, P. S. Badami, B. N. Reddy, S. A. Patil, *Trans. Met. Chem.* **31** (2006) 842
17. E. A. Guggenheim, *Trans. Faraday Soc.* **45** (1949) 714
18. E. A. Guggenteim, *Trans. Faraday Soc.* **47** (1951) 573
19. N. E. Hill, W. E. Voughan, A. H. Price, M. Davies, *Dielectric properties and molecular behaviour, The van Nostrands Series in Physical Chemistry*, van Nostvand Reinheard Company, London, 1961.

Journal of the Serbian Chemical Society
JSCS@tmf.bg.ac.rs • www.shd.org.rs/JSCS

J. Serb. Chem. Soc. 74 (6) 651–661 (2009)
JSCS–3863

UDC 54.024–039.7+54–145.2+546.791+
+613.163:537.635
Original scientific paper

EPR study of the production of OH radicals in aqueous solutions of uranium irradiated by ultraviolet light

MARKO DAKOVIĆ*, MILOŠ MOJOVIĆ and GORAN BAČIĆ

Faculty of Physical Chemistry, Studentski trg 12–16, 11000 Belgrade, Serbia

(Received 17 December 2008, revised 3 February 2009)

Abstract: The aim of the study was to establish whether hydroxyl radicals ($^{\bullet}$OH) were produced in UV-irradiated aqueous solutions of uranyl salts. The production of $^{\bullet}$OH was studied in uranyl acetate and nitrate solutions by an EPR spin trap method over a wide pH range, with variation of the uranium concentrations. The production of $^{\bullet}$OH in uranyl solutions irradiated with UV was unequivocally demonstrated for the first time using the EPR spin-trapping method. The production of $^{\bullet}$OH can be connected to speciation of uranium species in aqueous solutions, showing a complex dependence on the solution pH. When compared with the results of radiative de-excitation of excited uranyl ($^{*}UO_2^{2+}$) by the quenching of its fluorescence, the present results indicate that the generation of hydroxyl radicals plays a major role in the fluorescence decay of $^{*}UO_2^{2+}$. The role of the presence of carbonates and counter ions pertinent to environmental conditions in biological systems on the production of hydroxyl radicals was also assessed in an attempt to reveal the mechanism of $^{*}UO_2^{2+}$ de-excitation. Various mechanisms, including $^{\bullet}$OH production, are inferred but the main point is that the generation of $^{\bullet}$OH in uranium containing solutions must be considered when assessing uranium toxicity.

Keywords: uranium fluorescence; OH radicals; electron paramagnetic resonance; spin trap; DEPMPO.

INTRODUCTION

The uranyl ion and its luminescence have been the subject of intensive research for more than a 100 years.[1] There are several monographs and a large number of papers dealing with various aspects of this topic, including photochemical reactions between excited uranyl ($^{*}UO_2^{2+}$) and both inorganic and organic compounds.[1–6] These reactions are enabled by the fact that $^{*}UO_2^{2+}$ has a high oxidative potential ($E^{\ominus}(^{*}UO_2^{2+} / UO_2^{2+}) = 2.6$ V) and can readily oxidize different substrates.[7] During photochemical reactions, quenching of the uranyl fluorescence occurs, which is supposed to be the consequence of the pro-

* Corresponding author. E-mail: marko@ffh.bg.ac.rs
doi: 10.2298/JSC0906651D

duction of non-luminescent uranium forms, such as UO_2^{2+} and U(IV); this phenomenon is observed even in pure water solutions of inorganic uranyl salts.[8] Studies showed that the quenching is dependent on solution speciation, the presence of impurities, solution acidity and temperature.[9–11] There are several proposed mechanisms for explaining this process, which can be reduced to four: autoquenching, electron transfer, hydrolysis of excited uranyl and abstraction of hydrogen from the substrate.[7] However, due to the complexity of uranium speciation in solution[10] and the structure of the excited states of uranyl,[12] none of them can be considered as a complete description of the UO_2^{2+} fluorescence quenching process. Special interest has been shown in the photophysics and photochemistry of $^*UO_2^{2+}$ in aqueous solutions, probably because of their possible influence on the processes in the environment. In a series of papers dedicated to this problem,[8–11] a research group from the University of Coimbra (Portugal) proposed, as the most probable mechanism of UO_2^{2+} fluorescence quenching, OH radicals ($^\bullet$OH) produced in the process of hydrogen abstraction from water molecules. This process is thermodynamically favorable because the redox pair $^*UO_2^{2+}$ / / UO_2^{2+} has a higher oxidizing potential than the $^\bullet H^\bullet OH/H_2O$ pair ($E^\ominus(^\bullet H^\bullet OH/ /H_2O) = 2.48$ V).[7] However, the production of OH radicals has only been studied at relatively high uranium concentrations and low pH (where UO_2^{2+} are the dominant species), which is not the case in the environment and biological systems. It has been shown that the hydroxyl radical exists in uranyl solutions of high acidity (pH 1 or lower) or in the presence of polymolybdates, but the origin of those radicals is uncertain.[13–16] As a concurrent mechanism for the production of hydroxyl radicals, a reaction of water and organic radicals, previously formed in the interaction of an excited uranyl ion and a spin trap, was proposed.[16]

The aim of this work was to investigate the production of hydroxyl radicals in aqueous uranyl solutions irradiated by UV light, using EPR spin trap methods, in order to prove the existence of this species. To assess the influence of different forms of uranyl in solution on the production of $^\bullet$OH, the reaction was studied over a wide pH range with varying uranium concentration and in the presence of different counter-ions. The obtained results are discussed in terms of possible pathways of hydroxyl radical generation and the influence of different excited species of uranyl.

EXPERIMENTAL

Solutions of $UO_2(CH_3COOH)_2 \cdot 2H_2O$, $UO_2(NO_3)_2 \cdot 6H_2O$ and Na_2CO_3 were prepared by dissolving analytical grade chemicals (Merck, Germany) in deionized water (MiliQ). The pH values of the solutions were adjusted by adding of 0.10 M HCl and 0.10 M NaOH and controlled by a pH-meter. The spin trapping agent was DEPMPO, 5-(diethoxyphosphoryl)-5-methyl-1-pyrroline-*N*-oxide (Alexis, USA), because it can distinguish between different mechanisms of OH radical formation.[17] Solutions together with the spin trap were placed in quartz cuvettes and irradiated in a self-made UV reactor at a wavelength of 300±10 nm (UVB). The

wavelength of UV light was selected to be close enough to hat of an excitation laser (335 nm) frequently used in uranyl fluorescence studies. It was shown[18] that higher energy states of excited uranyl de-excite to the first excited state by internal conversion or non-radiative transfer to the surrounding molecules. Following irradiation, the solutions were transferred to Teflon tubes and the trapped radicals were measured using a Varian E104-A X-band EPR spectrometer (modulation amplitude: 2 G, power: 10 mW). The spectra were processed by Microcal Origin™ v. 7.5 software using window average smoothing. The intensity of the DEPMPO/OH peak in the adduct spectra was measured as the peak-to-peak height (line indicated by the arrow in Fig. 1). All experiments were performed at ambient temperature (22 °C).

Uranium shows complex behavior in aqueous solutions depending on the acidity and composition of the solution; hence it is necessary to predict the relative abundance of different uranyl species under various conditions. The theoretical calculation of their equilibrium concentrations was performed using Phreeqc v. 2.13 software (USGSC),[19] for which purpose, the program uses thermodynamic equilibrium constants data. As calculation input, temperature, composition and pH value of the solution were taken. The output file of the program contains information about the concentrations of all species present in the solution or in the solid phase (see Fig. 3).

RESULTS AND DISCUSSION

The EPR spectra of the DEPMPO adduct produced by irradiation of 4.2×10^{-5} mol dm^{-3} solution of uranyl acetate, which contained DEPMPO (0.10 mol dm^{-3}), at different pH values, are shown in Figs. 1b–1d. The corresponding spectra obtained for uranyl nitrate contained the same spectral lines. A typical spectrum of the DEPMPO/OH adduct is given for comparison in Fig. 1a. All the EPR spectra obtained in this study showed the presence of this adduct, which can be considered as proof for the production of OH radicals in UV irradiated solutions of uranyl ions. The blank probe, consisting only of irradiated deionized water and the spin trap, showed no EPR spectra. Also, a solution of uranyl and the spin-trap showed no EPR spectra (Fig. 1), and Fig. 1 shows that a small amount of some adducts other than DEPMPO/OH was present at higher pH values. A possible explanation for this in solutions containing CH_3COO^- could be the generation of an adduct with acetate radicals, formed in reaction with the excited uranyl ion. However, the existence of same lines in the spectra obtained for uranyl nitrate solutions and the fact that the formation of the acetate radicals is favored in solutions of low pH,[7] makes this explanation less probable. On the other hand, other excited uranyl species, which are present in solutions at the intermediate pH values, could have de-excitation pathways other than $^*UO_2^{2+}$; these routes may involve the production of free radicals. One of the proposed mechanisms for quenching uranyl fluorescence involves reversible crossing between two excited states of UO_2^{2+} (U^* and X^*) and separate routes of their de-excitation[7,9] (Fig. 2). It has been assumed that processes of non-radiative de-excitation of the X^* state include the generation of $^\bullet OH$.[9,16] However, in the case of complex uranyl species, even the de-excitation of the U^* state could involve free radical production other than hydroxyl in solution (see below).

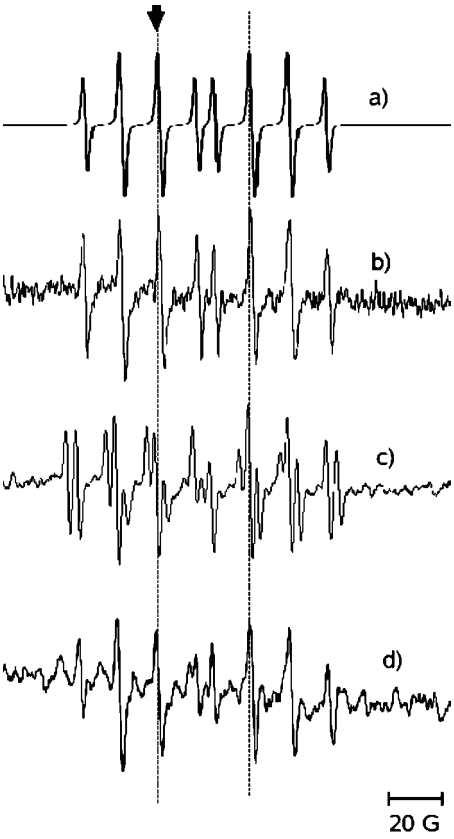

Fig. 1. EPR spectra of DEPMPO adducts: a) simulated EPR spectra of DEPMPO/OH[17] and spectra obtained by UV irradiation (wavelength: 300 nm) of uranyl acetate solution (the uranium concentration was 10 ppm, the concentration of the spin trap DEPMPO was 0.1 mol dm^{-3}) at different pH values: b) 2.0, c) 7.0 and d) 10.0. The arrow indicates the line which was the least affected by the presence and which was used for peak-to-peak measurements of the EPR signal height. The dashed line is used to indicate the alignment of the EPR spectra.

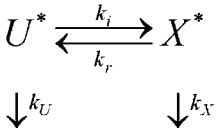

Fig. 2. The mechanism of quenching of uranyl fluorescence proposed by Formosinho,[9] where U* is the higher excited state of the uranyl ion, X* is the first excited state of UO_2^{2+}, k_i and k_r are constants of crossing between states, k_U and k_X are cumulative rate constants for the de-excitation processes.

The complexity of the EPR spectra obtained for solutions at intermediate pH somewhat complicates the quantitative assessment of DEPMPO/OH adducts; hence, for this purpose, the line which is the least affected by the presence of other adducts (indicated by arrow in Fig. 1) was selected.

It is well known that different uranyl species exist in aqueous solutions at different pH values,[20] which can be the explanation for the different DEPMPO adducts. The calculated distribution of uranyl species in the pure solutions used for UV irradiation is given in Fig. 3. In solutions of both uranyl acetate and uranyl nitrate at pH < 5, the most dominant specie is the free uranyl ion (with a hydration layer). Above this value, positively charged hydroxyl complexes of the uranyl ion become dominant, while at pH > 8, the only species present in the

solution is $(UO_2)_3(OH)_5^+$. As shown in Fig. 3, the concentration of these species is not equal to the total uranium concentration because of the existence of a solid phase in the form of $UO_2(OH)_2$ and $UO_2(OH)_2 \cdot 2H_2O$ (schoepite) in this pH range (the solid phases are not presented in the diagram). In solutions with an excess of carbonates, the hydroxyl complexes are replaced with carbonate complexes of uranyl, which are negatively charged and no solid phase is formed. It has been shown that the structure of the energetic levels of excited uranyl in complexes becomes altered in comparison to UO_2^{2+} (low pH), which in turn should have an impact on the uranyl fluorescence lifetime and spectra. Consequently, the production of OH radicals in the reaction of hydrogen abstraction[16] should also be affected by uranyl speciation.

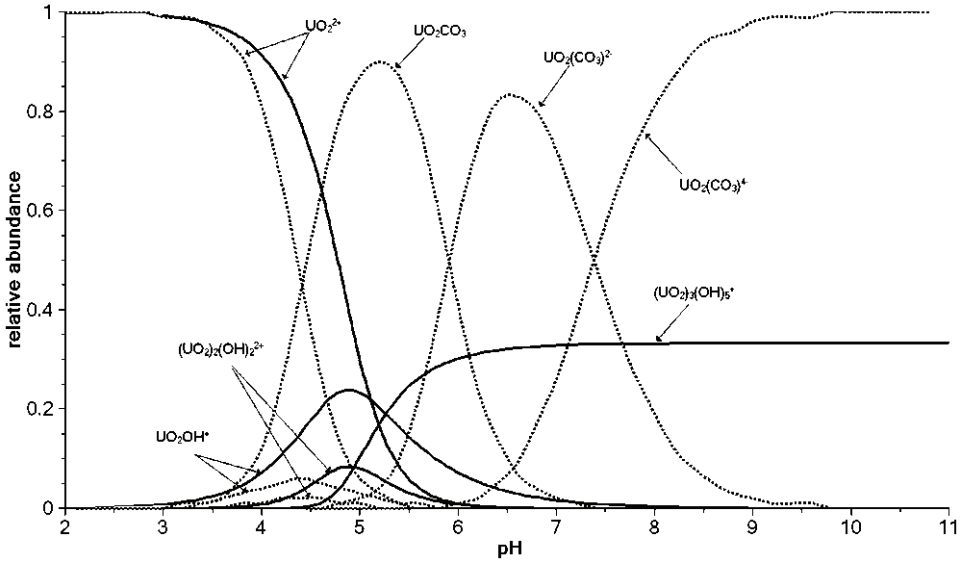

Fig. 3. Relative abundances of uranyl species in a solution of uranyl acetate: abundances in the absence (–) and in the presence (---) of carbonates.

The pH dependence of the signal height of the DEPMPO/OH adduct produced in a solution of uranyl acetate upon irradiation with UVB light is shown in Fig. 4. The pH profile of the adduct signal at pH < 6 qualitatively follows the concentration profile of the free uranyl ion, *i.e.*, a high and steady production of OH radicals up to pH 4, followed by a decline between pH 4 and 6 (see Fig. 3). This implies that $^*UO_2^{2+}$ plays a major role in $^{\bullet}OH$ production in this pH range. Fomosinho *et al.*,[9] considering uranyl fluorescence quenching in the pH range between 1 and 4, showed that the quenching constant depends on the pH of the solution, but the pH dependence of the profile showed an unexpected minimum around pH 3, which was explained by the presence of a strongly fluorescent hyd-

roxyl complex of uranyl. Since the EPR method directly measures the production of hydroxyl radicals while the study of $^{*}UO_2^{2+}$ de-excitation by fluorimetry just indirectly suggests their presence, the conclusion can be drawn of the co-existence of other non-radiative decay processes.

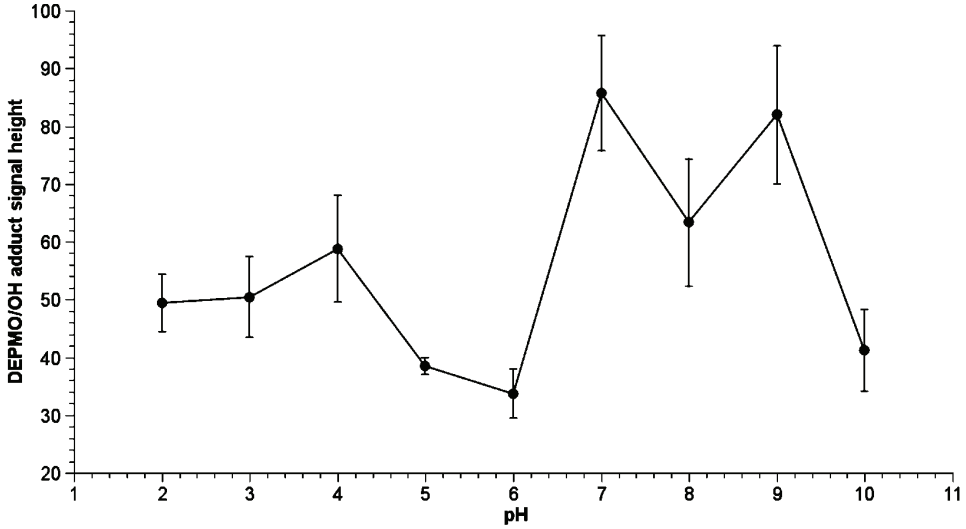

Fig. 4. pH dependence of the signal height of the DEPMPO/OH adduct produced in a solution of uranyl acetate (concentration of uranium: 10 ppm) by irradiation with UVB light.

In the pH range between 4 and 6, there is a drop in the production of OH radicals, which could be a consequence of various mechanisms. Firstly, uranium speciation in this range shows the presence of two hydroxyl complexes of uranyl ion with overlapping abundance profiles. Due to the low concentrations of these species, their impact on OH radical production should be small. However, Park *et al.*[21] observed that the fluorescence decay of uranyl above pH 3 has two components, which arise from two excited species: $^{*}UO_2^{2+}$ and $*(UO_2)_2(OH)_2^{2+}$; the fluorescence of the second species decays five times slower than the first one.[21] The concentration profile for $(UO_2)_2(OH)_2^{2+}$ (see Fig. 3) shows that it has a small abundance in this pH region. Considering the previously mentioned facts, the conclusion can be drawn that this species has a small influence on OH radical production. Secondly, in this pH range, the EPR spectra showed, in addition to the signal of the DEPMPO/OH adduct, additional lines which probably arise from the DEPMPO adduct of an unknown radical species (see Fig. 1c), the production of which could be a concurrent process to hydroxyl radical generation. A possible explanation could be the generation of organic radicals in reactions with excited uranyl ions, which was previously found in studies of UO_2^{2+} fluorescence quenching.[3,4] Since acetates were present in the solution, a reaction could occur

via hydrogen abstraction from C_α with the generation of acetate radicals. However, the fact that the additional signals also exist in solutions of uranyl nitrate in this pH range favors the assumption that $^*(UO_2)_2(OH)_2^{2+}$ shows different de-excitation pathways, one involving an OH radical and the other the production of an unknown free radical.

At pH values higher than 6, the signal of the DEPMPO/OH adduct first shows an increase, a slight variation around pH 8, followed by a drop of the signal height above pH 9. The speciation diagram (see Fig. 3) shows a dominance of the polyuranyl hydroxyl complex $(UO_2)_3(OH)_5^+$ in this region, the concentration of which remains unaltered throughout the region. In comparison with the OH radical yield in the region below pH 5, OH radical production in the pH region 7–9 showed higher efficiency. This could be explained by the formation of the uranyl exciplex species, $^*UO_2(UO_2)_2(OH)_5^+$ (or $^*UO_2(^*UO_2)_2(OH)_5^+$, which is less probable). The formation of exciplex species in a uranium solution is theoretically possible, but has not yet been experimentally confirmed,[8] and also the Phreeqc program cannot take into account the existence of such species. It is possible that the coordinated OH^- in this species can act as some kind of mediators in the process of $^\bullet$OH formation. It is premature to speculate whether this can explain the sudden drop of $^\bullet$OH production at pH 10.

The dependencies between the DEPMPO/OH adduct signal and the concentration of uranium at pH 2 for solutions of uranyl acetate and uranyl nitrate are shown in Fig. 5. It appears that $^\bullet$OH production is almost independent of the uranium concentration for both uranyl acetate and nitrate. The data for uranyl nitrate are in agreement with the concentration independence of the fluorescence decay constant of the excited uranyl ion,[9,21] but the authors did not give an explanation of such behavior. The same dependence was found in case of uranium acetate solutions, which may imply that the mechanism of OH radical production at pH 2 does not depend on the employed uranyl compound (acetate or nitrate). A slight increase in the DEPMPO/OH adduct signal in case of the nitrate solution was observed at higher uranium concentration. This can be explained by the following: the generation of hydroxyl radicals involves the production of UO_2^+ which is further converted to U(IV); this process is possible only in the presence of an $^\bullet$OH scavenger (hydroxyl radicals are good oxidants and can oxidize UO_2^+ back to the uranyl ion). However, if nitrates are present in a low pH solution, they can perform re-oxidation[7] of UO_2^+ to UO_2^{2+}. It is possible that above a certain uranyl nitrate concentration, this process becomes dominant; hence more UO_2^{2+} is "recycled" and available for excitation.

The same dependence but at pH 10.0 is shown in Fig. 6. The adduct signal showed no concentration dependence below 5 ppm for uranyl nitrate solutions, after which there was a steady increase in $^\bullet$OH production. A similar situation exists for uranyl acetate solutions, except that the threshold is at 3 ppm. The pro-

duction of $^{\bullet}$OH was generally higher in nitrate solutions. This again indicates that different species are involved in the production of OH radicals at different pH values, but also indicates that the counter ions play a significant role at high pH values. The Phreeqc calculation showed (not included in Fig. 3) the existence of small quantities of $UO_2NO_3^+$. There is thus a possibility of the formation of an excited mixed nitrate–hydroxyl complex, which could be de-excited easier by $^{\bullet}$OH production.

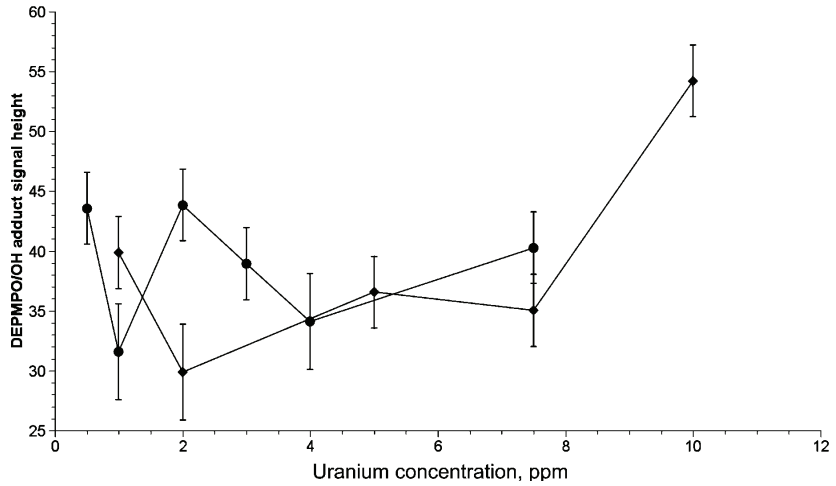

Fig. 5. Uranium concentration dependence of the signal of DEPMPO/OH, produced in solutions of uranyl acetate (●) and uranyl nitrate (♦),pH 2.0, by irradiation with UVB light.

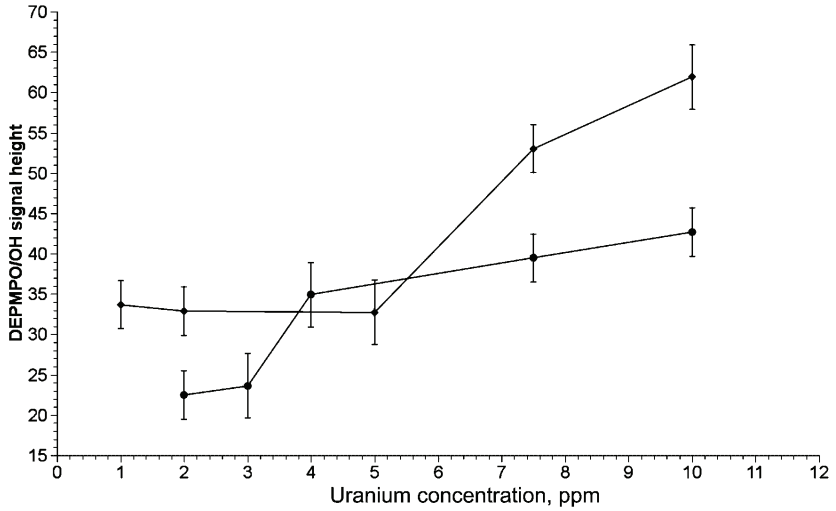

Fig. 6. Uranium concentration dependence of the signal of DEPMPO/OH, produced in solutions of uranyl acetate (●) and uranyl nitrate (♦), pH 10, by irradiation with UVB light.

The dependences between the signals of the DEPMPO/OH adducts and the concentration of uranium for solutions of uranyl acetate and uranyl nitrate in the presence of 0.010 M sodium carbonate, which is a realistic model for a natural aquatic environment, are shown in Fig. 7. The presence of 0.010 M carbonate maintains the pH value of the solution at pH 10.0, when carbonate complexes of uranyl are the only species present (Fig. 2). The found dependence of the DEPMPO/OH adduct signal on the uranium concentration could be a consequence of the replacement of hydroxyl ions in the coordination sphere of uranyl by carbonates. The dependencies for both compounds are linear, although with opposite slopes – negative for acetate and positive for nitrate.

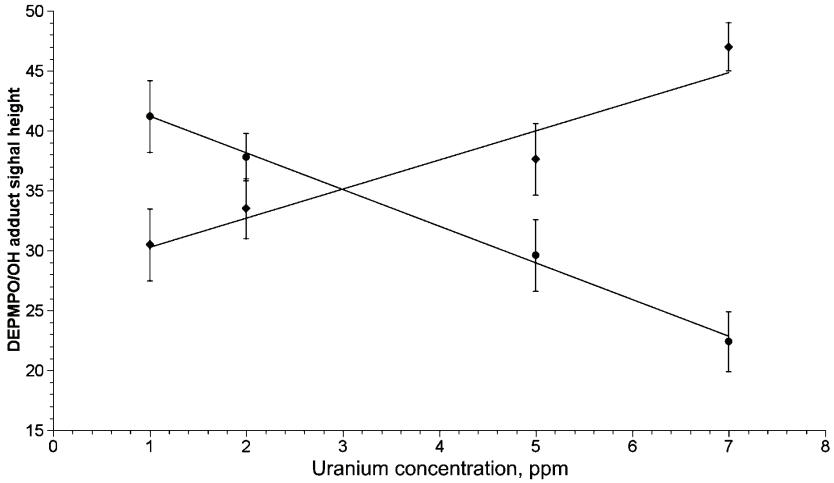

Fig. 7. Uranium concentration dependence of the signal of DEPMPO/OH, produced in solutions of uranyl acetate (●) and uranyl nitrate (♦) (0.010 M carbonate added) by irradiation with UVB light, on the uranium concentration.

The negative slope for uranyl acetate can be explained by a more efficient non-radiative energy transfer to acetate ions, probably *via* carbonates from the coordination sphere, which is favored by an increased concentration of acetates. Examples that this process is unfavorable from the aspect of the larger differrences in energy with organic matter are numerous, including action on bioorganic polymers such as proteins and nucleic acids.[22] The proposed mechanism is hydrogen abstraction from a reactive carbon atom, *i.e.*, a carbon atom in the states in the case of uranyl nitrate; hence there is a positive correlation between the amount of OH radicals and the concentration of uranium once the OH ions are removed from the coordination sphere.

Examples are uranyl ion interactions in the nearest vicinity of double bonds, hydroxyl, carbonyl or carboxyl group. Since it was shown in this study that $^{\bullet}$OH

are produced in uranyl solutions at physiological pH values, these mechanisms should be reconsidered to include the influence of hydroxyl radicals.

CONCLUSIONS

Using the EPR spin-trapping method, the production of OH radicals in uranyl solutions irradiated with ultraviolet light was unequivocally demonstrated. This is the first comprehensive study of this type, where their production was studied over a wide range of pH values (the only previous EPR study was constrained to a narrow, low pH range). Comparison of the obtained EPR results with those obtained by other authors using uranyl fluorescence quenching in aqueous solutions showed that production of OH radicals should be considered as one of the major mechanisms of UO_2^{2+} fluorescence decay. The effect of different counter ions and carbonate ions was also studied in order to assess their influence on production of hydroxyl radicals, attempting to reveal the mechanism of $^*UO_2^{2+}$ de-excitation. Although, further investigations are needed for a clarifycation of these mechanisms, the fact remains that potentially harmful OH radicals are produced under almost any circumstances encountered by biological systems, which should be taken into account when considering uranium toxicity.

Acknowledgements. This work was supported by grant no. 143016 from the Ministry of Science and Technological Development of the Republic of Serbia.

И З В О Д

ПРОУЧАВАЊЕ ПРОИЗВОДЊЕ ОН РАДИКАЛА У ВОДЕНИМ РАСТВОРИМА УРАНИЈУМА ПОД ДЕЈСТВОМ УЛТРАЉУБИЧАСТЕ СВЕТЛОСТИ

М. ДАКОВИЋ, М. МОЈОВИЋ и Г. БАЧИЋ

Факултет за физичку хемију, Студентски трг 1216, 11000 Београд

Циљ рада је испитивање услова при којим долази до продукције ОН радикала ($^\bullet$OH) у воденим растворима уранијумових соли под дејством ултраљубичастог зрачења. Генерисање $^\bullet$OH је проучавано помоћу EPR спин трап методе у широком опсегу pH и при различитим концентрацијама уранијума у растворима уранил ацетата и уранил нитрата. Установљено је да је производња хидроксилних радикала повезана са дистрибуцијом уранијумских врста у раствору и да на сложен начин зависи од pH вредности раствора. Добијени резултати, упоређени са претходно публикованим подацима за гашење флуоресценције уранил јона, указују да хидроксилни радикали играју главну улогу у овом процесу. У циљу даљег разјашњавања механизама деексцитације побуђеног стања уранила, продукција $^\bullet$OH је испитивана и у присуству карбоната, односно под условима својственим животној средини. Продукција хидроксилних јона у растворима уранијума озраченим ултраљубичастим зрачењем одвија се преко различитих механизама. Чињеница да $^\bullet$OH настају у овим растворима мора се узети у обзир код разматрања токсичних ефеката уранијума.

(Примљено 17. децембра 2008, ревидирано 3. фебруара 2009)

REFERENCES

1. E. Rabinowitch, R. L. Belford, *Spectroscopy and Photochemistry of Uranyl Compounds*, Pergamon Press, London, 1964
2. S. M. Fonseca, H. D. Burrows, M. G. Miguel, M. Sarakha, M. Bolte, *Photochem. Photobiol. Sci.* **3** (2004) 217
3. W. A. Massad, R. G. Badini, G. A. Argüell, *J. Radioanal. Nucl. Chem.* **240** (1999) 917
4. M. E. D. G. Azenha, H. Burrows, S. Formosinho, M. Miguel, *J. Chem. Soc. Faraday Trans. 1* **85** (1989) 2625
5. T. M. McCleskey, C. J. Burns, W. Tumas, *Inorg. Chem.* **38** (1999) 5924
6. W. K. Duerksen, *Photochemical Reduction of Uranyl Nitrate*, Rep Y/DZ-1019, Oak Ridge, TN, 1993
7. A. B. Yusov, V. P. Shilov, *Russ. Chem. Bull.* **49** (2000) 1925
8. S. Formosinho, M. Miguel, H. Burrows, *J. Chem. Soc. Faraday Trans. 1* **80** (1984) 1717
9. M. Miguel, S. Formosinho, A. Cardoso, H. Burrows, *J. Chem. Soc. Faraday Trans. 1* **80** (1984) 1735
10. S. Formosinho, M. Miguel, *J. Chem. Soc. Faraday Trans. 1* **80** (1984) 1745
11. H. Burrows, A. Cardoso, S. Formosinho, M. Miguel, *J. Chem. Soc. Faraday Trans. 1* **81** (1985) 49
12. C. Moulin, P. Decambox, V. Moulin, J. G. Decaillon, *Anal. Chem.* **67** (1995) 348
13. W. Mooney, F. Chauveau, T. H. Tran-Thi, G. Folcher, *J. Chem. Soc. Perkin Trans.* **2** (1988) 1479
14. A. Cox, T. Kemp, J. Reed, O. Traverso, *J. Chem. Soc. Faraday Trans. 1* **76** (1980) 804
15. S. Formosinho, M. Miguel, *J. Chem. Soc. Faraday Trans. 1* **81** (1985) 1891
16. S. J. Formosinho, H. D. Burrows, M. G. Miguel, M. E. D. G. Azenha, I. M. Saraiva, A. C. D. N. Ribeiro, I. V. Khudyakov, *Photochem. Photobiol. Sci*. **2** (2003) 569
17. M. Mojović, M. Vuletić, G. G. Bačić, *Ann. N. Y. Acad. Sci.* **1048** (2006) 471
18. M. Bouby, I. Billard, A. Bonnenfant, G. Klein, *Chem. Phys.* **240** (1999) 353
19. D. L. Parkhurst, S. A. J. Apelo, *User's guide to PHREEQC (version 2) – A computer program for speciation, batch reaction, one-dimensional transport and inverse geochemical calculations*, Water Resources Investigations, Report **99-4259**, Denver, CO, 1999
20. G. Meinrath, *J. Radioanal. Nucl. Chem.* **224** (1997) 119
21. Y. Park, Y. Sakai, R. Abe, T. Ishii, M. Harada, T. Kojima, H. Tomiyasu, *J. Chem. Soc. Faraday Trans.* **86** (1990) 55
22. M. Yazzie, S. L. Gamble, E. R. Civitello, D. M. Stearns, *Chem. Res. Toxicol*. **16** (2003) 524.

Journal of the Serbian Chemical Society
JSCS@tmf.bg.ac.rs • www.shd.org.rs/JSCS

J. Serb. Chem. Soc. 74 (6) 663–668 (2009)
JSCS–3864

UDC **Cetraria islandica* (L.) Ach.+544.723.3+54–
–145.15:546.36.027:582.29
Short communication

SHORT COMMUNICATION

Desorption of ^{137}Cs from *Cetraria islandica* (L.) Ach. using solutions of acids and their salts mixtures

ANA A. ČUČULOVIĆ[1*#], DRAGAN S. VESELINOVIĆ[2#] and ŠĆEPAN S. MILJANIĆ[2]

[1]*INEP – Institute for the Application of Nuclear Energy, Banatska 31b, 11080 Zemun and* [2]*University of Belgrade, Faculty of Physical Chemistry, 11001 Belgrade, P.O. Box 137, Serbia*

(Received 11 September 2008, revised 10 February 2009)

Abstract: The desorption of ^{137}Cs from *Cetraria islandica* (L.) Ach. lichen was investigated using the solutions: A) H_2SO_4–HNO_3–K_2SO_4, B) H_2SO_4–HNO_3–Na_2SO_4 and C) H_2SO_4–HNO_3–$(NH_4)_2SO_4$–$(NH)_4NO_3$ at pH 2.00, 2.58, 2.87, 3.28 and 3.75, similar to acid rain. After five consecutive desorptions using solutions A, B and C, from 44.0 % (solution B, pH 3.75) to 68.8 % (solution C, pH 3.28) of ^{137}Cs had been desorbed from the lichen. In all cases, the most successful ^{137}Cs desorption was the first one. In the presence of K^+ (solution A) the total amount of desorbed ^{137}Cs did not depend on the pH of the solution and this was confirmed by the analogous reactions of Cs^+ and K^+, due to their similar ionic radii. The dependencies of the non-desorbed content of ^{137}Cs on the number of desorptions gave curves indicating that at least two types of sorption occur. One of them can be dominant if suitable desorbants are used. The results indicate lichens as secondary sources of environment pollution with ^{137}Cs.

Keywords: *C. islandica* (L.) Ach. lichen; acid solutions; desorption; ^{137}Cs; radioisotope.

INTRODUCTION

In a previous study,[1] the extraction of ^{137}Cs from *Cetraria islandica* (L.) Ach. was investigated using solutions of HNO_3, H_2SO_4 and mixtures of these two acids, as well as a solution containing $(NH_4)_2SO_4$, *i.e.*, solutions with pH values similar to that of acid rain. H^+ and NH_4^+ were the dominant in these solutions. However, real rainfall also contains other ions originating from substances of different origin, such as sea spray, solid aerosols, *etc*.[2–4] Normal rain contains on average 2.0 mg Na^+, 0.30 mg K^+, 0.10 mg Cl^-, 0.60 mg SO_4^{2-}, about

* Corresponding author. E-mail: anas@inep.co.rs
# Serbian Chemical Society member.
doi: 10.2298/JSC0906663C

0.12 mg HCO_3^- and a series of other elements per 1 kg.[5] Their presence in rain is mostly due to natural processes.

In living organisms, the Cs^+ behaves as a chemical and biochemical homologue of potassium and follows its metabolism.[6,7] For this reason, an investigation of the influence of Na^+ and K^+ from atmospheric water on the desorption of Cs^+ from lichen is of interest, as cations of alkaline elements are similar to the Cs^+ and they can influence its desoprtion based on ion exchange, without other reactions. From this, the possible influence of these cations on the desorption of Cs^+ from lichen follows.

The purpose of this work was to investigate the influence of Na^+, K^+ and NH_4^+ on the desorption of ^{137}Cs from lichen, using solutions similar to acid rain, that thus become a secondary source of pollution with the ^{137}Cs.

EXPERIMENTAL

The apparatus, samples, and sample preparations were the same as in previous studies.[1,8]

Chemicals

H_2SO_4 p.a. and NH_4NO_3 p.a., Merck, Germany; HNO_3 p.a., Alkaloid, FYROM; $(NH_4)_2SO_4$ p.a., Euro Hemija, Serbia; Na_2SO_4, p.a. and K_2SO_4, p.a., Superlaboratory, Serbia; buffer solutions, pH 4.00 and 7.00, Carlo Erba, Germany, were used. The solutions were made in distilled water. Standard filter paper, Merck, was used for filtration.

The measurement error is given as the standard deviation of all the individual measurements of the same type (pH value) independent of the solution type.

Desorption solutions

Tree types of solutions were used: A) H_2SO_4–HNO_3–K_2SO_4; B) H_2SO_4–HNO_3–Na_2SO_4 and C) H_2SO_4–HNO_3–$(NH_4)_2SO_4$–NH_4NO_3. Solutions of H_2SO_4 (a) and HNO_3 (b) had pH values of 2.00, 2.58, 2.87, 3.28 and 3.75 (solutions 1 to 5). The H_2SO_4–HNO_3 solutions were obtained by mixing equivalent volume of solutions a and b, with the same pH values. Solutions A and B were obtained by adding 1.0 g of K_2SO_4 or Na_2SO_4 into H_2SO_4–HNO_3 solution. Solutions C were obtained by adding 0.50 g of $(NH_4)_2SO_4$ or NH_4NO_3 into 100 cm^3 of the H_2SO_4–HNO_3 solution.

Desorption procedure

After measuring the activity of the sample, 200 cm^3 of each solution was poured over 10.0 g of dried sample. The desorptions were performed at room temperature (≈ 22 °C) and lasted 24 h with occasional stirring. After this time, the solution was decanted, the sample dried and its activity remeasured.

Measurement of the ^{137}Cs activity in the sample

Before the first extraction and after every subsequent extraction, the filtrated and dried lichen sample was placed into a plastic vessel with a diameter of 7.5 mm and a volume of 150 cm^3. The activities of ^{137}Cs in every sample were measured under the same geometric conditions for 1 h using an HP Ge spectrometer (Ortec-Ametek), with 8193 channels, an energy resolution of 1.65 keV and a relative efficiency of 34 % at 1332.5 keV ^{60}Co. The activity values were used to calculate the specific activities (Bq/kg). The mass of the sample was reduced after extraction by 0.6 % (average value), *i.e.*, less than the error of the measurement.

RESULTS AND DISCUSSION

The content of ^{137}Cs in each sample was expressed as the percentage of the remaining radiocesium in the sample after each of the five consecutive desorptions, as related to its content in the original sample. All desorptions were repeated twice and the mean values are given in Tables I–III.

TABLE I. Activity[a] of ^{137}Cs (Bq/kg) in *C. islandica* lichen before desorption, totaly desorbed ^{137}Cs from lichen (%) and percentage of remaining ^{137}Cs in lichen after each desorption using the solution H_2SO_4–HNO_3–K_2SO_4 (A) (in relation to the starting content in lichen, 100 %). Room temperature (≈ 22 °C). Desorption time: 24 h. Mean measurement error: 1.64 %

pH value of solution A	Starting activity of ^{137}Cs in lichen before desorption, Bq/kg	Total desorbed ^{137}Cs from lichen %	Remaining ^{137}Cs in lichen after each desorption in relation to the starting content, %				
			Desorption				
			I	II	III	IV	V
2.00	2726	65.7	37.3	35.3	34.8	34.8	34.3
2.58	2938	67.0	40.3	35.5	33.7	33.2	33.0
2.87	2445	64.2	42.8	38.1	37.5	36.8	35.8
3.28	2435	64.5	38.8	37.5	36.7	36.2	35.5
3.75	2552	64.3	42.6	37.1	36.5	35.9	35.7

[a]Mean value from two measurements

TABLE II. Activity[a] of ^{137}Cs (Bq/kg) in *C. islandica* lichen before desorption, total desorbed ^{137}Cs from lichen (%) and percentage of remaining ^{137}Cs in lichen after each desorption using the solution H_2SO_4–HNO_3–Na_2SO_4 (B) (in relation to the starting content in lichen, 100 %). Room temperature (≈ 22 °C). Desorption time: 24 h. Mean measurement error: 1.64 %

pH value of solution B	Starting activity of ^{137}Cs in lichen before desorption, Bq/kg	Total desorbed ^{137}Cs from lichen %	Remaining ^{137}Cs in lichen after each desorption in relation to the starting content, %				
			Desorption				
			I	II	III	IV	V
2.00	2193	59.8	57.7	48.1	43.8	42.1	40.2
2.58	2266	61.0	53.4	47.9	46.1	40.5	39.0
2.87	2343	53.6	63.7	50.5	50.0	46.8	46.4
3.28	2140	52.9	63.8	51.7	49.8	47.2	47.1
3.75	2394	44.0	68.1	61.1	59.3	59.2	56.0

[a]Mean value from two measurements

According to the data in these Tables, high starting activity levels of ^{137}Cs (between 2140 and 3265 Bq/kg) were measured in all *C. islandica* samples. After five consecutive desorptions using solutions A, B and C, between 44.0 % (solution B, pH 3.75) and 68.8 % (solution C, pH 3.28) ^{137}Cs had been desorbed, leading to the conclusion that ^{137}Cs cannot be completely desorbed from lichen by this procedure. The solution pH influences ^{137}Cs desorption from lichen when the desorption was performed using solution B and to a lesser degree using solu-

tion C, which indicates an indirect or direct influence of H^+ in the desorption processes, besides the presence of Na^+ and NH_4^+ (Fig. 1).

TABLE III. Activity[a] of ^{137}Cs (Bq/kg) in *C. islandica* lichen before desorption, total desorbed ^{137}Cs from lichen (%) and percentage of remaining ^{137}Cs in lichen after each desorption using the solution H_2SO_4–HNO_3–$(NH_4)_2SO_4$–NH_4NO_3 (C) (in relation to the starting content in lichen, 100 %). Room temperature (≈ 22 °C). Desorption time: 24 h. Mean measurement error: 1.64 %

pH value of solution C	Starting activity of ^{137}Cs in lichen before desorption, Bq/kg	Total desorbed ^{137}Cs from lichen %	Remaining ^{137}Cs in lichen after each desorption in relation to the starting content, %				
			Desorption				
			I	II	III	IV	V
2.00	3265	62.7	47.3	38.9	38.5	37.9	37.3
2.58	2910	65.3	48.3	41.0	40.0	36.6	34.7
2.87	2902	65.4	47.4	41.9	39.7	39.0	34.6
3.28	2895	68.8	46.7	39.7	36.2	33.4	31.2
3.75	2863	63.3	51.6	43.8	41.8	40.1	36.7

[a]Mean value from two measurements

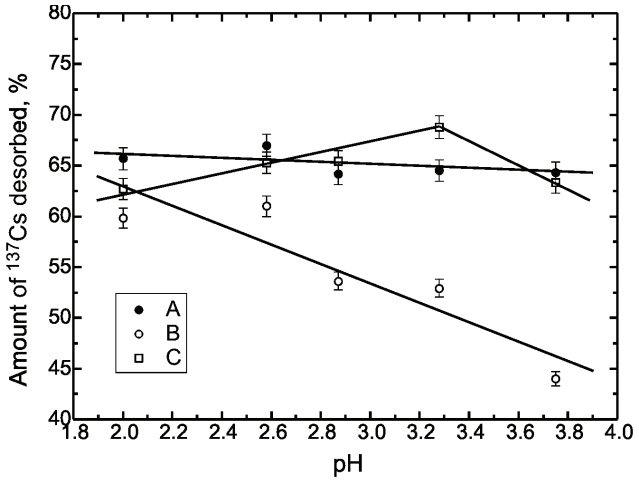

Fig. 1. Changes in the total amount of desorbed ^{137}Cs with the pH value of the desorption solutions A, B and C.

However, in the presence of K^+ (solution A), there were practically no changes in the amount of extracted ^{137}Cs with changing pH, indicating the specific and dominant influence of K^+ as compared to the influence of H^+ on ^{137}Cs desorption. This is in accordance with data obtained from the literature,[6,7] that Cs^+ in living organisms is the chemical and biochemical homologue of potassium, not HN_4^+. Also, the value of the ionic radius[9,10] (crystal) of Cs^+ (167 pm) is more

similar to the ionic radius of K^+ (133 pm) than to the ionic radius of Na^+ (97 pm), from which it differs significantly.

In all cases, the highest percentage of desorbed ^{137}Cs was achieved during the first desorption.

Consecutive desorptions with identical desorbent volumes led to changes in the amount of sorbed substance (c_x) with the number of desorptions (n_x). In order to analyze this dependence, the following equation was applied:

$$c_x = c_0 e^{-an} \quad (1)$$

where c_0 is the concentration of the sorbed substance (^{137}Cs) before desorption.[8]

Graphical representations using Origin 7.0 software[11] to the data given in Tables I–III gave curves showing an exponential dependence of the remaining amount of ^{137}Cs, *i.e.*, the desorbed amount, on the number of successive desorptions, regardless of the solution pH.

Application of the logarithmic form of Eq. (1) on the values given in Tables I–III resulted in two types of curves. A linear dependence was obtained using mixtures: A for pH 2.00 and 3.28; B for pH 2.58 and 3.75 and C for pH 2.87 and 3.28. This indicates that one sorption type is dominant in these cases. In all the other cases, curves like those given in Fig. 2 for selected examples were obtained. They are slightly different from those mentioned above and indicate the existence of at least two types of sorption, but when the corresponding desorbants were used, the desorption of ^{137}Cs was not sufficiently separated to be dominant. Desorptions performed with mixture A, pH 2.58, 2.87 and 3.75, B, pH 2.00, 2.87 and 3.28 and C pH 2.00, 2.58 and 3.75, gave this curve type. This shows the

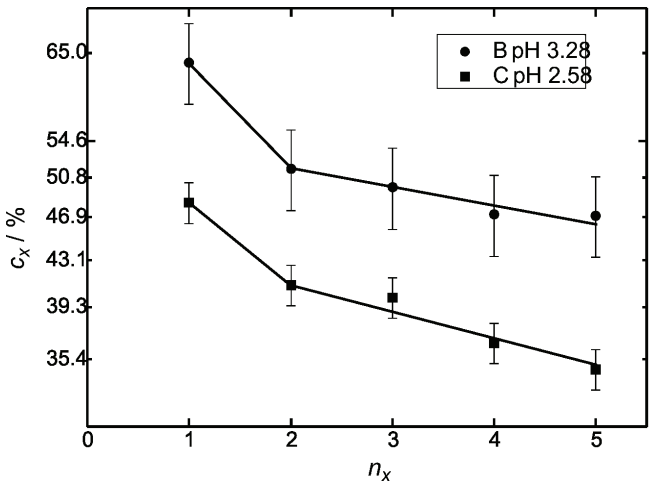

Fig. 2. Percentage of remaining ^{137}Cs content in lichen (shown on ln scale) as a function of the successive desorption number (n_x) according to Eq. (1), with solution B, pH 3.28 and solution C pH 2.58, for an equilibrium time of 24 h.

existence of the simultaneous action of H^+ and other cations that did not lead to the formation of dominant sorption, *i.e.*, a linear dependence according to Eq. (1).

The obtained results lead to the conclusion that *Cetraria islandica* lichen, *i.e.*, its remains, become sources of secondary pollution with radiocesium, not only due to the action of acid rain, *i.e.*, H^+, but also due to the action of K^+, *i.e.*, its compounds. To a lesser degree, the action of NH_4^+ is similar to that of K^+.

Acknowledgement. The Ministry of Science and Technological Development of the Republic of Serbia financially supported this work, Project No. ON142039.

ИЗВОД

ДЕСОРПЦИЈА ^{137}Cs ИЗ ЛИШАЈА *Cetraria islandica* (L.) Ach.
РАСТВОРИМА СМЕША КИСЕЛИНА И ЊИХОВИХ СОЛИ

АНА ЧУЧУЛОВИЋ[1], ДРАГАН ВЕСЕЛИНОВИЋ[2] и ШЋЕПАН С. МИЉАНИЋ[2]

[1]*ИНЕП – Институт за примену нуклеарне енергије, Банатска 31б, 11080 Земун и*
[2]*Факултет за физичку хемију, Универзитет у Београду, п.пр. 137, 11001 Београд*

Испитивана је десорпција ^{137}Cs из лишаја *Cetraria islandica* (L.) Ach. растворима: A) H_2SO_4–HNO_3–K_2SO_4, B) H_2SO_4–HNO_3–Na_2SO_4 и C) H_2SO_4–HNO_3–$(NH_4)_2SO_4$–$(NH)_4NO_3$ при pH 2,00; 2,58; 2,87; 3,28 и 3,75 сличним киселим кишама. После пет узастопних десорпција растворима A, B и C из лишаја је десорбовано од 44,0 % (раствор B, pH 3,75) до 68,8 % (раствор C, pH 3,28) ^{137}Cs. Најуспешнија десорпција ^{137}Cs је при првој десорпцији у свим случајевима. У присуству K^+ (раствор A) укупна количина десорбованог ^{137}Cs не зависи од pH раствора, што потврђује аналогне реакције Cs^+ и K^+, због сличних јонских пречника. Зависности недесорбоване количине ^{137}Cs од броја десорпција даје криве које указују да постоје најмање два типа сорпције, али да при коришћењу одговарајућих десорбенаса један од њих може да буде доминантан. Резултати указују да су лишајеви извори секундарног загађивања изотопом ^{137}Cs.

(Примљено 11. септембра 2008, ревидирано 10. фебруара 2009)

REFERENCES

1. A. Čučulović, D. Veselinović, Š. S. Miljanić, *J. Serb. Chem. Soc*. **72** (2007) 673
2. R. García, C. del Torres Ma, H. Padilla, R. Belmont, E. Azpra, F. Arcega-Cabrera, A. Báez, *Atmos. Environ.* **40** (2006) 6088
3. T. Ozeki, T. Ihara, N. Ogawa, *Chemom. Intell. Lab. Sys.* **82** (2006) 15
4. G. S. Zhang, J. Zhang, S. M. Liu, *Atmos. Res.* **85** (2007) 84
5. D. Veselinović, I. Gržetić, Š. Đarmati, D. Marković, *States and Processes in the Environment, Physicochemical Basics of Environmental Protection, Vol. 1*, Faculty of Physical Chemistry, Belgrade, 1995 (in Serbian)
6. I. Lovrenčić, M. Volner, D. Barišić, M. Popijac, N. Kezić, I. Seletković, S. Lulić, *J. Radioanal. Nucl. Chem*. **275** (2008) 71
7. Y.-G. Zhu, E. Smolders, *J. Exp. Bot*. **51** (2000) 1635
8. A. Čučulović, D. Veselinović, Š. S. Miljanić, *J. Serb. Chem. Soc*. **71** (2006) 565
9. *CRC Handbook of Chemistry and Physics*, CRC Press, Cleveland, OH, 1978
10. *Visual Elements: Group 1 – The Alkali Metals*, http://www.rsc.org/chemsoc/visualelements/Pages/data/intro_groupi_data.html (February, 2009)
11. Microcal Origin Software, version 7.0, http://www.OriginLab.com (February, 2009).

Journal of the Serbian Chemical Society
JSCS@tmf.bg.ac.rs • www.shd.org.rs/JSCS

J. Serb. Chem. Soc. 74 (6) 669–676 (2009)
JSCS–3865

UDC 547.783:543.544.5:665.58
Original scientific paper

Determination of methylparaben from cosmetic products by ultra performance liquid chromatography

MANUELA M. MINCEA[1,3], IOANA R. LUPŞA[3], DAN F. CINGHIŢĂ[1], CIPRIAN V. RADOVAN[1], IOAN TALPOS[2] and VASILE OSTAFE[1,2]*

[1]*West University of Timisoara, Faculty of Chemistry-Biology-Geography, Department of Chemistry, Pestalozzi Street, 16, Timisoara, 300115,* [2]*West University of Timisoara, Multidisciplinary Research Platform "Nicholas Georgescu – Roegen", Oituz 4, Timisoara and* [3]*Institute of Public Health Timisoara, Dept. of Food Hygiene, V. Babes 16–18, Timisoara 300226, Romania*

(Received 24 September 2008, revised 18 January 2009)

Abstract: A new method for the determination of methylparaben by ultra-performance liquid chromatography (UPLC) was developed. Methylparaben is often used as preservative, alone or in combination with other parabens, being added to cosmetic products, pharmaceutical products and foods to avoid microbial contamination. Due to its widespread use and potential risk to human health, assessing human exposure to this compound is of interest. A good determination and quantification of methylparaben was developed with a gradient elution using a mixture of methanol and water (60:40, v/v) within 1.455 min. Under optimized conditions, the linear working range extends over two orders of magnitude with relative standard deviations of intra- and inter-day precision below 2.3 %, and a detection limit of 0.02 ng μL^{-1} for methylparaben. The proposed method was successfully applied to the assay of methylparaben in cosmetic products with minimal sample preparation.

Keywords: UPLC; methylparaben; preservative; cosmetic products.

INTRODUCTION

Antimicrobial preservatives are used in cosmetics, foods, beverages and non-sterile pharmaceutical products (such as oral liquids and creams) to inhibit the growth of micro-organisms involuntarily introduced during manufacture or use.

Hydroxybenzoates (parabens) are alkyl esters of *p*-hydroxybenzoic acid with antibacterial and antifungal properties. While the antimicrobial activity increases with increasing alkyl chain length of the ester group, the aqueous solubility decreases, making the use of shorter chain esters more common because of their high solubility in water.[1] The activity may also be improved by combining two

* Corresponding author. E-mail: vostafe@cbg.uvt.ro
doi: 10.2298/JSC0906669M

hydroxybenzoates with short alkyl chains. Methylparaben ($C_8H_8O_3$, molecular mass 152.14 g mol^{-1}) is used alone or in combination with other parabens in some preparations, as they act as synergists.

Due to their broad antimicrobial spectra with relatively low toxicity, good stability and non-volatility,[2] parabens are commonly used as preservatives to prevent alteration and degradation of cosmetics, pharmaceuticals and foods from microbial and fungal contamination[3] and to protect the consumers.

Nearly all types of cosmetics products contain parabens, individually or in combination, which may come in touch with the skin, hair, scalp, lips, *mucosae*, *axillae* and nails, being used daily or occasionally,[1] in over 13200 formulations.[4]

The European Economic Community (EEC) Directive stipulates that parabens are permitted in a concentration of up to 0.8 % in cosmetics, with a maximum concentration for each individual one of 0.4 % (w/w), expressed as *p*-hydroxybenzoic acid.[5]

The super scale use of preservatives in cosmetics can result in potential health risks. Most of the preservatives may be harmful to the consumers due to their potency to induce allergic contact dermatitis. Some studies have reported that all commonly used parabens possess estrogenic activity in several *in vitro* assays and in animal models *in vivo*.[6–10]

Humans are exposed to low-dose but long-term levels of parabens and this type of preservative can be absorbed and retained in human body tissues without hydrolysis by tissue esterases to the common metabolite *p*-hydroxybenzoic acid. Consequently, a highly selective and sensitive method is required for the detection of methylparaben in cosmetic products.

The aim of this study was to develop a new, very fast and rapid method for the detection and quantification of methylparaben, the paraben most frequently used in cosmetic products.

EXPERIMENTAL

Reagents and chemicals

Methylparaben was obtained from Fluka, Switzerland. All the employed solvents were of HPLC grade and were obtained from Merck (Darmstadt, Germany). All other chemicals were analytical-reagent grade and deionized water was used to prepare all solutions.

UPLC instrument and conditions

The employed UPLC system was a Waters Acquity UPLC (from Waters, Mildford, USA, *via* Hemtek Co., Belgrade, Serbia and Chromaktiv, Bucharest, Romania), consisting of a binary solvent manager, a sample manager with an integral column heater module, a solvent tray module and a photo-diode array (PDA) detector. The analyte was determined using a BEH C_{18} (2.1×150) mm, 1.7 μm, column, also from Waters. Empower™ software was used. The column temperature was maintained at 30 °C. The autosampler temperature was set to 6 °C. The mobile phase A was 100 % methanol and mobile phase B was 0.05 % phosphoric acid in 60 % methanol. The flow rate was 0.250 mL/min. A gradient program was used starting with 100 % mobile phase B, followed by a linear increase in phase A until 30 % in 1 min and then

the percentage of mobile phase A was increased to 100 in the next 30 s. The column was eluted isocratically for 40 s and re-equilibrated for the next injection in 5 s. The injection volumes were varied between 1 and 7 μL (partial loop method). The UV signal was detected as the max plot in the range 190–400 nm (sampling rate: 20 pts/s). The advantages of the sub-routines of the Empower software, such as purity check and library match, were used throughout the sample analysis.

The UPLC mobile phases were freshly prepared daily and filtered through a 0.22 μm membrane filter (Millipore).

Stock solutions

The initial stock solutions of methylparaben (≈ 1 mg·mL^{-1}) were prepared by dissolving measured amounts of the analyte (approx. 0.01 g) in methanol (10 mL). Standard solutions were prepared by further dilution of the stock solutions with mobile phase B.

Sample preparation

The tested cosmetic products, including shampoo, shower gels, body lotions, balsams, body creams, sun creams, make-up removals, were obtained at local markets. A 5.0 mL volume of methanol was added to the cosmetic samples (0.50 g). The emulsions were sonicated for 10 min, diluted to 10 mL and filtered through 0.22 μm Millipore membrane filters.

RESULTS AND DISCUSSION

Optimization of the UPLC system

Using various liquid chromatography methods, several mobile phases have been reported for the separation of parabens, such as methanol–phosphate–water,[11–13] methanol–acetate buffer,[14] methanol–water,[1,15–18] acetonitrile–water,[19] acetonitrile–phosphate buffer,[20] acetonitrile–ammonium acetate,[21] methanol–acetic acid–water,[22] and acetonitrile–methanol–water.[23] In this work, the mobile phase of methanol–water–phosphoric acid was found to be suitable for the detection and quantification of methylparaben. Using a gradient mobile phase composed of methanol and water (60:40, v/v), the retention time of methylparaben was 1.455 min. A chromatogram of methylparaben, with PDA detection at the max-plot obtained under these conditions is shown in Fig. 1. The compounds were monitored by measurement of the peak area of methylparaben and the standard, and the ratio of peak area was calculated.

Linearity

Under the above-described optimum conditions, the calibration curve obtained with standard MP showed a good linear relationship in the interval 0.1–10 μg·mL^{-1}. A regression curve was constructed: $y = 2.07\times10^5x + 1.71\times10^3$, with $R > 0.9987$, where x represents concentration in μg mL^{-1} and y represents the UPLC peak area, which was automatically measured by the UPLC instrument, and R is the correlation coefficient. The detection limit for methylparaben, at a signal-to-noise ratio of three, was 0.02 ng μL^{-1} and the limit of quantification was 0.06 ng μL^{-1}. The calculations were performed by the Empower^{TM} program.

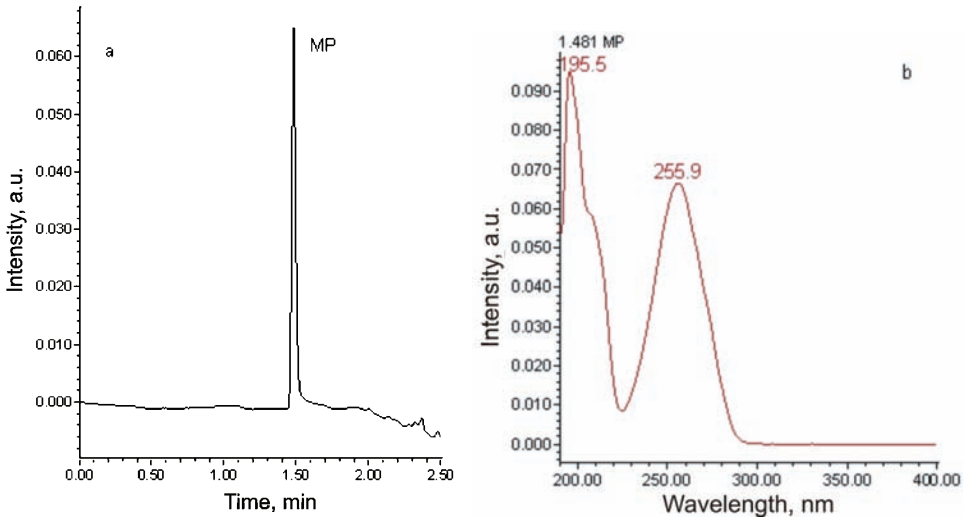

Fig. 1. A typical chromatogram of standard methylparaben using PDA detection at max-plot (a); for gradient elution, see the text; spectrum of methylparaben (b).

Precision

The intraday precision was tested with 5 repeated injections of methylparaben standard solutions at three concentration levels of 0.50, 1.0 and 5.0 $\mu g \cdot mL^{-1}$. The relative standard deviations (*RSD*) were below 2.3 %. The reproducibility of the chromatographic separation was very good as shown by the very narrow window of the retention time (Table I).

TABLE I. Precision and accuracy of the UPLC validation parameters of methylparaben

Characteristic	Type	Recovery, %	Peak area *RSD*, %	Retention time *RSD*, %
Precision	Intra-day	99–101	0.4–0.9	10^{-6}
	Inter-day	98.2–101.7	0.3–1.3	10^{-4}
Accuracy	Intra-day	97.7–102.1	0.9–2.1	10^{-4}
	Inter-day	96.5–103.1	1.4–2.8	10^{-4}

Accuracy

Five placebo samples of products without methylparaben were spiked with reference standard solutions. These samples were treated as described in the sample preparation procedure. The data obtained were compared with the theoretical concentrations. Under these conditions, the accuracy was expressed as percentage recovery. The relative standard deviations of the set results were determined. The extraction efficiency was determined by comparing the analysis of the standards solutions, and un-spiked and spiked samples.

Recovery

The recovery of spiked methylparaben in some cosmetic samples is shown in Table II. A comparison of an un-fortified and fortified shower gel sample is presented in Fig. 2.

TABLE II. The recovery of spiked methylparaben in cosmetic samples[a]

Spiked level, ng g^{-1}	Recovery, %		
	Balsam	Shower gel	Make-up removal (cleaning milk)
20	97.6±3.2	102.6±1.3	101.1±4.1
50	98.0±2.1	97.4±1.9	104.2±2.3
200	101.4±1.9	102.6±2.1	101.8±3.8

[a]Values are the means of three determinations ± standard deviation

It was found that the contents of methylparaben in the tested cosmetic products all satisfied the permitted concentration of the EEC Directive.

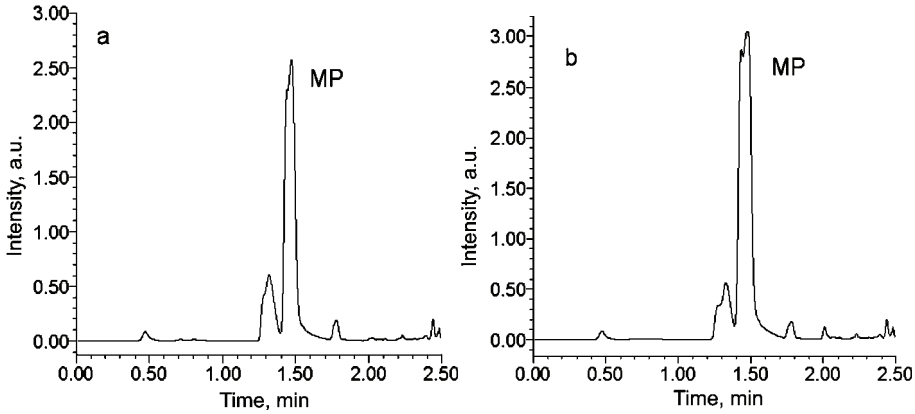

Fig. 2. Chromatogram of shower gel extract (a) and the same sample fortified with 90 ng g^{-1} MP (b).

Application of the method to cosmetic samples

The UPLC method was used for the quantification of methylparaben in various types of cosmetic products. The fact that in some sample methylparaben co-eluted with unidentified compounds was solved using the spectral analysis routine. The chromatogram of a hair balsam extract, as an example where methylparaben co-eluted with an unknown compound, is presented in Fig. 3. This drawback was, however, solved with the help of the purity check and library match routines of the Empower software.

Various types of cosmetic samples, including balsams, shower gels, sun creams, body lotions, anti-cellulite, feminine hygiene products and make-up removal (cleaning milk), were tested in this study. All the tested sample solutions

were found to contain between 16 and 680 mg·kg^{-1} methylparaben. In all the analyzed samples, the level of methylparaben was under 0.4 %, the high limit imposed by European regulations.

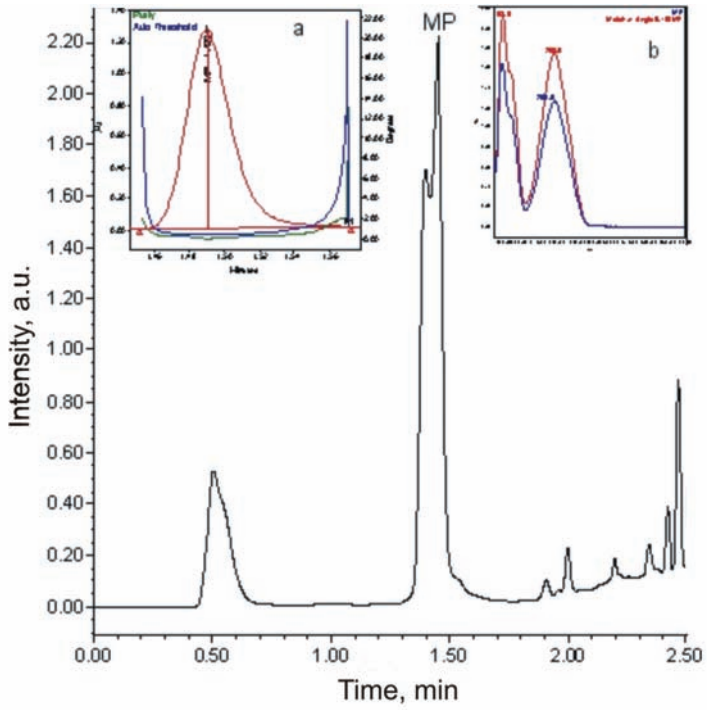

Fig. 3. Chromatogram of a hair balsam extract. The methylparaben co-eluted with an unknown compound. The peak purity check and library match routines helped in the identification and quantification of the analyte.

CONCLUSIONS

In conclusion, the proposed method allows a rapid and sound quantification of methylparaben in cosmetic samples, being based on a simple and rapid sample preparation procedure and a very fast and reliable chromatographic separation. The method can be used to monitor the occurrence at trace level of methylparaben preservative in cosmetic samples found on the market.

Acknowledgments. This project was financially supported by Romanian Grant CNCSIS, Type TD, Code No.111, and CNCSIS Grant No. 98/2006-2008, Multidisciplinary Research Platform “Nicholas Georgescu – Roegen”.

ИЗВОД

ОДРЕЂИВАЊЕ МЕТИЛПАРАБЕНА У КОЗМЕТИЧКИМ ПРОИЗВОДИМА ПРИМЕНОМ UPLC МЕТОДЕ

MANUELA M. MINCEA[1,3], IOANA R. LUPŞA[3], DAN F. CINGHIŢĂ[1], CIPRIAN V. RADOVAN[1], IOAN TALPOS[2] и VASILE OSTAFE[1,2]

[1]West University of Timisoara, Faculty of Chemistry-Biology-Geography, Department of Chemistry, Pestalozzi Street, 16, Timisoara, 300115, [2]West University of Timisoara, Multidisciplinary Research Platform "Nicholas Georgescu – Roegen", Oituz 4, Timisoara и [3]Institute of Public Health Timisoara, Dept. of Food Hygiene, V. Babes 16–18, Timisoara 300226, Romania

Развијена је метода за одређивање метилпарабена у козметичким производима применом UPLC методе. Из класе парабена, метилпарабени су најчешће коришћена једињења као конзерванси у козметичким и фармацеутским производима и храни. Анализа поменутог једињења је значајна имајући у виду широку употребу и потенцијални здравствени ризик због изложености. Идентификација и одређивање метилпарабена су изведени веома брзом процедуром, за око 1,5 min, са минималном припремом узорка, UPLC системом уз коришћење PDA детектора (BEH C_{18} (2,1×50) mm, 1,7 μm колона, градијентно елуирање смешом метанол–вода (60:40, v/v). Под оптималним условима радни линерани опсег одређивања метилпарабена обухвата два реда величине са релативном стандардном девијацијом до 2,4 %, и границама детекције од 2,45 ng ml^{-1}.

(Примљено 24. децембер 2008, ревидирано 18. јануара 2009)

REFERENCES

1. Q. Zhang, M. Lian, L. Liu, H. Cui, *Anal. Chim. Acta* **537** (2005) 31
2. F. F. Cantwell, *Anal. Chem.* **48** (1976) 1854
3. M. G. Soni, I. G. Carabin, G. A. Burdock, *Food Chem. Toxicol.* **43** (2005) 985
4. R. L. Elder, *J. Am. Coll. Toxicol.* **3** (1984) 147
5. Anon, Council Directive 76/768/EC, In: *Off. J. Eur. Commun.* L 262 (1976)
6. E. J. Routledge, J. Parker, J. Odum, J. Ashby, J.P. Sumpter, *Toxicol. Appl. Pharmacol.* **153** (1998) 12
7. S. Oishi, *Food Chem. Toxicol.* **40** (2002) 1807
8. R. M. Blair, H. Fang, W. S. Branham, B. S. Hass, S. L. Dial, C. L. Moland, W. Tong, L. Shi, R. Perkins, D. M. Sheehan, *Toxicol. Sci.* **54** (2000) 138
9. T. Okubo, Y. Yokoyama, K. Kano, I. Kano, *Food Chem. Toxicol.* **39** (2001) 1225
10. J. R. Byford, L. E. Shaw, M. G. B. Drew, G. S. Pope, M. J. Sauer, P. D. Darbrre, *J. Steroid Biochem. Mol. Biol.* **80** (2002) 49
11. E. Sottofattori, M. Anzaldi, A. Balbi, G. Tonello, *J. Pharm. Biomed. Anal.* **18** (1998) 213
12. M. J. Akhtar, S. Khan, I. M. Roy, I. A. Jafri, *J. Pharm. Biomed. Anal.* **14** (1996) 1609
13. S. H. Kang, H. Kim, *J. Pharm. Biomed. Anal.* **15** (1997) 1359
14. B. Saad, M. F. Bari, M. I. Saleh, K. Ahmad, M. K. M. Talib, *J. Chromatogr. A* **1073** (2005) 393
15. M. Thomassin, E. Cavalli, Y. Guillaume, C. Guinchard, *J. Pharm. Biomed. Anal.* **15** (1997) 831
16. G. Burini, *J. Chromatogr. A* **664** (1994) 213
17. X. Ye, A. M. Bishop, L. L. Needham, A. M. Calafat, *Anal. Chim. Acta* **622** (2008) 150
18. X. Ye, A. M. Bishop, L. L. Needham, A. M. Calafat, *Talanta* **76** (2008) 865

19. S. Scalia, D. E. Games, *Analyst* **117** (1992) 839
20. J. E. Belgaied, H. Trabelsi, *J. Pharm. Biomed. Anal.* **33** (2003) 991
21. A. Panusa, L. Gagliardi, *J. Pharm. Biomed. Anal.* **47** (2008) 786
22. L. Labat, E. Kummer, P. Dallet, J. P. Dubost, *J. Pharm. Biomed. Anal.* **23** (2000) 763
23. L. Nováková, P. Solich, L. Matysová, J. Sícha, *Anal. Bioanal. Chem.* **379** (2004) 781.

Journal of the Serbian Chemical Society
JSCS@tmf.bg.ac.rs • www.shd.org.rs/JSCS

J. Serb. Chem. Soc. 74 (6) 677–688 (2009)
JSCS–3866

UDC 543.544+66.097.8+577.15:577.121
Original scientific paper

Normal-phase thin-layer chromatography of some angiotensin converting enzyme (ACE) inhibitors and their metabolites

JADRANKA ODOVIĆ[1], MIRJANA ALEKSIĆ[1], BILJANA STOJIMIROVIĆ[2], DUŠANKA MILOJKOVIĆ-OPSENICA[3#] and ŽIVOSLAV TEŠIĆ[3*#]

[1]*Faculty of Pharmacy, University of Belgrade, P.O. Box 146, 11001 Belgrade,* [2]*School of Medicine, University of Belgrade, P.O. Box 840, 11000 Belgrade and* [3]*Faculty of Chemistry, University of Belgrade, P.O. Box 51, 11158 Belgrade, Serbia*

(Received 16 October 2008)

Abstract: The separation and chromatographic behaviour of five ACE (angiotensin converting enzyme) inhibitors and their four active metabolites were investigated by normal-phase thin-layer chromatography on silica using several mono- and binary non-aqueous solvent systems. The linear relationship between the R_M values and the composition of employed mobile phase was obtained. The hydrophobicity parameters R_M^0 and C_0 were determined from the regression data of the plots, analogous to reversed-phase chromatography. The chromatographically obtained hydrophobicity parameters were correlated with the calculated log *P* values. The current results were correlated with the lipophilicity of the studied ACE inhibitors and their metabolites, previously estimated by reversed-phase chromatography.

Keywords: ACE inhibitors; normal-phase thin-layer chromatography; hydrophobicity.

INTRODUCTION

Due to the utmost significance of structure/biological activity relationships of pharmaceuticals, interest in this field of research has been continually increasing. The biological activity of a substance depends on the structural, physiccal and chemical properties of its molecule and the lipophilicity (hydrophobicity), determining to a great extent biological activity, represents a very important feature. Thus, the well-known Lipinski "rule of 5" predicts that poor absorption or permeation of drugs is more likely when there are more than 5 hydrogen-bond donors or 10 hydrogen-bond acceptors, the molecular weight is greater than 500 and the calculated log *P* (*C* log *P*) is greater than 5.[1]

* Corresponding author. ztesic@chem.bg.ac.rs
# Serbian Chemical Society member.
doi: 10.2298/JSC0906677O

As early as 1964, Fujita *et al.*[2] introduced the concept of hydrophobicity and expressed it by the partition (distribution) coefficient as the log *P* value, defining it as the logarithm of the ratio of the concentrations of the examined substance in both phases of a saturated biphasic system consisting of 1-octanol and water:

$$\log P = \log \frac{c_o}{c_w} \quad (1)$$

where c_o represents the concentration of the substance in 1-octanol and c_w its concentration in water when the system is at equilibrium.

The so-called "shake flask" method represents a traditional approach for the determination of the lipophilicity of a molecule, *i.e.*, of the log *P* value.[3] However, since this method suffers from several drawbacks, such as poor reproducibility, time consuming, impossibility to be applied for extremely hydrophilic or lipophilic components, the lipophilicity of a biologically active substances is experimentally determined at present by chromatographic methods, primarily by the highly efficient reversed-phase liquid chromatography (RP-HPLC) and reversed-phase thin-layer chromatography (RP-TLC).[3–6] The chromatographic determination of lipophilicity is based on the distribution of the analyte between an expressively non-polar stationary phase (usually RP-18 silica gel) and a polar mobile phase (a binary system water – organic solvent with a relatively high water content). Taking into consideration that under the conditions of normal--phase chromatography, the analyte is distributed during the chromatographic procedure between the two phases significantly differing from each other in polarity, it is to be expected that this chromatographic method might be employed for the determination of relative lipophilicity. There are even several reports in the available literature describing such attempts.[7–9]

The chromatographic behaviour of different organic and inorganic, primarily biologically active substances, under conditions of reversed- and normal-phase planar chromatography has been the subject of our long-range project. Within the scope of these studies, the chromatographic behaviour of a series of ACE inhibitors has been examined by the methods of RP-TLC, applying conventional reversed-phase chromatography on a thin layer of RP-18 silica gel and binary systems water–organic solvent, as well as the salting-out TLC method.[10,11] Based on the obtained results, the parameters of lipophilicity of the examined compounds were calculated and correlated to computer-calculated log *P* values.

ACE inhibitors belong to a large and very significant family of pharmaceuticals. They are widely applied in clinical practice for the prevention and therapy of hypertension, heart failure and myocardial infarction. These drugs occur in pharmaceutical formulations as esters, which are enzymatically hydrolyzed under *in vivo* conditions to their di-acid forms representing their active metabolites. Lisinopril, already occurring in pharmaceutical formulation in its di-acid form

and captopril, which is not subjected to hydrolysis under *in vivo* conditions but forms disulfides, represent two exceptions among the examined ACE inhibitors.[12,13]

Among the approaches applied for the determination of ACE inhibitors and their metabolites in biological materials and pharmaceutical formulations, several methods, such as HPLC,[14,15] planar chromatography,[15] capillary zone electrophoresis,[16] spectrophotometry,[17] spectrofluorometry[17] and gas chromategraphy[18] have been employed so far. In addition, the activity and activity/physico-chemical properties relationships of these substances, mainly their lipophilicity,[19–21] were most frequently studied by reversed-phase liquid chromatography procedures.

As a continuation of studies on the chromatographic behaviour of ACE inhibitors, this work was concentrated on the examination of the retention of five ACE inhibitors and their metabolites employing the method of normal-phase thin-layer chromatography (NP-TLC) on silica gel plates. The main objective of this study was to investigate the feasibility of applying the NP-TLC method for the experimental determination of lipophilicity of these compounds.

EXPERIMENTAL

The substances investigated throughout the present study are listed in Table I.

The TLC experiments were performed on silica gel 10×10 cm TLC plates (Art. 5644, Merck, Darmstadt, Germany). The plates were spotted with 2 µl aliquots of freshly prepared ethanolic solutions of substances **1**, **3**, **5** and **8**, an aqueous solution of **7** and methanolic solutions of substances **2**, **4**, **6** and **9** (all about 2 mg/ml) and developed by the ascending technique. The solvent systems employed are listed in Tables II and III. All the components contained in the employed mobile phases were of analytical grade purity.

After development, detection was realised by exposing the plates to iodine vapour. All investigations were performed in triplicate at ambient temperature (22±2 °C).

TABLE I. The investigated substances

No	Structure	Name
1	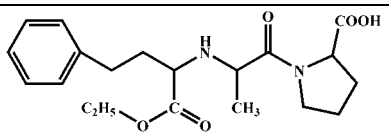	Enalapril, (*S*)-1-[*N*-[1-(ethoxycarbonyl)-3--phenylpropyl]-L-alanyl]-L-proline Krka Research and Development Division
2	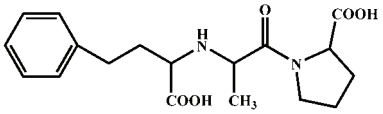	Enalaprilat, (*S*)-1-[*N*-(1-carboxy-3-phenylpropyl)--L-alanyl]-L-proline dehydrate Krka Research and Development Division
3	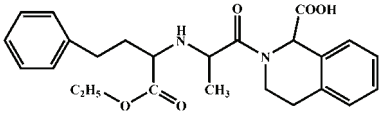	Quinapril, [3*S*-[2[*R**(*R**)],3*R**]]-2-[2-[[1-(etho-xycarbonyl)-3-phenylpropyl]amino]-1-oxopropyl]-1,2,3,4 -tetrahydro-3-isoquinolinecarboxylic acid Parke-Davis Pharmaceutical Research

TABLE I. Continued

No	Structure	Name
4	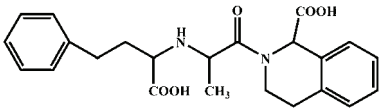	Quinaprilat, [3*S*-[2[*R**(*R**)],3*R**]]-2-[2-[(1-carboxy-3-phenylpropyl)- amino]-1-oxopropyl]--1,2,3,4-tetra- hydro-3-isoquinolinecarboxylic acid Parke-Davis Pharmaceutical Research
5	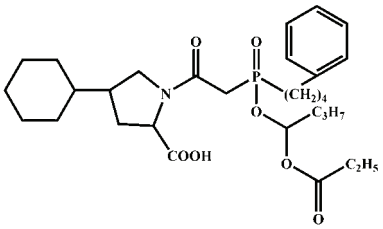	Fosinopril, [1 [*S**(*R**)],2α,4β]-4-cyclohexyl-1-[[[2--methyl-1-(1-oxo- propoxy)propoxy](4-phenylbutyl)-phosphinyl]acetyl]-L-proline Bristol-Myers Squibb Pharmaceutical Research Institute
6	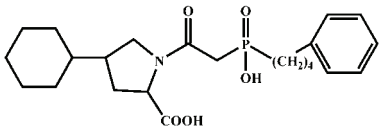	Fosinoprilat, *trans*-4-cyclo-hexyl-1-[[hydroxy(4--phenyl-butyl)phosphinyl]acetyl]-L- proline Bristol-Myers Squibb Pharmaceutical Research Institute
7	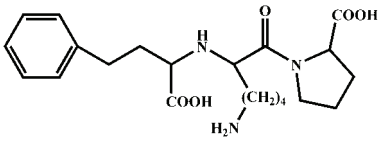	Lisinopril, (*S*)-1-[N^2-(1-carboxy-3-phenylpropyl)--L-lysyl]-L-proline dehydrate Belupo Pharmaceutical & Cosmetic Quality Control Department
8	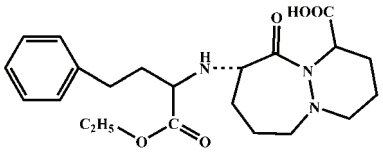	Cilazapril, [1*S*-[1α,9α (*R**)]]-9-[[1-(ethoxycarbonyl)-3-phenylpropyl]amino]octahydro--10-oxo-6*H*-pyridazino[1,2-*a*]- [1,2]diazepine--1-carboxylic acid monohydrate Roche Pharmaceuticals
9	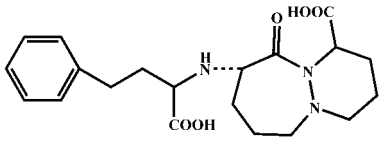	Cilazaprilat, [1*S*-[1α,9α (*R**)]]-9-[(1-carboxy-3--phenylpropyl)amino]octahydro-10-oxo-6*H*--pyridazino [1,2-a]- [1,2]diazepine--1-carboxylic acid Roche Pharmaceuticals

TABLE II. R_F×100 values of the investigated substances obtained by mono-component mobile phase

Mobile phase	Substance[a]								
	1	**2**	**3**	**4**	**5**	**6**	**7**	**8**	**9**
Methanol	81	54	92	86	94	86	12	64	35
Ethanol	77	22	88	71	92	80	11	44	37
n-Propanol	67	15	63	38	68	42	10	24	4
Isoropanol	60	8	63	22	75	55	0	20	0
Isobutanol	20	2	41	18	43	29	0	16	0
Acetone	18	0	25	12	14	4	0	8	0
Ethyl methyl ketone	30	0	41	17	19	14	0	11	0

[a]The numbers denote the substances, see Table I

TABLE III. R_F×100 values of the investigated substances obtained with two-component mobile phases

Substance[a]	*y*(ethanol) / %														
	Ethanol–ethyl methyl ketone					Ethanol–carbon tetrachloride					Ethanol–toluene				
	50	40	30	20	10	80	70	60	50	40	80	70	60	50	40
1	59	51	44	34	25	66	59	51	43	35	48	45	42	38	33
2	6	5	4	3	1	19	16	13	10	5	19	15	12	9	5
3	77	73	70	68	66	74	69	66	63	60	79	74	68	64	62
4	67	64	61	57	53	53	47	42	37	29	64	60	57	54	51
5	62	57	53	49	44	70	62	54	47	40	72	68	65	62	58
6	14	11	9	6	4	21	18	16	13	9	37	32	25	18	12
7	5	3	1	0	0	5	3	2	0	0	11	8	6	4	0
8	37	32	28	22	18	50	46	40	34	28	51	48	46	44	41
9	7	5	2	0	0	8	6	4	3	0	16	13	10	7	4

[a]The numbers denote the substances, see Table I

The R_M values were calculated for each solute in each mobile phase according to the Bate-Smith and Westall equation:[22]

$$R_M = \log (1/R_F - 1) \quad (2)$$

RESULTS AND DISCUSSION

The chromatographic behaviour of the examined ACE inhibitors and their metabolites and the feasibility of applying the normal-phase TLC method for the determination of their lipophilicity were investigated using thin-layer silica gel plates and several non-aqueous mono- and two-component solvents as the mobile phase. The results are summarized in Tables II and III, respectively.

The results obtained throughout the study of ACE inhibitors and their metabolites employing mono-component solvents (Table II) show a satisfactory accordance to their chromatographic behaviour with the method of normal-phase thin-layer chromatography. Namely, the retention order of the examined substances obtained by alcohols as the mobile phase is in agreement with the elution strength, ε^0, as well as with the polarity of the applied solvents, *i.e.*, the less polar the solvent, the stronger the retention. Hence, the strongest retention of the examined substances was recorded when isobutanol, as the least polar among the applied alcohols with a *P'* value of 3.9, was used and the weakest retention of the ACE inhibitors and their metabolites was observed when the very polar methanol (*P'* of 6.6)[23] was employed. However, such a regularity was not observed in case of ketones.

Also, the results obtained during the examinations of the ACE inhibitors and their metabolites applying two-component solvents (Table III) demonstrate a decrease of R_F values, *i.e.*, increased retention of the examined substances in paral-

lel with increasing concentrations of the less polar component in the mobile phase, which is in accordance with the normal-phase chromatographic mode.

The results summarized in Tables II and III indicate significant differences in the R_F values, *i.e.*, in the retention of the examined ACE inhibitors and their metabolites. In all instances, it was established that the metabolites exhibit a stronger retention, *i.e.*, they have lower R_F values compared to the corresponding parent ACE inhibitor. Such a behaviour of the examined substances under conditions of normal-phase TLC is contrary to that observed by reversed-phase chromatography (both the salting-out method and classical reversed-phase TLC chromatography on RP-18 silica) when the retention of the less polar ACE inhibitors was found to be much stronger than that of their metabolites.

This distinction in the chromatographic behaviour of the ACE inhibitors and their metabolites results from differences in their interaction with silica gel. Namely, due to the presence of two carboxylic groups in the molecule of the metabolites (including substance **7**), their specific interactions with silica gel (hydrogen bonds) are much stronger than those of the corresponding ACE inhibitors, containing only one carboxylic group within their molecule.

Based on the obtained retention parameters of the examined ACE inhibitors and the corresponding metabolites, separation factors (log α) were calculated (Table IV). Comparison of these values and the values of the separation factors calculated for two reversed-phase systems[11] revealed no significant differences in the separation selectivity of the ACE inhibitors and their metabolites between normal- and reversed-phase methods.

The retention behaviour of the examined substances obtained by reversed--phase TLC can be graphically presented as the relationship of the R_M value and the content of the less polar component of the mobile phase. The obtained linear relationships can be presented by the equation of a straight line $R_M = R_M^0 + mC$. The value of the intercept, R_M^0, represents the lipophilicity of the examined substance, while the value of the slope, m, corresponds to the specific hydrophobic surface area of this substance and C represent the content of the more polar component in the mobile phase. Based on the obtained intercept and slope values, another hydrophobic parameter, $C_0 = -R_M^0/m$, can be calculated. This hydrophobicity parameter corresponds to the parameter φ_0, previously defined for the HPLC method as the concentration of the organic component in the mobile phase for which the distribution of the analyzed substance between the mobile and stationary phase is equal (1:1).[25]

The same approach was applied in previous attempts to employ normal--phase chromatography for lipophilicity determinations.[7–9] Accordingly, the results obtained throughout the present study by normal-phase TLC are expressed analogously to those obtained by reversed-phase chromatography as the relationship of the R_M values and the content of ethanol, as the more polar component, in

the mobile phase. As seen from Fig. 1, linear relationships with very high values of the correlation coefficients were recorded for all employed solvent systems. Based on the intercept values and the slope of the plots, the parameter C_0 was calculated. The obtained regression parameters are presented in Table V. The results clearly demonstrate lower R_M^0 values for the more lipophilic compounds, *i.e.* the ACE inhibitors in relation to the corresponding metabolites. This phenomenon was the consequence of the application of normal-phase chromatographic method for the estimation of hydrophobicity of the examined substances and can be solved by presenting linear relationships of the retention and the content of less polar (instead of more polar) component in a binary non-aqueous mobile phase.

TABLE IV. The logarithm of separation factors calculated by relation: log $\alpha = |\Delta R_M|$[24]

Solvent system	y^a / %	Log $\alpha_{1,2}$	Log $\alpha_{3,4}$	Log $\alpha_{5,6}$	Log $\alpha_{8,9}$
Ethanol–ethyl methyl ketone	50[a]	1.353	0.217	1.001	0.892
	40	1.296	0.182	1.030	0.951
	30	1.174	0.174	1.057	1.280
	20	1.222	0.205	1.178	–
	10	1.519	0.236	1.275	–
Ethanol–carbon tertachloride	80	0.918	0.402	0.943	1.061
	70	0.878	0.400	0.871	1.125
	60	0.843	0.428	0.790	1.204
	50	0.832	0.462	0.773	1.222
	40	1.010	0.565	0.829	–
Ethanol–toluene	80	0.595	0.326	0.641	0.738
	70	0.666	0.278	0.655	0.791
	60	0.725	0.205	0.746	0.885
	50	0.792	0.180	0.871	1.019
	40	0.971	0.195	1.005	1.222
Water–methanol	40	1.091	1.059	–	1.173
	50	0.863	0.933	–	1.159
	60	0.654	0.701	0.272	0.815
	70	0.540	0.598	0.219	0.577
	80	0.593	0.528	0.340	0.511
Water–acetone	10	1.261	1.201	–	1.431
	20	1.113	0.983	0.505	1.189
	30	1.008	0.844	0.413	1.050
	40	0.806	0.800	0.403	0.957
	50	0.725	0.716	0.429	0.858

In order to check the applicability of normal-phase thin-layer chromategraphy for the determination of the lipophilicity of the examined substances, the hydrophobic parameters R_M^0 and C_0 were correlated with computer-assisted calculations of the values of log P[11] and with experimentally determined ones.[26] Experimentally determined log P values are available for substances **1** (2.45), **3**

(3.72), **5** (6.61) and **7** (–1.22). As it can be seen from Tables VI and VII, relatively satisfactory linear relationships[27] were obtained for all solvent systems employed in this study (in all instances r was statistically significant at the $P < 0.05$ level).

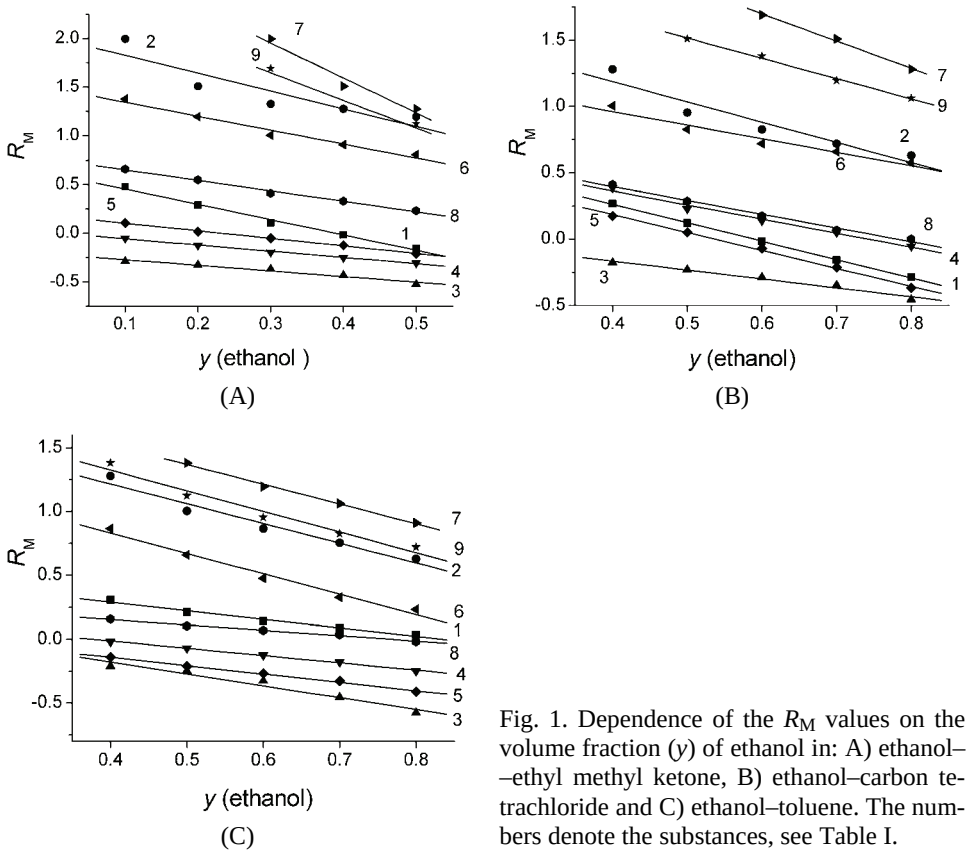

Fig. 1. Dependence of the R_M values on the volume fraction (y) of ethanol in: A) ethanol–ethyl methyl ketone, B) ethanol–carbon tetrachloride and C) ethanol–toluene. The numbers denote the substances, see Table I.

Comparison of these results with previous data obtained by reversed-phase TLC[11] strongly recommends normal-phase thin-layer chromatography as a suitable method for the estimation of the lipophilicity of the examined substances.

In addition, the hydrophobic parameters, R_M^0, obtained throughout the present study by normal-phase TLC using ethanol–ethyl methyl ketone, were correlated with the R_M^0 parameters obtained by reversed-phase TLC using water–methanol as the mobile phase. Based on the relationship presented in Fig. 2, it can be seen that the examined substances are classified into groups forming two series. The metabolites of the examined ACE inhibitors, being more polar than the corresponding parent molecules, belong to the first series and the second series includes the more lipophilic ACE inhibitors, themselves. The exception is fo-

TABLE V. Regression hydrophobicity parameters of the investigated compounds

No.[a]	Log *P*	Ethanol–ethyl methyl ketone				Ethanol–carbon tetrachloride				Ethanol–toluene			
		R_M^0	$-m$	$-r$	C_0	R_M^0	$-m$	$-r$	C_0	R_M^0	$-m$	$-r$	C_0
1	0.33	0.612±0.028	1.576±0.084	0.996	0.388	0.82±0.010	1.394±0.016	0.999	0.590	0.559±0.032	0.671±0.053	0.991	0.833
2	-0.59	2.011±0.165	1.832±0.498	0.905	1.097	1.801±0.163	1.532±0.264	0.958	1.175	1.836±0.112	1.549±0.182	0.980	1.185
3	1.77	–0.215±0.022	0.578±0.066	0.981	-0.371	0.104±0.036	0.673±0.059	0.989	0.155	0.194±0.068	0.930±0.110	0.980	0.209
4	1.12	0.006±0.007	0.638±0.022	0.998	0.010	0.789±0.045	1.061±0.072	0.993	0.743	0.216±0.015	0.571±0.025	0.997	0.378
5	8.93	0.179±0.007	0.774±0.022	0.999	0.231	0.727±0.026	1.353±0.042	0.997	0.538	0.121±0.016	0.655±0.026	0.998	0.185
6	5.38	1.489±0.045	1.434±0.134	0.987	1.038	1.372±0.079	1.026±0.128	0.977	1.338	1.472±0.077	1.599±0.124	0.991	0.920
7	-0.48	3.028±0.301	3.584±0.736	0.979	0.845	2.933±0.102	2.057±0.145	0.997	1.426	2.144±0.047	1.551±0.071	0.998	1.382
8	1.04	0.758±0.018	1.077±0.054	0.996	0.704	0.812±0.035	1.039±0.057	0.996	0.782	0.322±0.013	0.421±0.020	0.996	0.766
9	0.46	2.498±0.302	2.834±0.739	0.968	0.881	2.282±0.050	1.532±0.076	0.997	1.490	1.971±0.106	1.618±0.172	0.983	1.218

[a]The numbers denote the substances, see Table I

TABLE VI. Equations and correlation coefficients for R_M^0 and C_0 *vs.* the calculated log *P* values

Solvent system	Equation	–*r*	*SD*
Ethanol–ethyl methyl ketone	$R_M^0 = 1.874 \pm (0.355) - (1.212 \pm (0.372))\ \log P$	0.825	0.786
	$C_0 = 0.775 \pm (0.143) - (0.512 \pm (0.150))\ \log P$	0.836	0.317
Ethanol–carbon tetrachloride	$R_M^0 = 1.855 \pm (0.288) - (0.944 \pm (0.302))\ \log P$	0.813	0.638
	$C_0 = 1.130 \pm (0.154) - (0.424 \pm (0.162))\ \log P$	0.761	0.342
Ethanol–toluene	$R_M^0 = 1.488 \pm (0.247) - (0.868 \pm (0.259))\ \log P$	0.832	0.547
	$C_0 = 1.093 \pm (0.097) - (0.460 \pm (0.102))\ \log P$	0.897	0.215

TABLE VII. Equations and correlation coefficients for R_M^0 and C_0 *vs.* the experimentally determined log *P* values

Solvent system	Equation	–*r*	*SD*
Ethanol–ethyl methyl ketone	$R_M^0 = 2.019 \pm (0.650) - (0.387 \pm (0.161))\ \log P$	0.861	0.907
	$C_0 = 0.556 \pm (0.341) - (0.098 \pm (0.085))\ \log P$	0.632	0.477
Ethanol–carbon tetrachloride	$R_M^0 = 2.036 \pm (0.647) - (0.304 \pm (0.160))\ \log P$	0.801	0.902
	$C_0 = 1.042 \pm (0.303) - (0.126 \pm (0.075))\ \log P$	0.765	0.422
Ethanol–toluene	$R_M^0 = 1.527 \pm (0.332) - (0.267 \pm (0.082))\ \log P$	0.917	0.462
	$C_0 = 1.126 \pm (0.182) - (0.164 \pm (0.045))\ \log P$	0.931	0.254

sinoprilat, which practically represents an outlier for the metabolites. However, this deviation is in accordance with the structural diversity of the investigated substances: in contrast to the other studied metabolites that contain two carboxylic groups, fosinopirilat contains one carboxylic and one phosphinyl group. (As is known, a good correlation is only possible in closely related analogue series.[1])

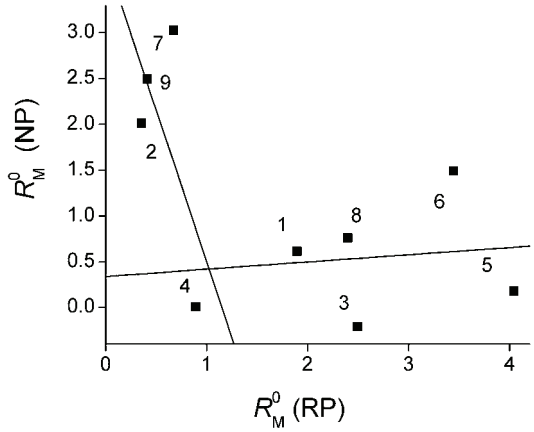

Fig. 2. Correlation between the NP (ethanol–ethyl methyl ketone) and RP (water–methanol) lipophilicity chromatographic data. The numbers denote the substances, see Table I.

CONCLUSIONS

The results obtained during the current study on the retention behaviour of several ACE inhibitors and their metabolites applying normal-phase TLC on silica gel plates, *i.e.*, conspicuous differences between the R_F values of these two

groups of substances, clearly demonstrate that this method is very suitable for their chromatographic separation. Based on the observed correlation of the chromatographically determined hydrophobicity parameters R_M^0 and C_0 and computer-assisted calculated log *P* values, it can be concluded that normal-phase TLC represents a reliable method for an estimation of the lipophilicity of the examined substances. Comparison of the results obtained by normal-phase TLC with those obtained by conventional reversed-phase TLC revealed no significant differences with regard to the estimation of the lipophilicity.

Acknowledgement. The authors are grateful to the Ministry of Science of the Republic of Serbia (Project No. 142062) for financial support.

И З В О Д

НОРМАЛНО-ФАЗНА ТАНКОСЛОЈНА ХРОМАТОГРАФИЈА НЕКИХ АСЕ ИНХИБИТОРА И ЊИХОВИХ МЕТАБОЛИТА

ЈАДРАНКА ОДОВИЋ[1], МИРЈАНА АЛЕКСИЋ[1], БИЉАНА СТОЈИМИРОВИЋ[2], ДУШАНКА МИЛОЈКОВИЋ-ОПСЕНИЦА[3] и ЖИВОСЛАВ ТЕШИЋ[3]

[1]*Фармацеутски факултет, Универзитет у Београду, п. пр. 146, 11001 Београд,* [2]*Медицински факултет, Универзитет у Београду, п. пр. 840, 11000 Београд и* [3]*Хемијски факултет, Универзитет у Београду, п. пр.51, 11001 Београд*

Хроматографско раздвајање и понашање пет АСЕ инхибитора (инхибитора ангио-тензин-конвертујућег ензима) и њихова четири активна метаболита испитивано је методом нормално-фазне танкослојне хроматографије на силика-гелу применом неколико једно- и дво-компонентних неводених система растварача. Добијена је линеарна зависност између R_M-вредности и концентрације етанола у мобилној фази. На основу одговарајућих регресионих података, по аналогији са реверзно-фазном хроматографијом, израчунати су параметри липофилности R_M^0 и C_0. Хроматографски добијени параметри хидрофобности корелисани су са израчунатим log *P* вредностима. Такође, R_M^0 –вредности добијене у овом раду корелисане су са R_M^0 –вредностима добијеним методом реверзно-фазне танкослојне хроматографије.

(Примљено 16. октобра 2008)

REFERENCES

1. C. A. Lipinski, F. Lombardo, B. W. Dominy, P. J. Feeney, *Adv. Drug Del. Rev.* **23** (1997) 3
2. T. Fujita, J. Iwasa, C. Hansch, *J. Am. Chem. Soc.* **86** (1964) 5175
3. S. K. Poole, C. F. Poole, *J. Chromatogr. B* **797** (2003) 3
4. K. Valko, *J. Chromatogr. A* **1037** (2004) 299
5. X. Liu, H. Tanaka, A. Yamauchi, B. Testa, H. Chuman, *J. Chromatogr. A* **1091** (2005) 51
6. A. Pyka, M. Miszczyk, *Chromatographia* **61** (2005) 37
7. M. L. Bieganowska, A. D. Szopa, A. Petruczynik, *J. Planar Chromatogr.* **8** (1995) 122
8. N. U. Perišić Janjić, T. Lj. Đaković Sekulić, S. Z. Stojanović, K. M. P. Gaši, *Steroids* **70** (2005) 137
9. N. U. Perišić Janjić, G. S. Usčumlić, N. Valentić, *J. Planar Chromatogr.* **18** (2005) 92
10. J. Odović, B. Stojimirović, M. B. Aleksić, D. Milojković-Opsenica, Ž. Tešić, *J. Planar Chromatogr.* **18** (2005) 102

11. J. Odović, B. Stojimirović, M. B. Aleksić, D. Milojković-Opsenica, Ž. Tešić, *J. Serb. Chem. Soc.* **71** (2006) 621
12. N. J. Brown, D. E. Vaughan, *Circulation* **97** (1998) 1411
13. J. Hoyer, K. L. Schulte, T. Lenz, *Clin. Pharmacokinet.* **24** (1993) 230
14. Ch. Abbara, G. Aymard, S. Hinh, B. Diquet, *J. Chromatogr. B* **766** (2002) 199
15. R. Bhushan, D. Gupta, S. K. Singh, *Biomed. Chromatogr.* **20** (2006) 217
16. J. A. Prieto, U. Akesolo, R. M. Jimenez, R. M. Alonso, *J. Chromatogr. A* **916** (2001) 279
17. A. El- Gindy, A. Ashour, L. Abdel- Fattah, M. M. Shabana, *J. Pharm. Biomed. Anal.* **25** (2001) 913
18. Y. Matsuki, K. Fukuhara, T. Ito, H. Ono, N. Ohara, T. Yui, Y. Nambara, *J. Chromatogr.* **188** (1980) 177
19. F. Zannad, *Am. J. Hyperten.* **8** (1995) 75S
20. C. Furberg, *Clin. Cardiol.* **23** (2000) IV 15
21. D. T. Nash, *Am. J. Cardiol.* **69** (1992) C26
22. E. C. Bate-Smith, R. G. Westall, *Biochim. Biophys. Acta* **4** (1950) 427
23. L. R. Snyder, *J. Chromatogr.* **92** (1974) 223
24. K. Saltoh, M. Kobayashi, N. Suzuki, *Anal. Chem.* **53** (1981) 2309
25. K. Valko, P. Slegel, *J. Chromatogr. A* **631** (1993) 49
26. A. C. Moffat, M. D. Osselton, B. Widdop, *Clarke's Analysis of Drugs and Poisons*, 3rd ed., Medical Toxicology Unit, Guy's Hospital, London, 2004.
27. A. G. Asuero, A. Sayago, A. G. Gonzalez, *Crit. Rev. Anal. Chem.* **36** (2006) 41.

Journal of the Serbian Chemical Society
JSCS@tmf.bg.ac.rs • www.shd.org.rs/JSCS
J. Serb. Chem. Soc. 74 (6) 689–696 (2009)
JSCS–3867
UDC 66.087:546.56+546.11:539.21
Original scientific paper

Cross-section analysis of the morphology of electrodeposited copper obtained in the hydrogen co-deposition range

NEBOJŠA D. NIKOLIĆ[1*#], VESNA M. MAKSIMOVIĆ[2], MIOMIR G. PAVLOVIĆ[1#] and KONSTANTIN I. POPOV[1,3#]

[1]*ICTM – Institute of Electrochemistry, University of Belgrade, Njegoševa 12, P.O. Box 473, 11001 Belgrade,* [2]*Vinča Institute of Nuclear Sciences, P.O. Box 522, 11001 Belgrade and* [3]*Faculty of Technology and Metallurgy, University of Belgrade, Karnegijeva 4, P.O. Box 3503, 11001 Belgrade, Serbia*

(Received 26 December 2008, revised 13 February 2009)

Abstract: Cross-section analysis of copper deposits electrodeposited in the hydrogen co-deposition range at a constant overpotential and in a pulsating overpotential (PO) regime was performed. It was shown that a complete structural analysis of these technologically very important electrodes is impossible without an analysis of their internal structure. An insight into the compactness (or porosity) of the deposits, as well as into the depth of the holes, can only be obtained by this type of analysis.

Keywords: electrodeposition; cross-section analysis; hydrogen; copper.

INTRODUCTION

Electrodeposition is a very suitable way to obtain open porous structures of copper and copper–tin alloys with an extremely high surface area. These structures are of high technological significance because they are ideally suited for electrodes in many electrochemical devices, such as fuel cells, batteries and chemical sensors.[1–3] They can be electrodeposited in both galvanostatic[1–3] and potentiostatic[4–12] regimes of electrolysis. The basic characteristics of these electrodes, denoted as both 3-D foam[1–3] and honeycomb-like ones,[4–12] are holes or pores formed due to attached hydrogen bubbles with agglomerates of copper grains among them. In constant regimes of electrolysis, the number, distribution and pore size can easily be controlled by the choice of appropriate electrolysis parameters.[7] In relation to constant regimes of electrolysis, a decrease in the diameter of the holes formed by attached hydrogen bubbles and an increase in their number can be achieved by the addition of specific substances to the plating bath,[2] or by application of periodically changing regimes of electrolysis.[13]

* Corresponding author. E-mail: nnikolic@tmf.bg.ac.rs
# Serbian Chemical Society member.
doi: 10.2298/JSC0906689N

The use of the scanning electron microscopy (SEM) technique was the most often used way for the examination of the structure of copper electrodes with an extremely high surface area. However, the use of this technique gives only information concerning the "top view" of these electrodes. Considering the high technological significance of deposits with an extremely high surface area, a complete analysis of deposits obtained in hydrogen co-deposition range is required. The detailed analysis cannot be realized without an insight into the interior of these structures. The most suitable way for a detailed analysis of deposits is cross-section analysis, because this type of analysis can give information related to the mechanism of formation and growth of deposits. For this reason, the aim of this study was the cross-section analysis of copper deposits obtained in the hydrogen co-deposition range at a constant overpotential and in a pulsating overpotential (PO) regime.

EXPERIMENTAL

Copper was electrodeposited from 0.15 M $CuSO_4$ in 0.50 M H_2SO_4 in an open cell at a temperature of 20±0.5 °C. Potentiostatic and square-wave pulsating overpotential techniques were used for the electrodeposition of copper. In the constant overpotential electrolysis, the employed deposition overpotential was 1000 mV. In the pulsating overpotential deposition, an overpotential amplitude of 1000 mV and a pulse duration of 10 ms were applied in all experiments. The pause duration was selected to be: 5, 20, 50 and 100 ms. Electrodeposition of copper was performed at cylindrical copper electrodes. In all experiments, the geometric surface area of the copper electrodes was 0.50 cm^2. The counter electrode was a copper foil of 0.80 dm^2 surface area placed close to the walls of the cell, while the reference electrode was a copper wire, the tip of which was positioned at a distance of 0.2 cm from the surface of the working electrode. Copper was electrodeposited with electricity quantities of 10 mA h cm^{-2}.

Doubly distilled water and analytical grade chemicals were used for the preparation of the solution for the electrodeposition of copper.

Cross-section analysis of the copper electrodes was performed using a Zeiss Axiovert 25 optical microscope equipped with a Panasonic WV-CD50 digital camera. In order to observe the cross-section of an obtained deposit, the electrode together with the deposit was mounted and fixed by an epoxy resin. In this way, the cross-section represented the plain parallel to the line of deposit growth. The samples were polished several times and the cross-section structure was observed in a non-etched state.

RESULTS AND DISCUSSION

It was shown by the scanning electron microscopy (SEM) technique that honeycomb-like deposits are formed by copper electrodepositions from 0.15 M $CuSO_4$ in 0.50 M H_2SO_4 at a constant overpotential of 1000 mV.[4–6,9] Honeycomb-like deposits can also be formed in the pulsating overpotential (PO) regime.[13] If the following parameters of a square wave PO were applied: an amplitude overpotential of 1000 mV, a deposition pulse of 10 ms and pause durations of 1, 5, 10, 20 and 50 ms, increasing the pause duration led to a decrease of the average diameter of the holes formed by attached hydrogen bubbles, as well as to an increase

in the number of holes formed at surface of copper electrodes compared to the size and number of holes obtained in the constant electrolysis regime.[13,14] Holes formed due to attached hydrogen bubbles were also formed in the PO regime with a pause duration of 100 ms, but their shape, size and number were completely different from those formed with shorter pause durations.[14]

The dependences of the average current on the electrodeposition time obtained at a constant overpotential of 1000 mV and in the PO regime with pause durations of 5, 20, 50 and 100 ms are shown in Fig. 1. From Fig. 1, it can be seen that increasing the pause duration led to a decrease of the average electrodeposition current. Also, these values were smaller than the current obtained in the constant regime of electrodeposition.

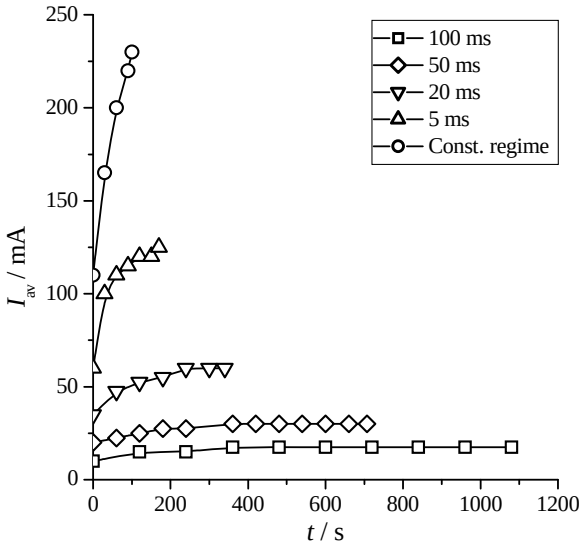

Fig. 1. The dependences of the average current on electrodeposition time, obtained at a constant overpotential of 1000 mV, and in the pulsating overpotential (PO) regime with pause durations of 5, 20, 50 and 100 ms.

Figure 2a shows the cross-section of a honeycomb-like structure electrodeposited from 0.15 M $CuSO_4$ in 0.50 H_2SO_4 at an overpotential of 1000 mV with a quantity of electricity of 10 mA h cm^{-2}. From this Figure, all elements of which honeycomb-like structures are constructed can be seen: "regular holes" formed by both attached hydrogen bubbles (part in circle denoted with A in Fig. 2a) and coalescence of neighboring hydrogen bubbles (part in circle denoted with B in Fig. 2a) and "irregular holes" formed due to the effect of current distribution at the growing surface (parts denoted by arrows labeled C in Fig. 2a).[6] The presence of channel structures formed through the interior of the deposit can be easily observed by cross-section analysis of this deposit at a higher magnification (Fig. 2b).

The mechanism of the formation of honeycomb-like structures was widely studied,[4–7] and it can be briefly presented as follows: in the initial stage of the electrodeposition process, both nuclei of copper and "nuclei" of hydrogen bub-

bles are formed at the active sites of the electrode surface.[6] The hydrogen bubbles isolate the substrate and then the current lines are concentrated around them making rings consisting of agglomerates of copper grains. The current lines are also concentrated at the nuclei of the copper formed in the initial stage between the hydrogen bubbles.

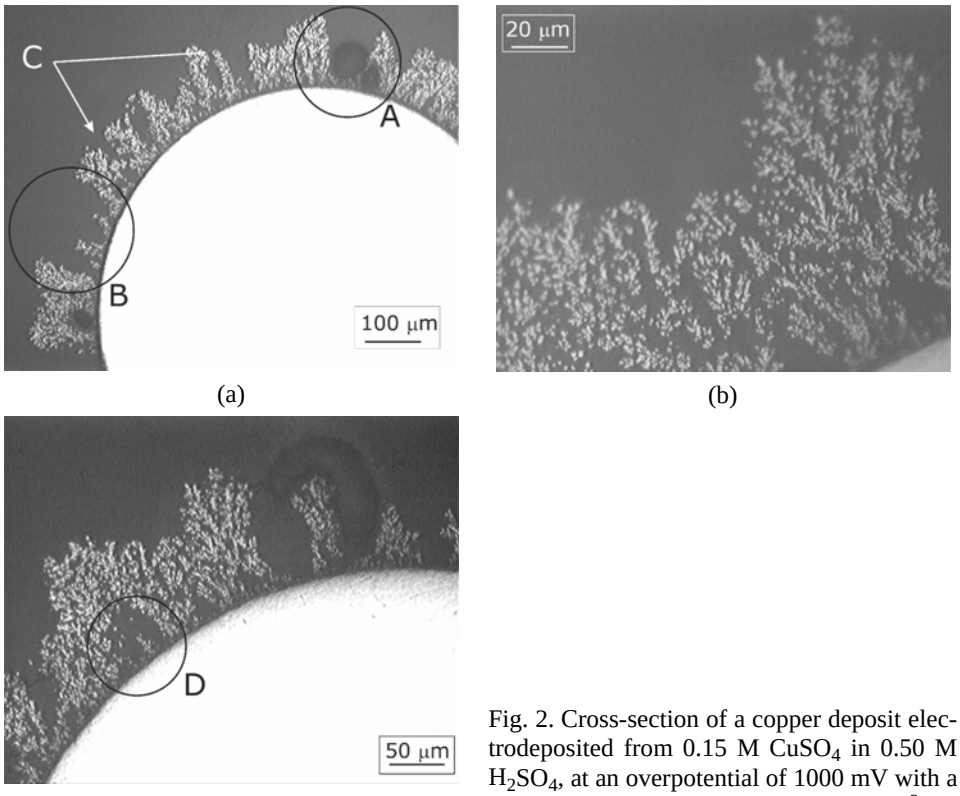

Fig. 2. Cross-section of a copper deposit electrodeposited from 0.15 M $CuSO_4$ in 0.50 M H_2SO_4, at an overpotential of 1000 mV with a quantity of the electricity of 10 mA h cm^{-2}.

As a result of the current distribution at the growing copper surface, new copper nucleation and hydrogen evolution occurs primarily at the top of these agglomerates. Some of the new, small, freshly-formed hydrogen bubbles which are formed at agglomerates around previously formed large hydrogen bubbles coalesce with them, leading to their growth with electrolysis time as already shown.[6] After detachment of these hydrogen bubbles from the electrode surface, “regular holes” are formed. In the growth process, the coalescence of closely-formed large hydrogen bubbles can also be observed.

Simultaneously, holes of irregular shapes are formed from nuclei of copper formed in the initial stage of the electrodeposition. The current distribution at the growing copper surface is responsible for the formation of this type of hole.[6]

Meanwhile, some of the freshly-formed hydrogen bubbles will not find a way to coalesce with the large hydrogen bubbles because they are situated among copper nuclei which initiate a barrier for their development into large hydrogen bubbles. This effect, together with the already discussed current density distribution leads to the formation of a porous channel structure through the interior of the copper deposit (Fig. 2b).

In the process of copper growth, due to the effect of the current distribution, some relatively large hydrogen bubbles can remain included in the interior of copper structure (part in the circle denoted with D in Fig. 2c), making the honeycomb-like structure obtained at a constant overpotential very porous. This enhanced porosity could not be seen by the SEM technique. Hence, complete analysis of the honeycomb-like structures was impossible without cross-section analysis.

The cross-section of morphology of the electrodeposited copper obtained in the PO regime with pause durations of 5, 20, 50 and 100 ms are shown in Fig. 3.

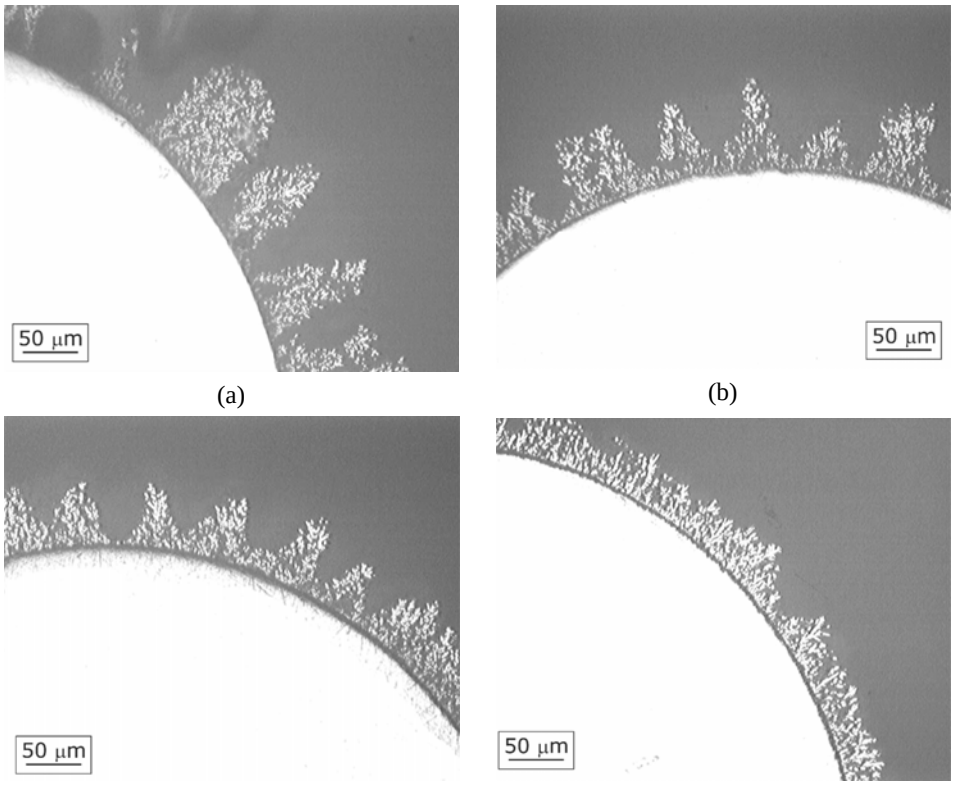

(a) (b)

(c) (d)

Fig. 3. Cross-section of copper deposits electrodeposited from 0.15 M $CuSO_4$ in 0.50 M H_2SO_4 in the pulsating overpotential (PO) regime with a pause duration of: a) 5, b) 20, c) 50 and d) 100 ms.

It can be seen that the compactness of the formed copper deposits increased with increasing pause duration. Also, the compactness of the deposits obtained in the PO regimes was larger than the one obtained in the constant regime of electrolysis (Fig. 2a). Prolonging the pause duration leads to a suppression of the coalescence of neighboring hydrogen bubbles. Coalesced hydrogen bubbles can be observed in the honeycomb-like structures obtained with a pause duration up to 20 ms. It can be seen from Figs. 2a and 3 that the application of a PO regime also leads to a loss of "irregular holes" formed due to the effect of the current distribution at growing copper surfaces. With prolonged pause duration, the pores or channels formed through the interior of the deposits were mutually coalesced, forming larger pores. In this way, the transport of electro-active species through the interior of the structures was facilitated, which is very desirable for an evaluation of electrochemical reactions.[1] Also, a decrease of the depth of the holes with the application of a PO regime can be observed. Prolonging the pause duration also leads to the appearance of dendrites in these copper structures. Dendritic particles were especially visible in the copper deposit obtained with a pause duration of 100 ms (Fig. 4). From Figs. 2 and 3, it is clear that the increase in the number of holes by the application of a PO regime cannot be only ascribed to suppressed coalescence of neighboring hydrogen bubbles, but to an improved current distribution at the growing copper surface by which the inclusion of hydrogen bubbles in the deposit was prevented. The effects observed by application of a PO regime are ascribed to the current density during the "off" periods (*i.e.*, during the duration of pause). Although this current density can be neglected in comparison with the current density during the "on" periods (*i.e.*, during the duration of the deposition pulses), it is clear that its effect on the formation of these deposits is very important.[13,14]

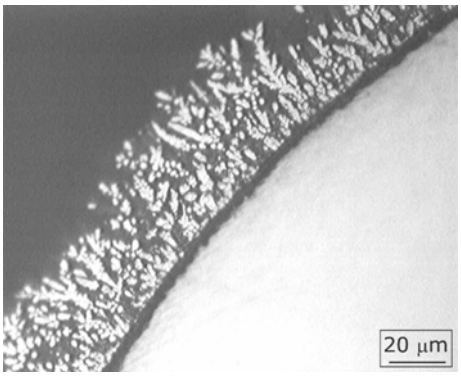

Fig. 4. Cross-section of a copper deposit electrodeposited from 0.15 M $CuSO_4$ in 0.50 M H_2SO_4 in the pulsating overpotential (PO) regime with a pause duration of 100 ms.

The formation of honeycomb-like structures is accompanied by vigorous hydrogen evolution, leading to a change in the hydrodynamic conditions in the near-electrode layer. The vigorous hydrogen evolution is only one of the possible

ways of changing the hydrodynamic conditions in the near-electrode layer. For example, a change of the hydrodynamic conditions can also be realized under imposed magnetic fields (magnetohydrodynamic effects),[15,16] in an ultrasonic field[17] or by rotating the electrode.[18] Certainly, the appearance of dendritic forms clearly indicates to a decreased effectiveness of the stirring of the copper solution by evolved hydrogen with increasing pause duration.

On the basis of the previous consideration, it is very clear that an estimation of porosity (or compactness) of deposits, the depth of holes and the size of the pores inside a structure is impossible without cross-section analysis of the deposit. This makes that cross-section analysis a necessity for a complete analysis of porous deposits.

On the other hand, the increased surface roughness at low levels of coarseness can be of interest for the polarization behavior of such electrodes. Obviously, an increased roughness at a low level of coarseness can lead to an increase of the apparent exchange current density, producing the same effect as a decrease of the reacting ion concentration, as stated in previous papers.[19,20] This will be the subject of our further investigations.

CONCLUSIONS

It has been shown that a complete analysis of honeycomb-like deposits, as potential electrodes for electrochemical devices, is impossible without the recognition of their internal structure. The pore size in the interior of a structure, the depth of both “regular” and “irregular” holes, as well as the overall compactness of a structure can only be estimated by cross-section analysis of these deposits.

Acknowledgement. The work was supported by the Ministry of Science and Technological Development of the Republic of Serbia under the research project: “Deposition of ultrafine powders of metals and alloys and nanostructured surfaces by electrochemical techniques” (No. 142032G).

И З В О Д

МОРФОЛОГИЈА ПОПРЕЧНОГ ПРЕСЕКА ПРЕВЛАКА БАКРА ДОБИЈЕНИХ ЕЛЕКТРОХЕМИЈСКИМ ТАЛОЖЕЊЕМ У ОБЛАСТИ КО-ДЕПОЗИЦИЈЕ ВОДОНИКА

НЕБОЈША Д. НИКОЛИЋ[1], ВЕСНА М. МАКСИМОВИЋ[2], МИОМИР Г. ПАВЛОВИЋ[1] и КОНСТАНТИН И. ПОПОВ[1,3]

[1]ИХТМ – Центар за електрохемију, Универзитет у Београду, Његошева 12, Београд, [2]Институт за нуклеарне науке “Винча”, Београд и [3]Технолошко–металуршки факултет, Универзитет у Београду, Карнегијева 4, Београд

Урађена је анализа попречних пресека талога бакра добијених у области ко-депозиције водоника на константној пренапетости и режимом пулсирајуће пренапетости. Показано је да комплетна структурна анализа ових технолошки веома важних електрода није могућа без анализе њихове унутрашње структуре. Увид у компактност (или порозност) талога, као и у дубину рупа може да се добије само овим типом анализе.

(Примљено 26. децембра 2008, ревидирано 13. фебруара 2009)

REFERENCES

1. H.-C. Shin, J. Dong, M. Liu, *Adv. Mater.* **15** (2003) 1610
2. H.-C. Shin, M. Liu, *Chem. Mater.* **16** (2004) 5460
3. H.-C. Shin, M. Liu, *Adv. Funct. Mater.* **15** (2005) 582
4. N. D. Nikolić, K. I. Popov, Lj. J. Pavlović, M. G. Pavlović, *J. Electroanal. Chem.* **588** (2006) 88
5. N. D. Nikolić, K. I. Popov, Lj. J. Pavlović, M. G. Pavlović, *Surf. Coat. Technol.* **201** (2006) 560
6. N. D. Nikolić, K. I. Popov, Lj. J. Pavlović, M. G. Pavlović, *J. Solid State Electrochem.* **11** (2007) 667
7. N. D. Nikolić, Lj. J. Pavlović, M. G. Pavlović, K. I. Popov, *Electrochim. Acta* **52** (2007) 8096
8. N. D. Nikolić, K. I. Popov, Lj. J. Pavlović, M. G. Pavlović, *Sensors* **7** (2007) 1
9. N. D. Nikolić, Lj. J. Pavlović, M. G. Pavlović, K. I. Popov, *J. Serb. Chem. Soc.* **72** (2007) 1369
10. N. D. Nikolić, G. Branković, M. G. Pavlović, K. I. Popov, *J. Electroanal. Chem.* **621** (2008) 13
11. N. D. Nikolić, Lj. J. Pavlović, S. B. Krstić, M. G. Pavlović, K. I. Popov, *Chem. Eng. Sci.* **63** (2008) 2824
12. N. D. Nikolić, Lj. J. Pavlović, G. Branković, M. G. Pavlović, K. I. Popov, *J. Serb. Chem. Soc.* **73** (2008) 753
13. N. D. Nikolić, G. Branković, M. G. Pavlović, K. I. Popov, *Electrochem. Commun.* **11** (2009) 421
14. N. D. Nikolić, G. Branković, V. Maksimović, M. G. Pavlović, K. I. Popov, *J. Solid State Electrochem.*, doi: 10.1007/s10008-009-0842-1, in press
15. H. Matsushima, A. Bund, W. Plieth, S. Kikuchi, Y. Fukunaka, *Electrochim. Acta* **53** (2007) 161
16. N. D. Nikolić, *J. Serb. Chem. Soc.* **72** (2007) 787
17. M. E. Hyde, O. V. Klymenko, R. G. Compton, *J. Electroanal. Chem.* **534** (2002) 13
18. G. Hinds, F. E. Spada, J. M. D. Coey, T. R. Ni Mhiochain, M E. G. Lyons, *J. Phys. Chem. B* **105** (2001) 9487
19. P. M. Živković, B. N. Grgur, K. I. Popov, *J. Serb. Chem. Soc.* **73** (2008) 227
20. P. M. Živković, N. D. Nikolić, M. Gvozdenović, K. I. Popov, *J. Serb. Chem. Soc.* **74** (2009) 291.

Journal of the Serbian Chemical Society
JSCS@tmf.bg.ac.rs • www.shd.org.rs/JSCS
J. Serb. Chem. Soc. 74 (6) 697–706 (2009) UDC 549.25+504.521;351.777.83+628.516(497.11)
JSCS–3868 *Original scientific paper*

Heavy metals concentration in soils from parks and green areas in Belgrade

MIRJANA D. MARJANOVIĆ[1#], MARIJA M. VUKČEVIĆ[1#], DUŠAN G. ANTONOVIĆ[1#], SUZANA I. DIMITRIJEVIĆ[1], ĐORĐE M. JOVANOVIĆ[2], MILAN N. MATAVULJ[3] and MIRJANA Đ. RISTIĆ[1*#]

[1]*Faculty of Technology and Metallurgy, University of Belgrade, Karnegijeva 4, Belgrade,* [2]*Ministry of Environmental Protection, Republic of Serbia, Omladinskih Brigada 1, Belgrade, and* [3]*Faculty of Sciences, University of Novi Sad, Trg D. Obradovića 2, Novi Sad, Serbia*

(Received 4 September, revised 31 October 2008)

Abstract: The current study included the investigation of several metals and their distribution in urban soils from parks and green areas in the city of Belgrade. The soils were sampled in January and February 2008. The concentrations of Cd, Co, Cu, Pb, Mn and Zn were measured, as well as the pH values and organic matter contents. The obtained results showed that there was a significant level of contamination in some samples, especially with lead, and that it was most probably caused by anthropogenic activities, mostly from traffic. The results were compared with the National legislation and Netherlands standards. Also, the recent results were compared with the data from previous work and it was concluded that there has been a certain increase of the Pb concentration in the past three years. The level of pollution in playground soil was very high and each analyzed sample exceeded the Dutch target value for Cd, Co and Pb.

Keywords: pseudo-total metal contents; urban soil; parks; green areas; pollution.

INTRODUCTION

Trace elements, especially heavy metals, are considered to be one of the main pollutants in the environment, since they have a significant effect on its ecological quality.[1]

Expanding interest in the field of heavy metal research is associated with an increasing world production of metals and their common usage in the past century and, consequently, with their increasing emissions into the environment. This has resulted in a growing hazard to human health posed by elevated metal concentrations in the air, water and food.[2] The problem with heavy metals is their persistence, making it impossible to eliminate them from the environment.[3]

* Corresponding author. E-mail: risticm@tmf.bg.ac.rs
# Serbian Chemical Society member.
doi: 10.2298/JSC0906697M

The majority of the studies[4–10] agreed that urban soils contained enriched levels of trace elements relative to the natural background levels.[11] While usually natural forms are presented in relatively low concentrations, in recent years a number of anthropogenic sources, such as emissions of industrial plants, vehicle exhausts, thermal power stations and commercial product waste, have made notable contributions to the increase of environmental metal concentrations.[4, 12–14]

The heavy metal contents of urban soils may influence public health *via* direct contact with contaminated dust or soil or by inhalation.[3] Children are the most sensitive target group of exposure.[15,16] Due to their higher sensitivity, as well as characteristic behaviors (outdoor activities, hand–mouth activity, deficient hygienic habits, *etc.*), children are at greater risk of exposure to the toxic elements from contaminated soils than adults.[12] Bearing in mind that children are more susceptible to metals, since they are in the early stage of development, determining the heavy metal contents in playground soils is of particular importance.

The aim of the current study was to investigate the metal contents in urban soil in Belgrade and to obtain some knowledge about possible changes of the metal concentrations with time. The current study included the investigation of several metals and their distribution in urban soils in Belgrade. Special attention was paid to playground sampling in parks where children spend most of their time.

EXPERIMENTAL

Sites of investigation

Belgrade is the capital and the largest city in Serbia, located in southeastern Europe, between 44 and 49° of the northern latitude and 20 and 27° of the eastern longitude, 90–120 m above sea level. Belgrade has a moderate continental climate, with an average annual air temperature of 11.9 °C. January is the coldest month with an average temperature of 0.1 °C and July is the hottest month with an average temperature of 22.1 °C. A characteristic of the Belgrade climate is the Košava, a southeast–east wind which brings clear and dry weather. It blows mostly in autumn and winter, in 2–3 days intervals. The average annual rainfall on Belgrade and its surroundings is 669.5 mm. The months with the most rainfall are May and June.

Belgrade is situated at the confluence of the Sava and the Danube Rivers. It is an important intersection of roads and industry and the commercial center of the country. With a growing population (around 1.8 million citizens) and economic development, the environmental quality of the urban soils is becoming more important considering human health. Numerous heating plants, coal or crude oil used for domestic heating, leaded gasoline and diesel vehicle exhaust, are some of the potential sources of pollutions in urban soils and they are major problems in Belgrade.[17,18]

Sampling strategy

In the study areas, there are no specific point-sources of heavy metals and therefore, heavy metal contamination of the soils is derived from continuous urbanization and development, which can adversely affect human health in the contaminated area.

Soil samples were taken from 15 locations from parks and green areas in the urban parts of Belgrade (Fig. 1) in January and February 2008. Most of the locations were chosen within the main public parks and green areas in the central zone of Belgrade. Each location was re-

presented with 2 or 3 samples, one sample from the children's playground and one or two samples near a street or crossroad. At each sampling point, three sub-samples, from top 10 cm layer, within a 20 cm×20 cm surface, were taken and mixed to obtain a bulk composite sample. Such a sampling strategy was adopted in order to reduce the possibility of random influence of urban waste not clearly visible.[5] Samples were collected with a stainless trowel and transferred to the laboratory in plastic bags. Stones and foreign objects were hand-removed, and the samples were air-dried for seven days.

Fig. 1. The study area and sampling locations. Legend: 1. Tašmajdan, 2. Karađorđev park, 3. Kalemegdan, 4. Pionirski park, 5. Skupština, 6. Zemun, 7. Manjež, 8. Studentski park, 9. Novi Beograd, 10. Mostarska petlja, 11. Ada Ciganlija, 12. Ušće, 13. Finansijski park, 14. Vukov spomenik, 15. Slavija.

Analytical procedure

The dry samples were gently crushed and sieved to 2 mm and 1.00±0.02 g was weighed for analysis. Measurements of the pH values were realized on a 1:5, soil:deionized water suspension.[19] The content of organic matter was determined as the weight loss after heating 1 g soil at 550 °C for 2 h.

"Pseudo-total metal contents" were obtained by digesting soil samples in *aqua regia*. The term pseudo-total accounts for the *aqua regia* digestion not completely destroying silicates. This method is widely used in environmental studies and, for example, recommended by the National Government Regulation of Italy.[5]

One gram of dried and homogenized portion of the soil fraction smaller than 2 mm was digested with 18 ml HCl and 6 ml HNO_3 by heating under reflux until most of the solvent was removed. After cooling, the digestion was repeated. Cool suspension was filtered into 50 ml volumetric flask and made up to the volume with deionized water. The concentrations of Cd, Co, Cu, Pb, Mn, and Zn were measured using a Pye Unicam SP9 atomic absorption spectrometer.

RESULTS AND DISCUSSION

The obtained results for pH values of soil–deionized water suspension and organic matter content determined by loss-on-ignition are presented in Table I. The results are given as mean value for each location, which included 2 or 3 samples. The range for the acquired values at the locations is also given. The measured pH values indicated that all the analyzed samples were sub-alkaline or alkaline, which could affect a lower solubility and greater retention of metals in soils.[20] The range of the organic matter content was generally 6.11–13.11 %, with two exceptions: an extremely low value at location 12 (3.38 %) and an extremely high value at location 11 (23.65 %).

TABLE I. Mean and range of pH values and organic matter content (*OM*)

Location	pH		*OM* / %	
	Range or value	Mean	Range or value	Mean
1	8.07–8.57	8.31	6.11–9.09	9.49
2	8.44–8.75	8.60	8.27–8.93	8.60
3	8.00–8.62	8.36	8.72–11.69	10.22
4	8.38–8.58	8.45	7.17–11.22	8.65
5	8.72–9.32	9.02	9.55–11.26	10.41
6	8.32–8.57	8.41	7.09–11.19	9.11
7	8.23–8.44	8.35	7.44–9.46	8.77
8	8.63–9.01	8.82	8.95–9.72	9.34
9	8.64–9.00	8.82	7.53–7.69	7.61
10	8.35–8.38	8.36	12.13–13.1	12.62
11	8.55–9.21	8.83	8.13–23.65	13.37
12	8.56–9.72	8.97	3.38–8.42	6.11
13	8.34–8.62	8.50	7.54–10.92	9.17
14	8.58	–	8.93	–
15	8.18–8.30	8.24	6.52–7.23	6.88

The minimum, maximum, and average metal concentrations are summarized in Table II. The average heavy metal concentrations for each of the 15 locations are shown in Fig. 2.

All of the investigated metals had a wide range of concentration values, depending on location and sampling point at a specific location. High concentra-

tions coupled with wide range of values suggests anthropogenic sources for these elements.[21]

TABLE II. Minimum, maximum and average metal concentrations (mg/kg soil)

Concetration	Cd	Co	Cu	Pb	Mn	Zn
Min	1.1	4.4	8.8	$\leq LOD$[a]	281.8	63.2
Max	3.1	36.0	251.3	785.7	688.9	691.1
Average	1.8	16.5	46.3	298.6	417.6	174.2

[a]Limit of detection for Pb is 5 mg/kg dry sample

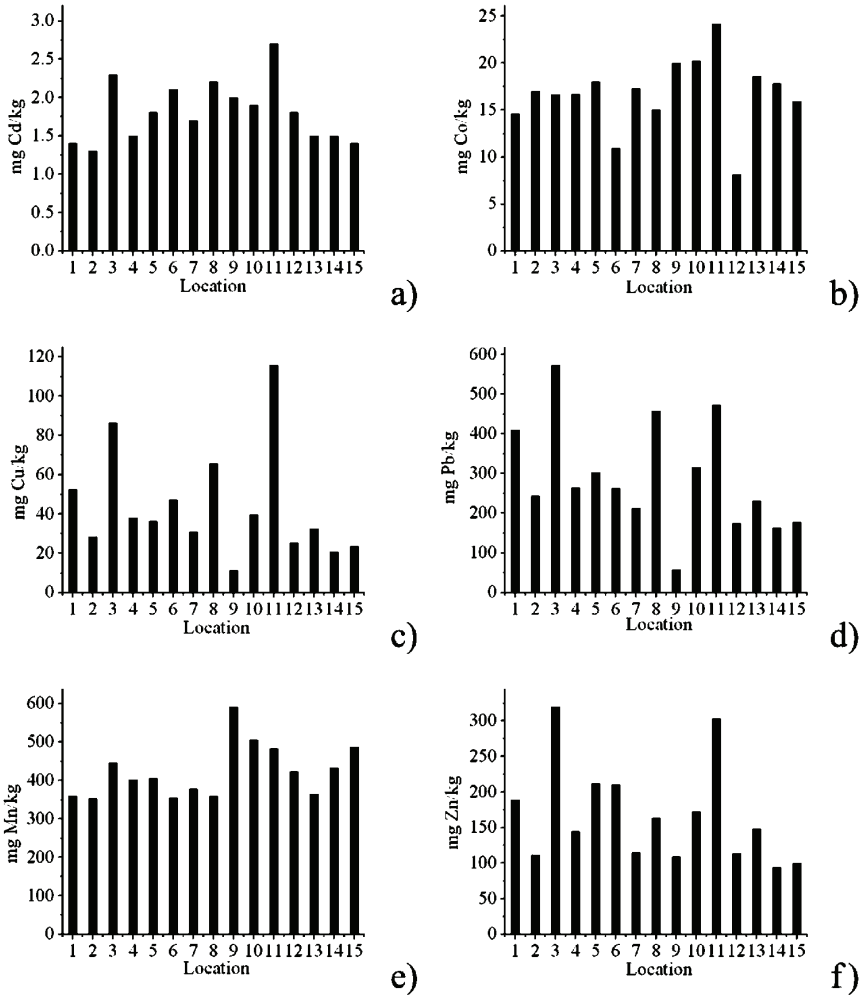

Fig. 2. Mean values of a) Cd, b) Co, c) Cu, d) Pb, e) Mn and f) Zn concentrations (mg/kg).

According to the National legislation,[22] 93.3 % of the analyzed samples were contaminated with lead (maximum allowed concentration for lead in soil is

100 mg/kg); 13.3 % of the samples were contaminated with zinc (maximum allowed concentration for zinc in soil is 300 mg/kg); 6.7 % of samples were contaminated with copper (maximum allowed concentration for copper in soil is 100 mg/kg). There was no soil contamination with cadmium (maximum allowed concentration for cadmium in soil is 3 mg/kg). Manganese and cobalt are not regulated with the National legislative.

The possible contamination can also be estimated according to the Netherlands Soil Quality Standard,[23] an often cited standard in similar studies.[4,24–26] The Dutch target values (Table III) indicate the level at which there is a sustainable soil quality. This means that soils are relatively unpolluted if they meet the target values. According to the Netherlands Standard, 93.3 % of the examined samples were polluted with Pb and Co, 60 % were polluted with Zn and 53.3 % were polluted with Cu. The soil intervention values are representative of the level of contamination above which there is a serious case of soil contamination. According to this, 6.7 % of analyzed soil samples exceeded the intervention value for the concentration of Pb, which means that these locations require remediation. Comparing the obtained Zn, Cd, Cu, and Co concentrations with the intervention values, the contamination was not sufficiently high to require remediation. The manganese concentration is not defined with this standard.

TABLE III. Target and intervention values for selected metal concentrations (mg/kg) in soils from the Ministry of Housing, Spatial Planning and Environment Directorate, Netherlands[23]

Value	Cd	Co	Cu	Pb	Zn
Target	0.80	9.0	36	85	140
Intervention	12	240	190	530	720

Comparing results obtained in this study and the results from the previous study,[27] it could be concluded that there was a significant increase in average concentrations for Pb in urban soils of Belgrade. The mean concentration for Pb was 299 mg/kg in the year 2008, which was approximately twofold higher than the mean concentrations in 2003 and 2005, 151 and 125 mg/kg, respectively. It is also worth noting that the maximum Pb concentration from the previous study[27] was 238 mg/kg, which was more than three times lower than the maximum concentration obtained in 2008. Possible explanations for the obtained data could be the growing density of the traffic in the past few years or the fact that sampling was performed during the winter season, when heating plants could be a potential source of pollution. On the other hand, the concentration of Cu was more than twofold lower than the concentration acquired in 2005 (95.7 mg/kg) and almost the same as the concentration in 2003 (53.3 mg/kg). The decrease in the concentration of Cu suggests that some of this metal was removed by rain or irrigation. The mean concentrations for Zn and Cd were similar as in the previous study (mean concentrations for Zn were 152 and 214 mg/kg; and for Cd they were 1.3 and 1.9 mg/kg for the years 2003 and 2005, respectively).

It is a common practice to compare mean concentrations of trace metals in urban soils from different urban settings.[28] It is obvious that the existing level of contamination in Belgrade with Cd, Co, Cu, Pb, Mn, and Zn is significantly higher than comparable levels in several other cities over the world (Table IV). Considering that all the studies were published in the last year or two, the only explanation for extremely high Pb contamination is the use of leaded gasoline, which is still available in Belgrade and is more often in use than unleaded gasoline.[17] The other investigated metals (Cd, Co, Cu, and Zn) were also present in higher concentrations than in other cities, but they were similar or lower than the concentrations measured in the previous study.

TABLE IV. Average metal concentrations (mg/kg) in urban soils from different cities across the world

City	Cd	Co	Cu	Pb	Mn	Zn	Reference
Galway	–	6	27	58	539	85	8
Hong Kong	0.36	3.55	16.2	88.1	–	103	7
Madrid	0.14	–	14	22	249	50	29
Hangzhou	–	9.25	36.57	46.15	415.27	116.07	21
Belgrade	1.8	16.5	46.3	298.6	417.6	174.2	This paper

The results obtained by analyzing the playground soil samples are presented separately because high amounts of the examined metals were found in some of them. The results obtained for the concentrations of Cd, Co, Cu, Pb, Mn and Zn are shown in Table V.

TABLE V. Heavy metal concentrations (mg/kg) in soils from playgrounds

Location[a]	Cd	Co	Cu	Pb	Mn	Zn
1	1.20	10.21	17.17	151.52	282.51	90.86
2	1.31	14.04	15.11	221.43	299.59	101.83
3	1.55	16.01	71.01	535.71	372.22	122.02
4	1.41	13.91	26.78	190.95	365.58	146.68
5	1.53	17.80	20.56	176.80	443.41	97.29
6	1.67	12.08	23.91	192.86	372.22	119.64
7	1.80	14.19	15.27	180.38	352.86	98.06
8	2.14	12.08	50.92	550.00	331.43	157.65
9	1.89	20.02	8.79	99.01	506.54	121.67
10	1.90	24.16	36.51	157.14	471.81	156.14
11	3.10	35.96	251.32	300.00	563.35	495.82
13	1.07	17.98	22.65	207.14	388.14	113.70
15	1.53	15.85	19.94	190.95	425.68	109.05

[a]No playgrounds were at Locations 12 and 14

According to the National Legislation, 12 of the 13 playground soils were polluted with Pb and one of them (Location 11) was also polluted with Zn, Cd and Cu. On Location 9, the concentration of lead was almost the same as the ma-

ximum allowed by the National Legislation. In all the analyzed playground soil samples, the Dutch target values for Pb, Cd and Co were exceeded and in 4 of the 13 playground soil samples, the target values were exceeded for Zn and Co. Locations 3, 8 and 11 should be remediated since the intervention values for Pb (Locations 3 and 8) and Cu (Location 11) were exceeded. High levels of investtigated metal concentrations at Location 11 could be related to the high level of organic matter (23.65 %), as soils high in organic matter adsorb and bind heavy metals by forming complexes with organic acids, which increases the retention of metals in soils.[3] Children playing in parks could come in contact with soil polluted with metals, especially with lead. This could have negative effect on children's health, particularly for six-year olds and younger children.[15]

CONCLUSIONS

Cadmium, cobalt, copper, lead, manganese, and zinc are good indicators of contamination in soil because they appear in gasoline, vehicle exhausts, car components, industrial emissions, *etc*. According to the National Legislation, 93.3 % of the analyzed samples were contaminated with lead, 13.3 % of the samples were contaminated with zinc and 6.7 % of samples were contaminated with copper. A comparison between the obtained results with those from the previous study indicated that there was a significant increase in concentrations of Pb in the urban soils. Target values for Cd, Cu Pb and Zn in the analyzed soil samples from playgrounds were exceeded and also intervention values for Pb and Cu in some of the samples were exceeded. Furthermore, according to the National Legislation, 92.3 % of playgrounds were polluted with Pb and 7.7 % were polluted with other metals.

Acknowledgements. The authors wish to thank the Ministry of Environmental Protection of the Republic of Serbia for financial support. This study was also partially financially supported by the Ministry of Science and Technological Development of the Republic of Serbia through Project No. 142002.

ИЗВОД

КОНЦЕНТРАЦИЈА ТЕШКИХ МЕТАЛА У ЗЕМЉИШТУ ПАРКОВА И ЗЕЛЕНИХ ПОВРШИНА У БЕОГРАДУ

МИРЈАНА Д. МАРЈАНОВИЋ[1], МАРИЈА М. ВУКЧЕВИЋ[1], ДУШАН Г. АНТОНОВИЋ[1], СУЗАНА И. ДИМИТРИЈЕВИЋ[1], ЂОРЂЕ М. ЈОВАНОВИЋ[2], МИЛАН Н. МАТАВУЉ[3] и МИРЈАНА Ђ. РИСТИЋ[1]

[1]Технолошко–металуршки факултет, Универзитет у Београду, Карнегијева 4, 11000 Београд, [2]Министарство заштите животне средине, Омладинских бригада 1, 11070 Нови Београд и [3]Природно–математички факултет, Универзитет у Новом Саду, Трг Д. Обрадовића 2, 21000 Нови Сад

Циљ овог рада био је испитивање дистрибуције тешких метала у земљишту паркова и зелених површина у Београду. У узорцима земљишта, прикупљеним током јануара и фебруара 2008. године, одређиване су концентрације кадмијума, кобалта, бакра, олова, мангана и цинка, као и pH вредност и садржај органске материје. Добијени резултати показују значајан степен загађења код појединих узорака. Изузетно висок садржај олова забележен је код свих

испитиваних узорака, и највероватније је последица антропогених активности, пре свега саобраћаја. Поређењем резултата са ранијим испитивањима примећено је знатно повећање садржаја олова у земљишту у протекле три године. Изузетно забрињавајућа је и чињеница да је земљиште узорковано у дечијим игралиштима загађено тешким металима. Такође, поређењем добијених резултата са холандским стандардом, закључено је да су код свих узорака концентрације испитиваних метала више од концентрација дефинисаних тим стандардом.

(Примљено 4. септембра, ревидирано 31. октобра 2008)

REFERENCES

1. J. Sastre, A. Sahuquillo, M. Vidal, G. Rauret, *Anal. Chim. Acta* **462 (**2002) 59
2. J. Weber, A. Karczewska, *Geoderma* **122** (2004) 105
3. M. Sieghardt, E. Mursch-Radlgruber, E. Paoletti, E. Couenberg, A. Dimitrakopoulus, F. Rego, A. Hatzistathis, T. Barfoed Randrup, *Urban Forests and Trees*, Springer, Berlin, 2005, p. 281
4. X. D. Li, C. S. Poon, P. S. Liu, *Appl. Geochem*. **16** (2001) 1361
5. D. S. Manta, M. Angelone, A. Bellanca, R. Neri, M. Sprovieri, *Sci. Total Environ.* **300** (2002) 229
6. L. Madrid, E. Diaz-Barrientos, F. Madrid, *Chemosphere* **49** (2002) 1301
7. S. L. Lee, X. D. Li, W. Z. Shi, C. N. Cheung, I. Thornton, *Sci. Total Environ.* **356** (2006) 45
8. C. Zhang, *Environ. Pollut*. **142** (2006) 501
9. M. Romić, T. Hengl, D. Romić, S. Husnjak, *Comput. Geosci.* **33** (2007) 1316
10. L. Miao, R. Xu, Y. Ma, J. Xu, J. Wang, *Geochem. Explor*. **96** (2008) 43
11. E. De Miguel, M. Jimenez de Grado, J. F. Llamas, A. Martin-Dorado, L. F. Mazadiego, *Sci. Total Environ.* **215** (1998) 113
12. S. Granero, J. L. Domingo, *Environ. Int.* **28 (**2002) 159
13. K. Ljung, O. Selinus, E. Otabbong, *Sci. Total Environ*. **366 (**2006) 749
14. J. W. S. Wong, N. K. Mak, *Environ. Technol.* **18** (1997) 109
15. H. W. Mielke, C. R. Gonzales, M. K. Smith, P. W. Mielke, *Environ. Res.* **81** (1998) 117
16. M. Sanchez-Camazano, M. J. Sanchez-Martin, L. F. Lorenzo, *Sci. Total Environ.* **146/147** (1994) 163
17. M. Aničić, M. V. Frontasyeva, M. Tomašević, A. Popović, *Environ. Monit. Assess.* **129** (2007) 207
18. D. Crnković, M. Ristić, D. Antonović, *Soil Sediment Contam.* **15** (2006) 581
19. ISO 10390: Soil Quality – Determination of pH (1994)
20. B. Škrbić, S. Čupić, *J. Environ. Sci. Health. A* **A39** (2004) 1547
21. T. Chen, X. Liu, M. Zhu, K. Zhao, J. Wu, J. Xu, P. Huang, *Environ. Pollut.* **151** (2008) 67
22. *Regulations about allowed quantities of dangerous and harmful matters in soil and irrigating waters and methods about their analysis*, Official Herald of the Republic of Serbia, No. 23/94 (in Serbian)
23. Ministry of Housing, Spatial Planning and Environment Directorate-General for Environmental Protection, *Circular on target values and intervention values for soil remediation*, Netherlands Government Gazette, 2000, p. 39
24. S. Rodrigues, M. E. Pereira, L. Sarabando, L. Lopez, A. Cachada, A. Duarte, *Sci. Total Environ.* **368** (2006) 40
25. I. Ivančev-Tumbas, J. Tričković, E. Karlović, Z. Tamaš, S. Rončević, B. Dalmacija, O. Petrović, M. Klašnja, *Int. Biodeterior. Biodegrad.* **54** (2004) 311

26. C. S. C. Wong, X. D. Li, *Sci. Total Environ.* **319** (2004) 185
27. M. Ristić, M. Marjanović, *CI&CEQ* **12** (2006) 236
28. N. S. Duzgoren-Aydin, *Sci. Total Environ.* **385** (2007) 182
29. E. De Miguel, I. Iribarren, E. Chacon, A. Ordonez, S. Charlesworth, *Chemosphere* **66** (2007) 505.